AN ABSTRACT OF THE DISSERTATION OF

Raúl Eduardo Avelar Morán for the degree of Doctor of Philosophy in Civil Engineering presented on April 10, 2012.

Title: Safety Performance of Curve Advisory Speed Signs

Abstract approved: ______________________________

Karen K. Dixon

Posting advisory speed signs at sharp horizontal curve sites is a practice well established in the United States. The purpose of these signs is to provide the driving public with a safe speed to negotiate such curves; however, the link between these signs and safety has not yet been clearly established.

The first manuscript in this dissertation presents an effort to model safety as it relates to curve advisory speed signs. It proposes a statistical model relating crash frequency at 2-lane rural highways in Oregon to curve advisory speed signs and other influential factors. The Advisory Speed Crash Factor (ASCF) emerges as a sub-model that characterizes the safety effect of advisory speed signs. Results indicate that safety may be compromised if the advisory speed is either excessively prohibitive or excessively permissive.

The second manuscript extends the use of the proposed ASCF to develop the OSU posting method, a new procedure that procures the "optimal" advisory speed derived from the ASCF. A field validation analysis, also presented in this manuscript, verified the meaningfulness of the proposed ASCF sub-model.

The third manuscript outlines another methodology, named 'the Hybrid OSU Posting Method' in an effort to mitigate the well documented variability associated with using the Ball Bank Indicator (BBI). This method determines the advisory speed using the BBI in combination with the ASCF. Though benefits in safety performance and consistency resulted from using the Hybrid OSU method, this method is still outperformed by the computational OSU method.

Note: The Oregon Department of Transportation funded most of this effort; Therefore, copies of parts or this entire document may be published by the Oregon Department of Transportation or their agents.

Safety Performance of Curve Advisory Speed Signs

by

Raúl Eduardo Avelar Morán

A DISSERTATION

submitted to

Oregon State University

in partial fulfillment of
the requirements for the
degree of

Doctor of Philosophy

Presented April 10, 2012
Commencement June 2012

Doctor of Philosophy dissertation of Raúl Eduardo Avelar Morán presented on April 10, 2012.

APPROVED:

____

Major Professor, representing Civil Engineering

____

Head of the School of Civil and Construction Engineering

____

Dean of the Graduate School

I understand that my dissertation will become part of the permanent collection of Oregon State University libraries. My signature below authorizes release of my dissertation to any reader upon request.

____

Raúl Eduardo Avelar Morán, Author

ACKNOWLEDGEMENTS

First of all, I would like to thank God and His infinite Grace. No work would have been possible without the gifts of life, health, a sufficient set of talents, the opportunities to nurture them, and the presence of great people to help and inspire me. *Sanctificetur Nomen Tuum, Dominus.*

I would like to thank Dr. Karen Dixon for her kindness, wise counsel, and the trust granted throughout my entire career at OSU.

I would like to thank the Department of Civil and Construction Engineering for providing me with a research assistantship to fund my education.

I also would like to thank my parents, Ricardo Avelar and Lupita Morán, for their continuous support throughout my studies in the U.S., and ultimately for their unconditional support through all of my life. *Sin ustedes, padres queridos, no sería la mitad del hombre que soy. Con todo mi cariño y sinceridad: ¡Mil gracias!*

Finally, I would like to thank many friends and spiritual brothers who in the recent or in the distant years have provided me with camaraderie and made my life tremendously rich. You have stirred me to pursue my goals as passionately as you have chased and reached your own. Some of you make incredible achievement look easy and ordinary. You all inspire and humble me truly.

CONTRIBUTION OF AUTHORS

Dr. Karen Dixon provided valuable input during the initial phases of crash data collection and filtering, as well as in their preliminary analysis. She provided valuable feedback and funding for the data collection effort toward the validation analysis. She also devoted several hours to co-editing and formatting the manuscripts for publication.

TABLE OF CONTENTS

Page

TABLE OF CONTENTS (Continued)

Page

TABLE OF CONTENTS (Continued)

Page

TABLE OF CONTENTS (Continued)

Page

TABLE OF CONTENTS (Continued)

Page

LIST OF FIGURES

LIST OF FIGURES (Continued)

LIST OF TABLES

LIST OF EQUATIONS

LIST OF EQUATIONS (Continued)

LIST OF APPENDICES

LIST OF APPENDIX TABLES

LIST OF APPENDIX EQUATIONS

ACRONYMS, INITIALISMS AND ABBREVIATIONS IN THIS DISSERTATION

AADT	Average Annual Daily Traffic
AASHTO	American Association of State Highway and Transportation Officials
AIC	Akaike Information Criterion
AASCF	Absolute Advisory Speed Crash Factor
ASCF	Advisory Speed Crash Factor
ASD	Advisory Speed Differential
BBI	Ball Bank Indicator
BV Poisson	Bivariate Poisson
CPF	Cumulative Probability Function
DOT	Department Of Transportation
FHWA	Federal Highway Administration
mph	Miles Per Hour
MUTCD	Manual on Uniform Traffic Control Devices
ODOT	Oregon Department of Transportation
OSU	Oregon State University
pcph	Passenger Cars per Hour
Q-Q	Quantile - Quantile plot
SE	Superelevation
SFD	Side Friction Demand
SPR	State Planning and Research
TCD	Traffic Control Devices
TTI	Texas Transportation Institute
vpd	Vehicles per day

DEDICATION

Ad majorem Dei Gloriam. Ad Jesum per Mariam.

En honor a mis padres, Ricardo y Lupita.

Dieses Werk ist Katies -meines Sonnenscheins- gewidmet.
„...Denn so wie es ist und so wie du bist...“.

A todos mis hermanos.

SAFETY PERFORMANCE OF CURVE ADVISORY SPEED SIGNS

1. General Introduction

In the United States it is common practice to post advisory speed signs at sharp horizontal curve sites. The purpose of these signs is to provide the driving public with a safe speed to negotiate such curves. Current literature has repeatedly verified that the driving public tends to choose speeds above the speeds indicated on these signs. This author verified such trend in a previous research effort, which showed that 73% of drivers in western Oregon drive above the advisory speed (Avelar, 2010).

Current literature offers a myriad of studies with conflicting results regarding the effectiveness of these signs. Some argue that these signs are ineffective; some that researchers cannot draw conclusions about the signs; and some argue that these signs are costly or even counterproductive (Chowdhury, Warren, Bissell, & Taori, 1998), (Courage, et al., 1978), (Gates, Carlson, & Hawkins Jr., 2004), (Kanellaidis, 1995), (Koorey, et al., 2002), (Lyles, 1982), (Lyles & Taylor, 2006), (Ritchie, 1972), (Zwahlen, 1987), (Zegeer, Stewart, Council, Reinfurt, & Hamilton, 1992).

In any case, the link between these signs and the safety performance at posted sites has not yet been clearly established. In spite of the well documented fact of operating speeds exceeding the speeds displayed at these signs, it is still not clear if drivers use the signs as a reference to select their speeds at posted sites, and if so to what extent. These signs would be associated with a safety benefit if they conveyed information that drivers may find useful to choosing their speeds around curves.

1.1. Background and Relevant Premises on Traffic Control Devices at Horizontal Curves

In general, the use of traffic control devices (TCDs) at horizontal curves intends to provide guidance to safe operation at these locations. Zegeer et al. (1992) performed an assessment of the effectiveness of typical curve countermeasures, including TCDs. The authors also recommend general guidelines on horizontal alignment design. These guidelines encompass cost-effective strategies, such as signing, marking and delineation. NCHRP report 500 in its seventh volume (Torbic, et al., 2004) presents a detailed set of strategies to reduce the likelihood of curve related crashes, or to reduce the consequences of departing the travel lane at horizontal curves. The strategies that this report outlines include recommendations on the use of TCDs.

Curve-specific TCDs include a wide variety of warning signs (that may be supplemented with flashers), chevron signs, advisory speed signs, and various types of pavement signs and markers. The specifications and recommended uses of these TCDs are contained in the *Manual on Uniform Traffic Control Devices* (MUTCD).

Figure 1-1: Warning and Advisory Speed Signs

The most common curve TCDs are the horizontal alignment warning sign, the advisory speed warning sign, the chevron sign, and the large directional arrow sign. Figure 1-1 shows a curve warning sign and its companion advisory speed.

The wide array of possible combinations of curve TCDs intends to inform drivers about various degrees of hazardous conditions at horizontal curves. There are two widely used supplements to the MUTCD (FHWA, 2009): the Traffic Engineering

Handbook (Institute of Transportation Engineers, 2009) and the Traffic Control Devices Handbook (Pline, 2001). These documents intend to promote consistency in the use of TCDs, extending specific guidelines for practitioners.

Low-Cost Treatments for Horizontal Curve Safety, a Federal Highway Administration publication (McGee & Hanscom, 2006), offers a set of guidelines for applying TCDs at curve locations, including the ones in the MUTCD, other traditional TCDs, and some innovative configurations.

Another set of guidelines is provided by Bonneson, Miles and Carlson in their *Curve Signing Handbook* (2007). This document stresses the importance of consistency in determining the need of curve TCDs. The authors argue that lack of consistency may explain, to a significant extent, driver disregard for these types of signs.

There is a body of work suggesting that current advisory speed posting practice is not consistent, and there are several different views on their effectiveness, as discussed in the literature review sections of chapters 2, 3, and 4 of this dissertation.

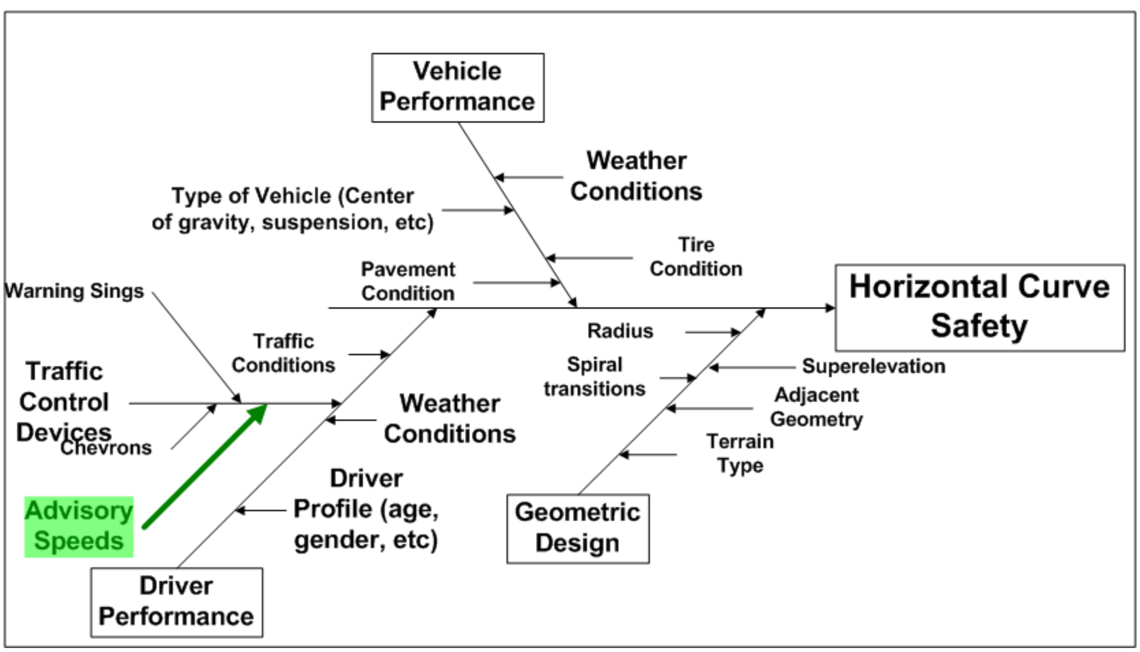

Figure 1-2: Advisory Speeds in the Context of Horizontal Curve Safety

Given this brief background review, a need to study advisory speed signs safety becomes apparent. This dissertation will add to that discussion from a stand point that has been minimally explored: safety performance.

It is expected that advisory speeds play a role on curve safety as contextually depicted in Figure 1-2. Chapter 2 in this dissertation provides a meaningful articulation of such a safety effect, from the stand point of a statistical model provided in that chapter.

1.2. Research Questions Addressed in this Dissertation

The purpose of this dissertation is to provide robust scientific answers to the following research questions:

1. After accounting for other relevant factors with known safety effects, is there a safety benefit associated with the use of advisory speed warning signs?

   If there is indeed such a safety benefit:

2. Is it dependent on the advisory speed value displayed in these signs?
3. Is this benefit also dependent on the criteria that were used to determine the advisory speed?
4. How robust is the evidence in favor of such a safety benefit?
5. Is it possible and feasible to determine an advisory speed value such that it will yield maximum safety benefit?

Chapter 2 in this dissertation presents a safety performance evaluation of curve sites, an effort that sheds light on research questions one through three. The fourth and fifth research questions are addressed by chapters 3 and 4, where the focus is on expanding the evidence favoring the safety effect of these signs -as just established in chapter 2- and on developing new methodologies to post better safety performing advisory speeds.

1.3. The Organization of this Dissertation

Chapter 1 of this dissertation presents a general introduction to advisory speeds, introduces the research questions addressed in this work, and presents a general outline of the document. The main body of this dissertation consists of three journal research papers, henceforth referred to as manuscripts, presented as chapters 2, 3, and 4 respectively. The research questions are addressed, to this author's satisfaction, throughout these three manuscripts.

The first two manuscripts have already appeared in the proceedings of national and international conferences. The first manuscript is under review for publication by *Accident Analysis & Prevention*, a well-known international Journal; the second manuscript was accepted for publication by the *Transportation Research Record, Journal of the Transportation Research Board of the National Academies*, a referential journal in the United States. The third manuscript is under consideration for publication by the *Journal of Transportation of the Institute of Transportation Engineers.*

The first manuscript, chapter 2 in this dissertation, presents a statistical analysis, an effort to modelling the safety performance of horizontal curve sites as it relates to advisory speed signs and other influential factors. Though two candidate statistical specifications were explored, this modelling effort ultimately utilized a Poisson Generalized Linear Model linking the crash frequency at 2-lane rural highways in the state of Oregon to geometric, operational and posting characteristics. The Advisory Speed Crash Factor (ASCF) is a sub-model that characterizes the safety effect of advisory speed signs, after accounting for other influential factors. This manuscript also explores and explains the engineering and human factors implications of the proposed ASCF sub-model. A closer examination to the distribution of ASCF values throughout the available sample suggests that safety performance may be compromised at sites with either excessively prohibitive or excessively permissive advisory speeds. Finally, this manuscript also presents an assessment and a brief discussion of the adequacy of the model and the fulfillment of its underlying assumptions in the available sample.

The second manuscript develops a new computational posting procedure, named “the OSU posting method”, based on the “optimal advisory speed”, a concept derived from the ASCF formulation. Additionally, this manuscript shows a comparison between the expected performance of the new method and two reference sets of advisory speeds. Finally, this chapter includes a brief review of a series of field validation tests this author performed using a new sample of sites in order to test the robustness of the proposed ASCF function. Chapter 5 provides more ample coverage of the details of these validation analyses.

The third manuscript outlines a mixed methodology, named ‘the Hybrid OSU Posting Method’, focusing on mitigating the well documented variability of using the Ball Bank Indicator (BBI), while producing an advisory speed based on safety performance. Inherent variability to the BBI is an issue that inevitably affects advisory speeds determined using this device. But since the BBI is the most widely used posting method, the Hybrid OSU method emerges in anticipation of practitioners being reluctant to stop using the BBI, despite the well documented volatility of its readings. The proposed methodology uses the BBI in combination with the ASCF to arrive at an advisory speed that is based on the optimal advisory speed value, as outlined in the second manuscript.

Complementary, chapter 5 presents relevant material that was not included in the manuscripts, and chapter 6 provides a general conclusion to the dissertation. Finally, Appendices A and B supplement this dissertation with materials that are related to this work, but without which this dissertation can sustain itself as a coherent whole.

2. Modelling the Safety Effect of Advisory Speed Signs: A Bivariate Multiplicative Factor on Number of Crashes based on the Speed Differential and the Side Friction Demand

Raul E. Avelar and Karen K. Dixon

Accident Analysis & Prevention ISSN: 0001-4575

Elsevier
3521 Riverport Lane
Maryland Heights, MO 63043

Paper presented at the 3rd International Conference on Road Safety and Simulation 2011; Along with 30 others, this paper was selected from the 180 papers presented in the conference for a special issue of the journal Accident Analysis & Prevention (SI: RSS 2011); paper is currently under peer review.

Modelling the Safety Effect of Advisory Speed Signs: A Bivariate Multiplicative Factor on Number of Crashes based on the Speed Differential and the Side Friction Demand

Raul E. Avelar

Graduate Research Assistant, School of Civil and Construction Engineering, Oregon State University, Corvallis, OR, USA, e-mail: avelarr@engr.orst.edu

Karen K. Dixon

Associate Professor, School of Civil and Construction Engineering, Oregon State University, Corvallis, OR, USA, e-mail: karen.dixon@oregonstate.edu

3rd International Conference on Road Safety and Simulation, September 14-16, 2011, Indianapolis, USA

ABSTRACT

Posting advisory speed signs at sharp horizontal curve sites is a practice well established in the United States. The purpose of these signs is to provide the driving public with a safe speed to negotiate such curves; however, the link between these signs and safety performance has not yet been clearly established. This paper presents a recent Oregon effort to model the safety performance as it relates to these curve advisory speed signs. The authors developed a Generalized Linear Model that parameterizes the crash frequency at 2-lane rural highways in the state of Oregon in terms of curve advisory speed signs and other factors. This paper presents an analysis based on the Poisson model, as it provided the most appropriate fit to the data. The authors also tested an alternative Negative Binomial (NB) model. This research found that a bi-linear polynomial, contained in the selected statistical model, convincingly establishes a link between the presence of advisory speed signs and the expected numbers of crashes at these sites. Such a link also proved meaningful from the engineering and human factors perspectives. By using the developed sub-model, the authors estimated the safety effectiveness of advisory speeds. This research estimates that, for the state of Oregon, these signs are linked to an approximate reduction of 27% in the expected number of crashes. In general, this research found that advisory speed signs tend to enhance safety. However, the authors also determined that, under certain conditions, advisory speed signs may not be displaying the value that offers the greatest potential for safety enhancement. Furthermore, some advisory speeds can actually be negatively associated with safety performance. Based on the findings of this research, this negative relation can occur at sites with either excessively prohibitive or excessively permissive advisory speeds.

Keywords: advisory speed, safety, Side Friction Demand

2.1. Introduction

Curve advisory speed signs are companions to curve warning signs. Their purpose is to recommend a safe speed for vehicles to negotiate horizontal curves. Although the practice of posting these signs is well established, a convincing linkage between these signs and their hypothesized long term safety benefit has not been clearly established. Current literature includes repeated documentation of poor adherence to these signs, but the authors of this paper believe that such lack of operational compliance may not directly translate into similar safety expectations. This paper presents a statistical analysis in pursuit of quantifying a potential safety benefit of advisory speed signs.

The research effort as summarized in this paper includes six general sections: (2.2) past and current advisory speed posting practices, () data characteristics and filtering, (3) statistical analysis, (4) the effects of advisory speed signs, (5) an evaluation of the resulting model adequacy, and (6) conclusions and recommendations.

2.2. Past and Current Advisory Speed Posting Practices

Advisory speed signs in the United States have been in use since the 1930s. The standardized practice of posting these signs dates back to the 1948 *Manual on Uniform Traffic Control Devices* (MUTCD), where the use of the ball bank indicator is recommended to determine safe speeds for horizontal curves. In its latest edition, the 2009 MUTCD recognizes the potential use of alternative methods to establish advisory speeds. According to this document, advisory speeds shall be determined by an “engineering study that follows established engineering practices” (FHWA, 2009, p. Section 2C.08). This version of the MUTCD indicates that using the ball bank indicator, the geometric design equation, or an accelerometer are examples of such advisory speed engineering assessment practices. The most widely implemented assessment technique is the ball bank indicator. The thresholds for this method have been continually updated through subsequent editions of the MUTCD (FHWA, 2009).

Available literature consistently indicates that advisory speed values, developed using the standardized ball bank indicator procedure, have a large variation in recommended values (Chowdhury, et al., 1998; Courage, et al., 1978). Furthermore, a recent study by Dixon and Rohani (2008) found that a large proportion of curve sites in the state of Oregon do not comply with the state policy. Various authors argue that such lack of consistency results in poor adherence to advisory speeds (Lyles, 1983; Bonneson, et al, 2009).

Surprisingly, there does not appear to be any available literature that quantifies how advisory speed signs actually play a role in enhancing safety performance at horizontal curve locations. The only reference that assigns a flat effect to the mere presence of these signs is that of Elvik and Vaa (Elvik & Vaa, 2004), from which it appears that the signs are beneficial. This paper investigates the possibility that these signs, despite potentially poor operational compliance, are conveying additional and meaningful information to the public about the severity of downstream horizontal alignments. Accordingly, drivers may respond by adjusting, in some way, their driving behaviour at posted horizontal curves, and this heightened awareness at these locations may result in fewer crashes.

2.3. Data Characteristics and Filtering

This research is based upon the data from a probability sample of 210 directional horizontal curve sites located at 2-lane rural highways in Oregon. The sites were selected from the road inventory database of state maintained highways in Oregon. Dixon and Rohani (2008) collected geometric data at these sites to assess the consistency of posting practice in the state. The researchers used probability sampling to ensure representativeness of their results to the state of Oregon. A detailed quantification of the underlying probability structure of a subset of these sites is documented in detail in further work by Avelar (2010). The data collected on site include: curve length, number of lanes, lane and shoulder width, superelevation, vertical grade and vertical signage. Dixon and Rohani determined the corresponding horizontal radii by analyzing aerial images. Additionally, they also collected the Average Annual Daly Traffic, available from the Oregon Department of Transportation (ODOT).

Subsequently, the authors of the current paper compiled the crash records for the sampled sites using ODOT's State-wide Crash Data System. This research used crashes from the period of 2000 to 2004, which closely preceded the site data collection so as to ensure the crash records were appropriately linked to the physical site characteristics at the time of the crash.

Before performing the statistical analysis, the authors filtered the crash data to exclude those crashes that were likely associated with intersections, driveways, and other features not typical to segment locations where the horizontal curve-related crashes could be located. In order to draw meaningful comparisons, the authors of this paper compiled all the crashes that occurred along the 2-mile study corridors and linked them to curve locations, where present. Isolated crash records where mile point locations were recorded to a whole number were suspicious due to potential rounding errors, and therefore were noted and then excluded from further analysis. More detail regarding the data characteristics, sites selected, distribution of crashes, and data filtering is available in Dixon and Avelar (2011).

2.4. Statistical Analysis

In an effort to assess the associated safety effects of advisory speed signs, the authors determined that an univariate statistical test with a simplified direct comparison between crashes at sites with and without advisory speed signs would not suffice due to the large number of potential factors associated with horizontal curve locations at the rural two-lane study sites. For instance, the associated horizontal radius is a natural choice to compare the crashes that occurred within horizontal curves with and without advisory speeds posted, but the wide range of candidate horizontal curve radii within the study sample prohibited a meaningful comparison. The analysis should simultaneously incorporate the effect of radii and other relevant factors, and any associated assumptions should be verifiable. The following sections of this paper review the types of statistical models available, the model selection process, and the results of the modelling procedures.

2.4.1. **Overview of Statistical Models**

Traditionally, Poisson regression models have been used for regressing count responses to a vector of potential explanatory variables; however, overdispersion with respect to the Poisson distribution is commonly encountered in crash data. The use of negative binomial regression models (NB) is an attractive alternative to cope with this issue as such models represent Poisson-overdispersion using an additional parameter in the conditional variance of the Poisson model, while still preserving the conditional expectation of the mean as the regressed parameter. In fact, when the dispersion parameter is equal to one, the Poisson model emerges as a particular case of the NB model.

The two simpler forms of NB models are known as NB1 and NB2. The difference between these two specifications is represented by the conditional variance function, particularly with relation to how the dispersion parameter is specified. The conditional variance for the NB1 model is a simple linear function of the conditional mean, while the conditional variance for the NB2 model is a quadratic function of the conditional mean. Naturally, NB models with more complex parameterizations are also available, but were not incorporated as part of this analysis.

The authors of this paper, therefore, explored the use of Poisson and NB2 models only. It is the NB2 model and not the NB1 that may be formulated as a Generalized Linear Model (GLM), and thus, model evaluation metrics are easily obtainable. A quick and more direct comparison with the significance and fit of Poisson models is therefore easily attained. As previously indicated, as long as the data is not over-dispersed, the Poisson model results are equally valid to the NB2 model results.

Although the Poisson and NB2 regression models have a relatively simple structure, some complexity arises in this case because the authors chose to explicitly account for interactions among the explanatory variables. Explicitly modelling variable interactions creates departures from both simple linearity of the mathematical form and an independent-like covariance structure among predictors (both typical assumptions of non-interacting linear regression models). The authors paid special attention to the fact that using interrelated variables as predictors increases the risk of encountering multicollinearity and its derived issues. These issues, however, when assessed and well accounted for, do not invalidate the procedure; they simply require additional computational efforts and further interpretation of the results.

2.4.2. **Model Selection**

Crash occurrences may be understood as a Poisson process. This Poisson process may be homogeneous, in which case a Poisson regression model would be appropriate, or heterogeneous, in which case the NB2 specification would be a more appropriate choice to develop the corresponding GLM (assuming a Gamma distribution as the mix-function for the Poisson parameter).

It is important to mention that since over-dispersion issues were not present in the data, both the Poisson and NB model specifications could be used interchangeably in this case. The magnitudes and p-values are essentially the same for the resulting parameterization. The authors selected the Poisson model for this analysis, in spite of the availability of a dual but comparably well fitted NB model, for the following reasons: (1) the principle of parsimony, and (2) the straightforward implications that derive from the simpler structure and well known statistical properties of the Poisson Model. These properties enabled testing the model goodness of fit beyond the statistical software output, by performing a Convoluted Poisson Distribution test. The authors performed an extended assessment of the selected model to dispel any doubts regarding the adequacy of the Poisson GLM. This assessment is presented following the model results and interpretation. Beyond the preferred statistical distribution, the authors deem one contribution of this paper lies upon the parameterization of the mean itself, as the interpretation of selected Poisson specifications are equivalent to the more general NB model for this particular case.

The authors performed the statistical procedures summarized in this paper with a regression package and the statistical computing language R (Fox & Weisberg, 2011), (R Development Core Team, 2011).

2.4.3. **Model Results**

The resulting safety effects model is depicted in Table 2-1. The functional form of the expected number of crashes is provided by Equation 2-1.

Table 2-1: Selected Poisson Regression Model for Crash Data

Term	Estimate	Standard Error	z-value	p-value	Significance[1]
(Intercept)	-1.862	2.259	-0.824	0.410	
LnAADT	0.931	0.108	8.635	< 2e-16	***
LnCurveLength	-0.956	0.246	-3.886	1.02E-04	***
LaneWidth	-0.282	0.129	-2.182	0.029	*
Radius	0.001	0.000	1.868	0.062	º
Angle	0.892	0.686	1.299	0.194	
Radius:Angle	0.002	0.001	2.791	0.005	**
Radius:Adv.SpdPresent	-0.004	0.001	-4.439	9.03E-06	***
Adv.SpdPresent:Angle	-1.211	0.538	-2.250	0.024	*
Adv.SpdPresent	4.026	0.724	5.563	2.65E-08	***
ASD	0.024	0.023	1.048	0.295	
SFD	5.799	2.275	2.549	0.011	*
ASD:SFD	-0.553	0.151	-3.668	2.44E-04	***

[1]*Significance values are as follows:*
º p<0.1; * p < 0.05; ** p < 0.01; and *** p < 0.001

Equation 2-1: Functional Form of Selected Model

$$
\begin{aligned}
\#Crashes = exp[&-1.862 + 0.931Ln(AADT) - 0.931Ln(CurveLength) - 0.282(LaneWidth)\\
&+ 0.892(Angle) + 0.001(Radius) + 0.002(Angle \times Radius)\\
&- 0.004(AdvSpdPresent \times Radius) - 1.211(AdvSpdPresent \times Angle)\\
&+ 4.026(AdvSpdPresent) + \{5.799(SFD) + 0.024(ASD) - 0.553(ASD \times SFD)\}]
\end{aligned}
$$

Where:

AADT	=	Annual Average Daily Traffic (vpd);
CurveLength	=	Length of the Curve (ft);
LaneWidth	=	Width of travel lane (ft);
Radius	=	Horizontal Radius (ft);
Angle	=	Horizontal Curve Central Angle (Radians);
SFD	=	Side Friction Demand at Advisory Speed (no units);
ASD	=	Advisory Speed Differential, defined as speed limit minus posted advisory speed (mph); and
AdvSpdPresent	=	Indicator variable equals to one when advisory speed signs are present, otherwise the value is zero.

The authors assessed the option of removing the Angle and ASD constituent terms from the model since they appear statistically insignificant as shown in

Table 2-1; however, each variable is associated with significant interactions and so their effects cannot be considered independent of these associated interacting variables. As a result, the coefficients of the constituent terms should be interpreted in conjunction with these identified interactions. This model includes three variables associated with advisory speeds: ASD (the difference between the speed limit and the posted advisory speed), SFD (the Side Friction Demand that a vehicle would experience if it navigates the curve at the advisory speed), and *AdvSpdPresent* (a binary variable indicating the presence of posted advisory speeds). Based on the statistic AIC used for model selection, these variables, although interrelated, improved the information quality of the model. The authors also tested and discarded other relevant variables based on the model selection algorithm that ultimately converged and stabilized to the model shown. The authors monitored this algorithm to avoid simultaneity of variables that could destabilize the convergence of the algorithm to attain maximum likelihood of estimates, or extreme increments in the Variance Inflation Factors (VIFs) as these are clear indicators of extreme multicollinearity. For instance, once the working model had significantly increased the AIC value by including the ASD variable with an interaction term, the inclusion of variables for the advisory speed and the speed limit created convergence issues to the fitting algorithm. For these cases, the authors explored two separate branches of the step-wise model selection and chose the model with a better AIC value.

2.5. The Effect of Advisory Speed Signs

It is important to evaluate the influence of relevant geometric design and posting practice concepts as they relate to the rather complex vector of predictors generated as a result of the structure of the model. Due to the presence of interaction terms in the regression model, it is not possible to gather a simple "independent" effect for some of the variables in the model. Instead, the effect of a set of interacting variables is interpreted jointly as a composite multivariate entity affecting the number of crashes. Before presenting a formal multivariate assessment, however, the authors deem appropriate to present an interpretation of the model variables and their perceived influence on safety performance.

2.5.1. Model Interpretation

Figure 2-1 represents conceptually how relevant variables fall into the three influential categories of geometric design, signage, and operations. This diagram only includes the significant variables indicated as a result of the statistical analysis. As the figure shows, many of the variables do not perform independently and some overlap can be expected as a result. For instance, the SFD can be understood as both an operational and a geometric variable, since this variable is a function of speed, radius, and superelevation.

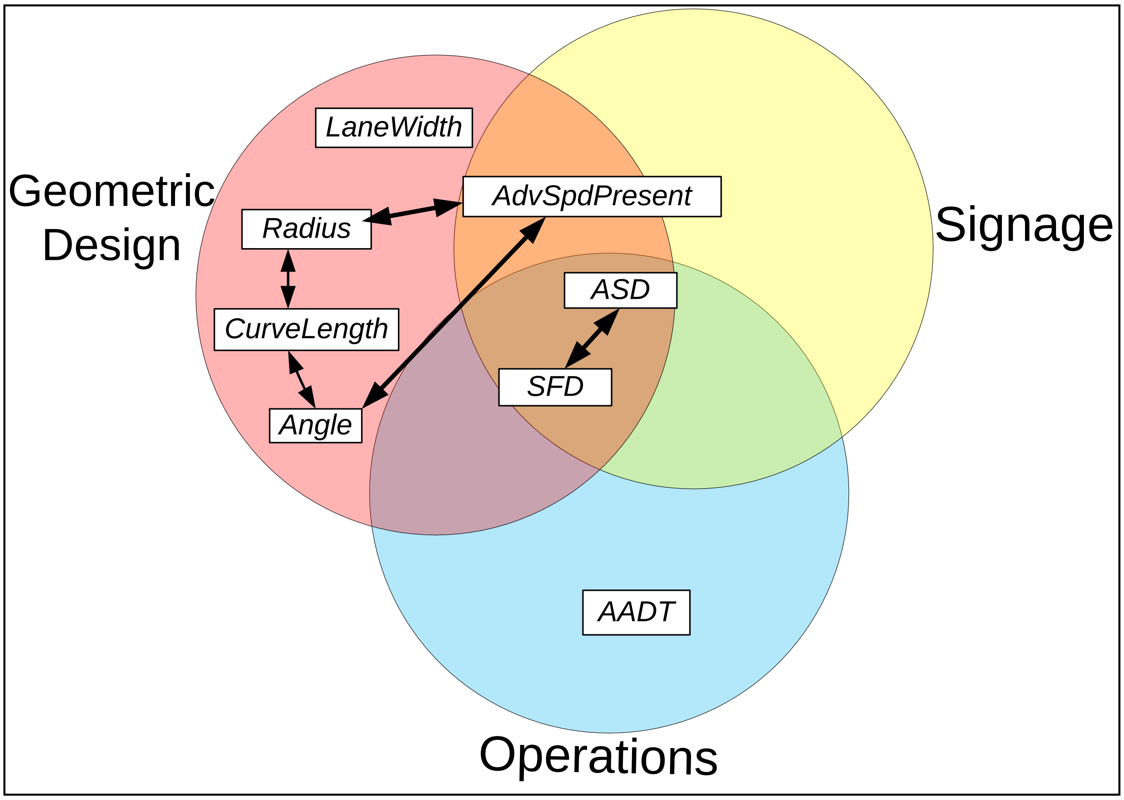

Figure 2-1: Model Variables Schematic

In addition to the variables shown in the diagram, the step-wise model selection procedure included additional interaction terms as indicated by the two-headed arrows in Figure 2-1. The researchers did not find these interactions surprising, given that the established geometric design methods and MUTCD posting procedures ensure the interrelation between the three depicted categories of variables.

It is important to note that an interaction term between two variables may be seen as the conditioning of the marginal effect of one variable to a particular value of the other. Additional information regarding the statistical interpretation of this type of model can be found in Brambor et al. (2006). Since a purely statistical interpretation may tend to disregard known engineering relationships, however, the authors felt that it would be helpful to further articulate an interpretation of the model interactions based on a transportation engineering perspective.

Based on the three categories of variables depicted in Figure 2-1, the authors hypothesize that safety performance emerges from the model in the following way: geometry and signage impact safety by changing road operations, which will result in higher or lower crash frequencies over an extended period of time. According to this premise, interactions in the model should translate into a shift in the short-term operations, ultimately impacting the long-term likelihood of crashes. As an example, the authors believe that the mere presence of the speed plaques (located at warranted curve locations) and the information the drivers may gather from the displayed values may trigger a change in behaviour, which would translate into a shift in operations. A mix of pre-existing road geometry factors, such as radius and cross-slope, in combination with the expected operations upstream (roughly captured by the speed limit) ultimately dictate the advisory speed plaque message which then can influence the likelihood of a crash.

Based on this interpretation, if a variable capturing an aspect related to advisory speeds was part of an interaction with another model variable, regardless of the direct link one may draw from the mathematical form, it may make more sense to think of the signage variable shifting the effect of the other, more influential variable. This is a relevant observation, since the model contains two such interactions: the presence of advisory speeds interacting with a geometric characteristic (Radius and Angle). A shift towards fewer crashes in the effects of these geometric variables is indicated by corresponding negative coefficients of the interaction terms. However, to quantify the total joint effect and draw meaningful conclusions, each advisory speed variable and the corresponding interactions should be explored in order to draw a holistic interpretation of the effect of advisory speeds in safety performance.

2.5.2. The Marginal Effects of Advisory Speed Model Variables

Although the presence of advisory speed plaques seems to affect the likelihood of crashes by shifting the effects of geometric variables, the two other advisory speed variables appear to directly contribute to the overall safety of the studied sites. These variables are the SFD and the ASD (previously defined in Equation 2-1). The SFD can be computed using Equation 2-2, an equation available from any highway design book.

Equation 2-2: Side Friction Demand

$$SFD = \frac{V^2}{15R} - 0.01e$$

Where:

SFD	=	Side Friction Demand;
V	=	Advisory Speed (mph);
R	=	Horizontal Radius (ft); and
e	=	Superelevation (%).

The SFD variable emerges from the known associations of the geometric and operations categories as depicted in Figure 2-1. Since this value is a function of vehicle dynamics as well as road geometrics, it plays an important role in establishing the appropriate advisory speed at curve locations. The authors hypothesize that the SFD variable implicitly captures the drivers' expected discomfort associated with negotiating the curve safely. Although the actual SFD would vary among drivers (e.g. varying vehicle capabilities, driving aggressiveness, etc.), research shows that ultimately drivers would tend to respond similarly to a higher degree of discomfort (Bonneson, Pratt, & Miles, 2009), (Chowdhury, Warren, Bissell, & Taori, 1998), (Avelar, 2010). On the other hand, drivers may judge the severity of an approaching curve based on how small the posted advisory speed is, or relative to the speed limit, how large they perceive the Advisory Speed Differential (defined as the speed limit minus the advisory speed value). This value would provide information supplemental to their individual visual assessment (based on perceiving the curvature and length of the curve as the driver approaches the curve). For this reason, the ASD spans the signage category as well as the operations and geometric categories in Figure 2-1.

As previously indicated, the resulting statistical model included an interaction between the SFD and ASD. A simple description of this effect may prove challenging; however, the authors speculate that the underlying relationship captured by this bivariate function is as follows: The long-term safety benefit of advisory speeds would emerge as drivers adjust their behaviour considering information these variables carry jointly (how much slower should they be taking the curve as suggested by the ASD, and how severe the associated discomfort can be expected as represented by the SFD variable).

From a mathematical stand point, this bivariate function may be seen marginally for each of the involved variables. This perspective implies, however, that both the marginal effect and the statistical significance of one variable will depend on the particular values of the other variable. The authors judge that a brief review of both marginal effects may prove helpful.

2.5.3. **Marginal Effect of ASD and SFD**

A simplified approach to understanding the effect derived from the interaction of the ASD and SFD is to look at the marginal effect of the involved variables. Figure 2-2 displays the marginal Effect of ASD.

Three items are worth noting regarding the marginal effect of the ASD: (1) all factors are smaller than one, which means that this effect is beneficial; (2) as the SFD increases the marginal effect improves; and (3) the model does not exhibit a statistical significance for the marginal effect at SFD values smaller than 0.14. Complementary, Figure 2-3 shows the marginal effect of Side Friction Demand at different levels of the ASD.

There are two features worth noting in the case of the marginal effect of the SFD. First, this marginal effect appears severely adverse for an ASD of 5 mph, and mildly adverse for ASDs of 10 mph. It is worth noting that these marginal effects are not statistically significant, given the data set available.

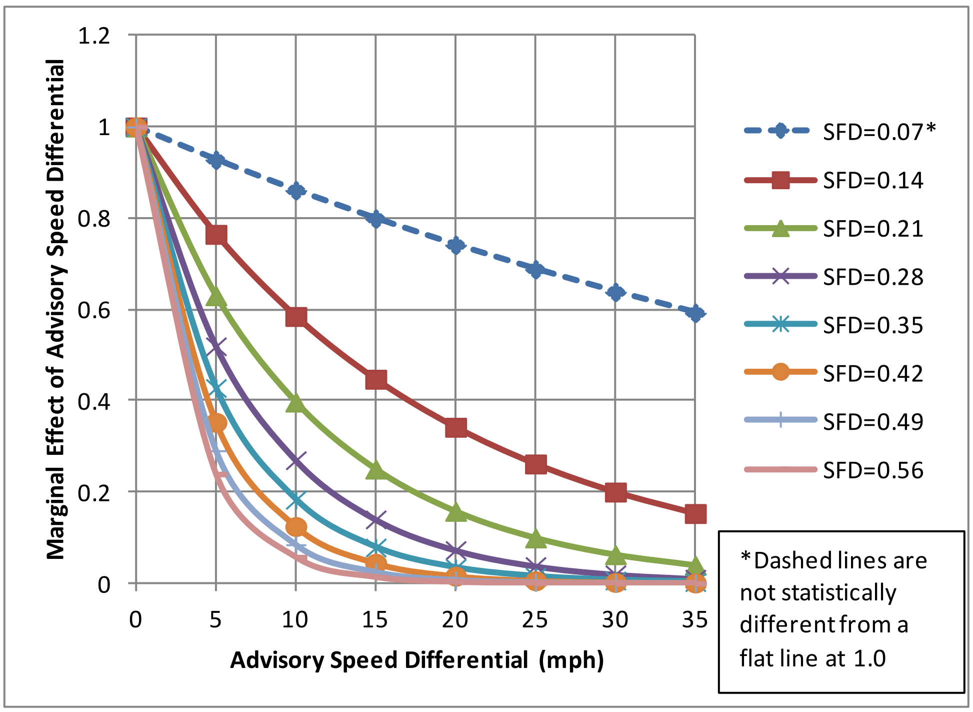

Figure 2-2: Marginal Effect of ASD at Different SFD Levels

An ASD value of 5 mph means that the advisory speed is 5 mph below the speed limit. However, this marginal effect should be interpreted in a different way. In Oregon the standard posting procedures do not require an advisory speed sign if the recommended advisory speed is only 5 mph below the speed limit. Since the drivers are not presented with an advisory speed plaque, it would be expected that the effect is null. This is suggested by the lack of statistical significance. Similarly, the marginal effect of SFD is not significant for ASD values of 10 and 15 mph. That is not surprising for the case of ASD=10mph, since this value falls very close to a flat line of 1.0. In general, the authors speculate that these two marginal effects may have actually proven to be statistically significant for a larger data set with more observations in these boundary regions.

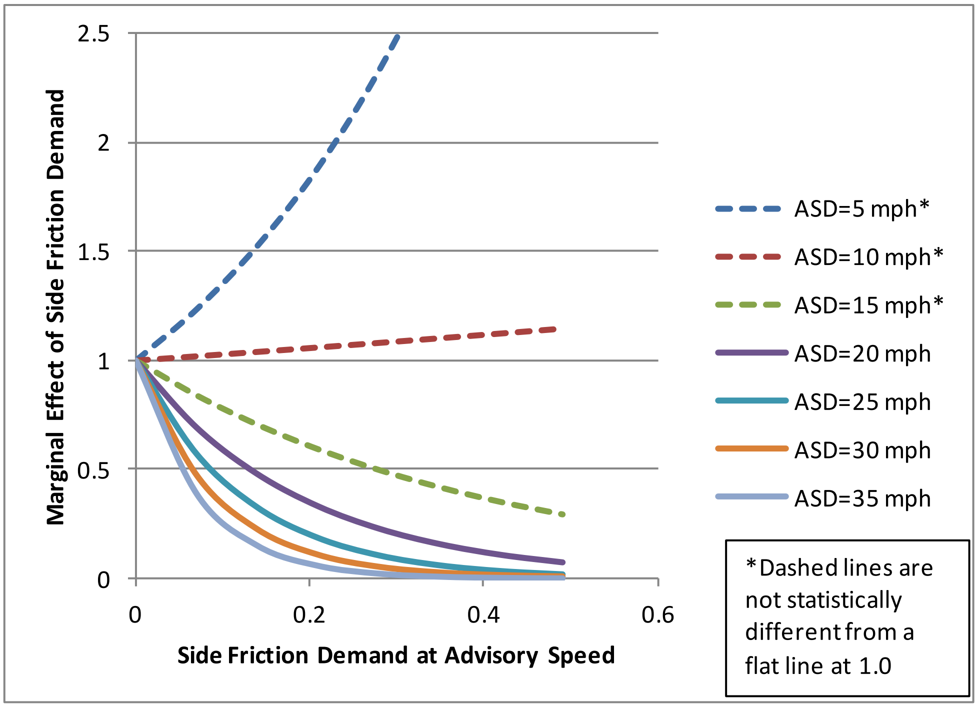

Figure 2-3: Marginal Effect of SFD at Different ASD Values

By examining the marginal effects for both the SFD and ASD, the authors emphasize the following points: (1) advisory speeds tend to be beneficial (both marginal effects are smaller than one when advisory speed signs are present); (2) advisory speed signs provide more safety benefits as their values tend to differ from the regulatory speed limit (larger SFD marginal effect for larger ASDs); and (3) advisory speed signs are more beneficial when greater driver discomfort results from driving at the suggested speeds (larger ASD marginal effect for larger SFDs).

The use of marginal effect trends, as those shown in Figure 2-2 and Figure 2-3, is most useful when the purpose is to isolate the effect of a single variable and its interaction with a less critical variable in the model. However, the authors recognize that a disjoint interpretation of the marginal effects in this particular case may appear contradictory from the traffic engineering stand point: to reap the safety benefit of posting advisory speeds, one needs to increase both the ASD and the SFD, but to increase the ASD one needs to post low advisory speeds, which in turn have small SFD associated. These marginal effects are closely intertwined, and their isolated view, as discussed here, is merely informative. Both the SFD and the ASD should be considered jointly. Thus, the authors recognize that the global effect of advisory speeds may be more informative by interpreting the complete bi-linear interpolant polynomial of ASD and SFD as a single entity.

2.5.4. **The Advisory Speed Crash Factor**

In a Poisson regression model, the effect of a non-interacting variable is a multiplicative factor to the average expectancy of the response variable. The corresponding multiplicative factor emerging from the unconditional bi-linear interpolant polynomial may be computed by disregarding the marginal effects and evaluating directly the ASD and SFD values in the polynomial. An additional benefit of this procedure is that the mathematical form is simple and clear enough to provide a direct interpretation in the scale of the response.

This section focuses on deriving and describing the corresponding multiplicative factor of the bi-linear interpolant polynomial of ASD and SFD. This newly developed multiplicative factor is denoted as the Advisory Speed Crash Factor (ASCF) from this point forward. Equation 2-3 depicts the mathematical form of the ASCF. Notice that this value is derived directly from Equation 2-1. As a result, the ASCF functions as a sub-model contained in the full Poisson regression model.

Equation 2-3: The Advisory Speed Crash Factor

$$ASCF = exp[5.799(SFD) - 0.5528(ASD \times SFD) + 0.0237(ASD)\,]$$

The authors explored the mathematical properties of the ASCF to determine if this sub-model is meaningful in describing the safety effect of advisory speeds. Because the ASCF is the ordinate of two explanatory variables, it can be represented as response surface or by a contour map. Figure 2-4 and Figure 2-5 are, respectively, the response surface and the contour map representations of the ASCF.

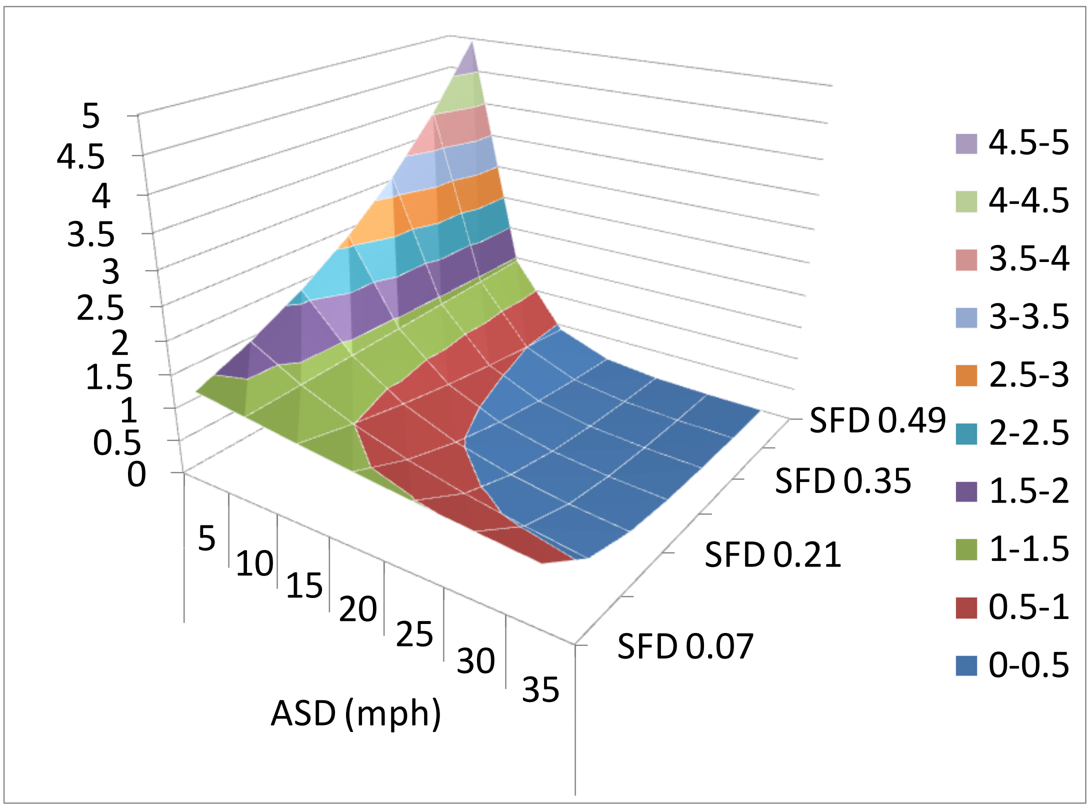

Figure 2-4: Response Surface Representation of the ASCF

The dotted line in Figure 2-5 corresponds to a multiplicative crash factor equal to 1.0. This is the level at which there is no effect on the expected number of crashes. The region to the left and below this dotted line corresponds to ASCF values larger than one, indicating more crashes.

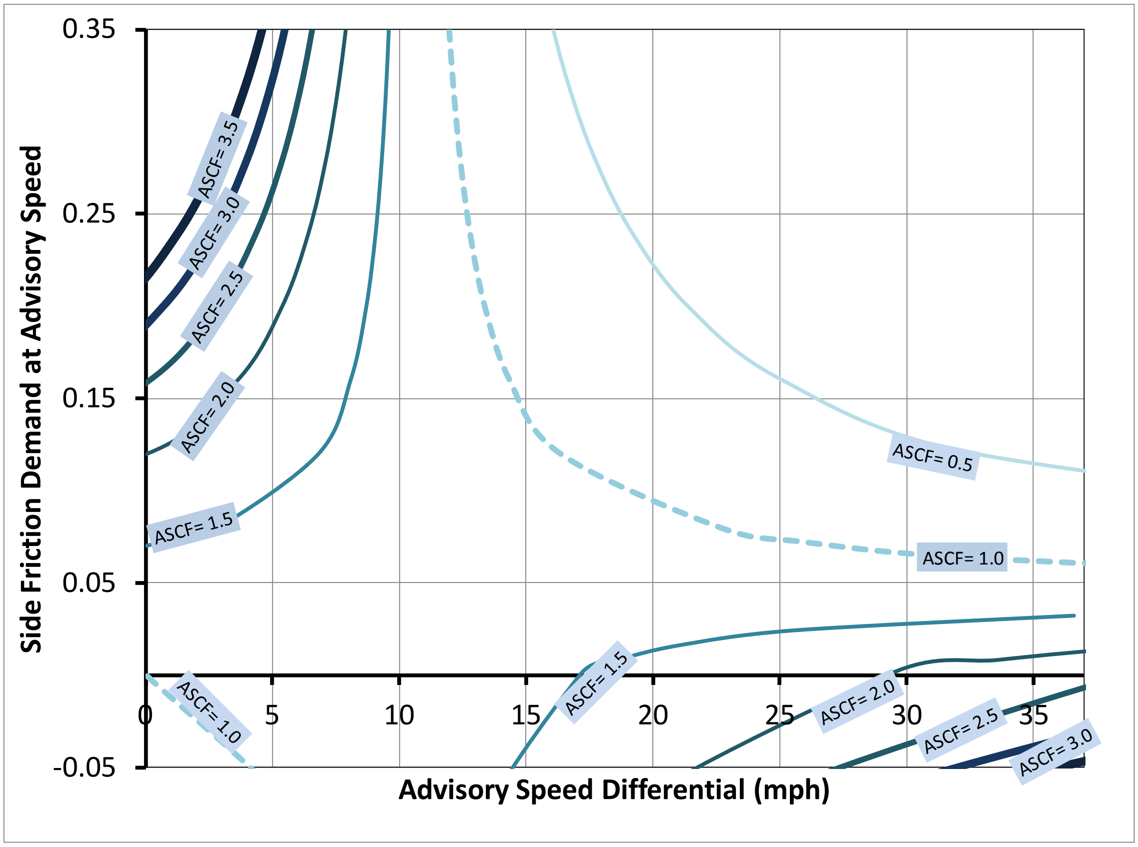

Figure 2-5: Contour Map Representation of the ASCF

Finally, the region to the right and above the dotted line corresponds to ASCF values less than one, suggesting fewer expected crashes. This mathematical representation of the ASCF corresponds with the marginal view of its two components, the ASD and the SFD.

2.5.5. **Effectiveness of Advisory Speeds in Oregon**

Given the complexities of the model structure, it is not simple to draw a generalized conclusion about the effectiveness of advisory speeds. According to the model, such effectiveness depends jointly on how much the advisory speed differs from the speed limit and on the degree of discomfort associated with navigating the curve at such an advisory speed. Furthermore, as of the steep areas in Figure 2-5, it appears that advisory speeds may have a detrimental effect if they are either too low for the associated SFD or too high in general.

In order to assess the effectiveness of current posting practices, the authors used the available probability sample of advisory speeds from the state of Oregon. This assessment consists of a theoretical exercise of “virtually removing” advisory speed signs and observing the expected safety effect, as predicted by the model. The actual effect for this hypothetical scenario would likely be very different: informational campaigns about the change would result in an immediate rise in familiar drivers’ awareness of the altered signage and would initially reduce the likelihood of crashes. Eventually, drivers would reach a new generalized perception of the driving environment, at which point the ASCF surface would be completely unrepresentative of the new operations and associated safety. However, the authors consider this exercise of some use, in order to extract the extent of the safety benefit of advisory speed plaques.

The computed measure of effectiveness is the ratio of ASCF before the hypothetical removal of advisory speed plaques to the ASCF after the removal. This quantity is referred to as absolute ASCF, or AASCF. Figure 2-6 shows a graphical display of AASCF versus ASD. This trend has an AASCF overall average of 0.728. This value suggests that advisory speed plaques may reduce crash frequency, on average, by 27.2% in the state of Oregon. It is reasonable to consider, however, that the AASCF values ranging from 0.951 to 1.05 correspond to sites with virtually no benefit associated with advisory speeds. Interestingly, 99 out of 210 sites exhibit AACSF values within this range. Additionally, there is 1 site in the sample for which the model predicts an adverse effect of advisory speeds (i.e. AASCF larger than 1.0).

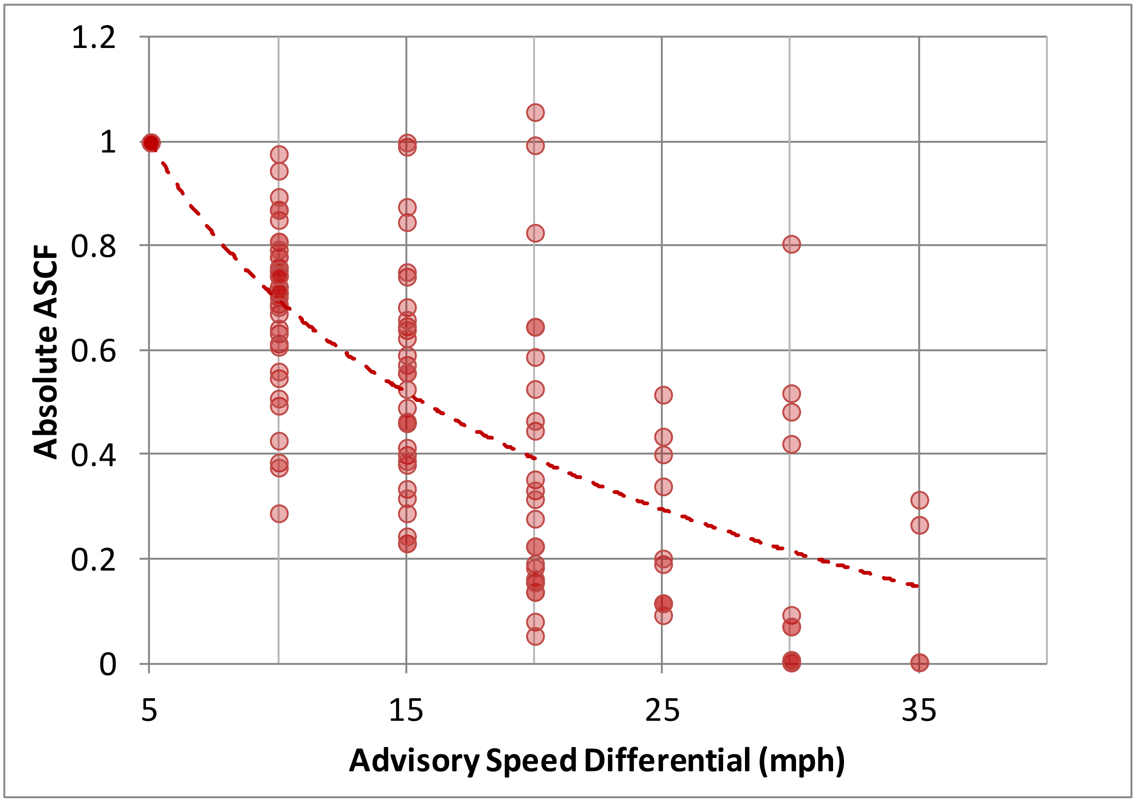

Figure 2-6: AASCF vs. Advisory Speed Differential

The authors recognized some important elements from this assessment: (1) 91 out of 99 sites with values of AASCFs close to 1.0 have an associated ASD of 5 mph. This ASD value corresponds to sites without advisory speeds signs; (2) the absolute effect on crashes appears beneficial for most of the remaining sites (i.e. AASCFs smaller than 1); (3) the AASCF diminishes systematically as the ASD increases, which in general indicates a good balance of ASD and SFD values underlying current posting practices in Oregon; (4) the range of AASCF values roughly remains the same as the ASD increases; and (5) despite the observed general benefits of advisory speed signs, there is one site in the sample with AASCF slightly larger than 1.0 (suggesting an advisory speed value that mislead rather than guide drivers). This preliminary evaluation suggests that cost-effective measures, such as changing the advisory speed displayed at such sites or even removing the plaque, have a potential to improve safety.

Table 2-2 demonstrates the impact of modifying advisory speeds at 5 of the sites with different advisory speed values.

Table 2-2: Effect of Modifying Advisory Speeds at Selected Sites

Site	**Speed Limit (mph)**	**Radius (ft)**	**Superelevation (%)**	**Current Advisory Speed (mph)**	**Current AASCF**	**Modified Advisory Speed (mph)**	**Modified AASCF**
1	55	1770	11	NA	1.000	NA	1.000
2	55	900	11	NA	1.000	45	0.906
3	55	575	14.5	45	0.743	40	0.738
4	55	700	12.5	35	1.058	45	0.814
5	55	520	11	35	0.588	40	0.528
6	55	300	14	25	0.519	35	0.202

Except for site 3, it is expected that all of the sites already displaying advisory speed plaques would benefit by increasing their posted advisory speed (sites 4, 5 and 6). Incidentally, these three sites display 25 and 35 mph advisory speeds. This observation is not surprising, given that previous research indicates that the posting policy in Oregon is among the most conservative in the United States (Dixon & Avelar, 2011). An extreme case is site 4, which would require an increment of 10 mph. This site is also abnormal in that it has the only AASCF larger than one in the whole sample. Site 3, though, would benefit from lowering its advisory speed, which suggests that the plaque may be too permissive. Finally, while site 1 would still not require an advisory speed plaque, site 2 would improve its safety performance by displaying a new one. Conditions at all sites except site 1 are such that an AASCF value smaller than 1.0 is achievable. According to this research, therefore, current advisory speeds in Oregon may not be exploiting all of their potential safety benefit. Though this simplistic example demonstrates how the AASCF can be used as an indicator of expected safety performance, it is clear that the use of this AASCF method (similar to the common crash modification factor) can help engineers assess the potential for safety improvements as one consideration in advisory speed selection.

2.6. Evaluation of Model Adequacy

Prior to developing concluding comments, this section addresses concerns that may arise regarding the adequacy of the selected model. Specifically, this section explores the following three associated issues: structural correlation in the response data, multicollinearity for both potentially correlated covariates and the statistical structure of interactive models, and general goodness of fit to the data.

2.6.1. Assessing the Structural Correlation in the Response Variable

For the rural 2-lane 2-way study corridors used for this analysis, every "curve site" in the study comprises two directions of travel, and each pair contains relevant common factors (e.g. driving population, traffic volume, and horizontal radius). As a result, the authors expect a high correlation between the numbers of crashes from each pair of directions of travel. It would be problematic to use both directions of travel in fitting the regression if such a correlation is substantial and beyond the explanatory power of the statistical model. Doing so would be equivalent to artificially duplicating the number of data points; however, assessing both directions of travel as one site is also problematic since issues such as direction of curve and relative cross slope would differ (be exactly opposite for most locations).

It is reasonable to expect that many similarities exist for the pairs of directions of travel and that these characteristics are, to some extent, explicitly accounted for by the corresponding regression variables. The horizontal radius, AADT and curve length, for instance, are the same for the two directions of travel at each location. Rather than simply eliminating 50% of the candidate sites and given this potential correlation, the authors then assessed how the correlation in the paired data compared to the predicted (based on regression) correlation from pairs of independent Poisson variables stemming from the fitted univariate model.

The authors paired the data by site and computed the correlation for the total sample of 105 pairs of crash counts and found a correlation value of 0.698. The authors compared the correlation in the sample to the distribution of correlations that arise from repeated realizations of the theoretically independent Poisson distributions.

The authors developed a synthetic sample of the paired-sites correlation distribution by using the technique of static simulation of paired but independent Poisson distributions, so that the observed distribution of correlations emerges only from the pairing of similar independent, univariate realizations such as from the regression model. The synthetic sample consisted of 200 replications of the overall correlation.

Simulation results suggest that a normal curve could approximate this distribution (simulated data have very small 3rd and 4th moments; a -0.10 skewness indicating rough symmetry and a normalized kurtosis of -0.623 indicating a peakness that is close to the normal distribution). The authors used the mean and the standard deviation of the simulated data to assess the statistical significance of the correlation from the crash data. The actual correlation of 0.698 compares very closely to the mean simulated correlation (0.581). Using the simulated standard deviation (0.088), a 0.184 two-sided p-value may be obtained from the standard normal distribution. Comparably, an empirical one-sided p-value of 0.09 may be computed from the raw synthetic sample as the proportion of simulated correlations that resulted in values larger than 0.698, the sample statistic.

From the results, the authors conclude that the correlation observed between the pairs of directions of travel in the sample is not atypical, and that it is reasonable to expect such a degree of correlation from pairs of truly independent Poisson variables with similar parameters such as those associated with the regression model.

2.6.2. **Discussion on Multicollinearity among Regressors**

It is worthwhile to notice that a certain degree of multicollinearity was unavoidable in the model, despite the variable selection procedure that included strategies to minimize multicollinearity. One such strategy, for instance, was to avoid including two highly correlated variables simultaneously as predictors. However, the authors included interaction terms to contribute to improving the quality of information in the model (i.e. significant drops in AIC), but also included these terms because the joint interpretation with their constituent terms explain reasonably expected transportation engineering safety behaviour. The mathematical structure of the ASCF, the main sub-model developed in this paper, similarly rests upon a bi-linear interpolant polynomial emerging from two interacting variables. The only drawback of choosing an interacting model, as of this paper, is the requirement of slightly more complex procedures for joint interpretation of the co-dependent terms.

It is recognized that the degree of multicollinearity increases when the covariates are no longer independent. If the severity and the effects of multicollinearity among predictors are properly treated in the modelling process (mainly monitoring VIFs and algorithm convergence issues) and with adequate interpretation of the results, the authors advocate for the use of interactive models, especially because of their ability to represent complex interrelationships. Furthermore, the explicit account of multicollinear predictors may become attractive because of the need to account for factors that are not entirely independent. Such interdependency may transcend into explaining the response variable, and if that is so, interactions between variables are a useful tool to explicitly model such joint effects. However, a model structure that includes interactions implies a potential source of multicollinearity due to the model structure itself in addition to that resulting from the use of co-dependent covariates.

Multicollinearity manifests itself as an inflation of the standard errors from the regression. This circumstance, in turn, results in convergence issues in the fitting algorithm. The authors observed convergence issues in the early and intermediate stages of the step-wise procedure, for both the NB and Poisson models. Some judicious decisions were necessary in order to manually exclude some of the correlated variables as a requirement of the step-wise procedure. One such decision was to exclude advisory speed related variables in favor of keeping horizontal geometry covariates in the early models. Later the model selection procedure allowed advisory speed and synthesized variables, such as the ASD and SFD. Ultimately, some of these variables were included in the model because of their significant contribution to the quality of the information in the model (i.e. significant drops in AIC).

After the adjustments described in this section, the fitting algorithm did not indicate convergence issues, nor did the VIFs exhibit extreme values. Additionally, almost all of the coefficients in the model present small enough standard errors to indicate statistically significant results. Only two terms are not statistically significant, but each of them is of prime importance to derive statistically significant marginal or joint effects, as shown in previous sections of this paper. After this assessment, the authors believe that no serious multicollinearity issues required further attention.

2.6.3. **Goodness of Fit**

It is important that a representative statistical model have an overall good fit to the data. To establish the appropriateness of the Poisson model in describing the data, the authors tested the goodness-of-fit at three different conceptual levels: residual deviance, dispersion, and Poisson distribution suitability.

2.6.4. **Approximate Chi-Squared Test on Model Residual Deviance**

The authors used an approximate chi-squared test to assess the residual deviance. This quantity, obtained from the Maximum Likelihood Estimation (MLE) algorithm, is expected to converge in distribution to the chi-squared function as the sample size increases (i.e. by virtue of the Central Limit Theorem). This test resulted in a p-value of 0.6413 from a 184.35 chi-squared statistic (i.e. the residual deviance) for 197 degrees of freedom suggesting a lack of evidence against the appropriateness of the model fit to the data.

2.6.5. **Approximate Dispersion Parameter**

A good fit to the Poisson distribution can be evaluated when the ratio of the variance to the mean of the response variable is approximately equal to one. This expected mean-variance relationship can be estimated using the ratio of the residual deviance to its degrees of freedom from the regression algorithm. This ratio is referred to as the dispersion parameter in some literature. In this case, a value of 0.961 indicates that there is no significant over-dispersion present in the data. Since the expected value of a chi-squared distribution is its associated degrees of freedom, a corresponding p-value for this statistic assumes a null hypothesis that the expected ratio parameter was 1.0. This value corresponds to the p-value of the residual deviance statistic of 0.6413 as previously shown. This result also suggests that if a NB regression were used instead, the magnitude and statistical significance of the coefficients would have been virtually the same.

2.6.6. **Convoluted Poisson Distribution Test on Total Number of Crashes**

The discrete convolution theorem applied to Poisson distributions (Samaniego, 1976) states that the distribution of a sum of independent Poisson variables is also a

Poisson variable with a scale parameter equal to the sum of the scale parameters for each data point. This evaluation is depicted by Equation 2-4.

Equation 2-4: Convoluted Poisson Probability Function

$$P\left(\sum Y_i = z\right) = e^{-(\sum l_i)} \times \frac{(\sum l_i)^z}{z!}$$

Where:

Y_i	=	Observed number of crashes at site i;
z	=	Arbitrary value from the domain of Y; and
l_i	=	Predicted number of crashes at site i per the regression model.

The test statistic is the total number of crashes and the associated p-value is obtained from the convoluted Poisson distribution. Since the statistic percentile is rather large (one tailed p-value of 0.4914 from a convoluted Poisson random variable statistic of 180 with an expectation of 180.67), the test clearly failed to reject the hypothesis that the sample is a realization of the convoluted distribution emerging from the model fitted values.

Given the results of these tests, the researchers are confident that the Poisson model is appropriate to describe the available crash data. Since the Poisson is a particular case of the NB2 distribution, these tests also mean that an NB2 model with dispersion parameter approximately equal to 1.0 also describes the data satisfactorily.

2.7. **Conclusions and Recommendations**

The authors of this paper developed a mathematical model to describe the safety impact of advisory speed signs. The purpose of this paper is to quantifiably link the displayed value of advisory speeds to the safety performance of the sites.

The basis of this mathematical model is a statistical analysis involving 210 randomly selected directional sites located in the state of Oregon. The functional form of the model included a bi-linear interpolant polynomial of two quantities linked to advisory speeds: the advisory speed differential (ASD) and the side friction demand (SFD). This effect was named the advisory speed crash factor (ASCF). Because the Poisson regression model did not suffer from overdispersion when fitting the data, either the Poisson or the NB2 specifications can be used interchangeably when accounting for the ASCF. This is convenient, as the NB2 specification is the naturally assumed posterior distribution (i.e. Safety Performance Function) for widely accepted Empirical Bayes and Full Bayes analyses for before-after studies.

The ASCF consists of a multiplicative value that directly affects the expected number of crashes for a curve rural 2-lane road location. The concept of the ASCF is analogous to the crash modification factor (CMF). Currently, the most closely associated reference work (Elvik & Vaa, 2004) proposed the use of a CMF that suggests a single value that ranges from 0.71 to 0.87 depending on crash severity. The ASCF resulting from the work outline in this paper, however, is more suitably referred to as a crash modification function as it varies based on the specific advisory speed value and site conditions.

This paper introduced a new element referred to as the absolute ASCF (AASCF) that helps to assess the notional impact of advisory speed signs as opposed to a theoretical scenario where the plaques are not displayed. The values proposed by Elvik and Vaa (2004) are aligned with the derived AASCF average value of 0.728 which functions as a measure of the overall effectiveness of advisory speeds in Oregon.

Although most of the sites included in this study appeared to benefit from the practice of posting advisory speeds, there was one instance in which the posted advisory speed seemed detrimental to safety. The ASCF further provides a computational tool to assess the safety effect of particular values of advisory speeds. Therefore, the authors expect that the concept developed in this paper is a useful function to evaluate safety performance.

Additionally, the authors recognize that the AASCF is a detailed functional form that results in a value comparable to the crash modification factor for advisory speeds similar to that recommended by Elvik and Vaa (2004). As such, the authors anticipate that the AASCF may be used as a crash modification function to improve the accuracy of current HSM procedures.

The authors believe that the ASCF may also be used as the criterion for an improved safety-based posting procedure. Recent work by Dixon and Avelar (2011) proposed such a procedure as a computational alternative to the currently wide-spread ball-bank indicator method. The authors recognize that such a method allows for further improvement, particularly with the potential combination of instrumentation based procedures, such as those developed by Pratt, Bonneson and Miles (2011). To enhance this method for transferable posting procedures, the authors recommend further research in order to field validate the concept of ASCF in Oregon and other states.

Finally, the authors also recommend future work to explore and strengthen the link of the ASCF to field operational data, since this type of data would closely contribute to the overall validation of the ASCF concept. Specifically future research should explore how the operating speed relates to the components of the ASCF bivariate function.

Acknowledgments

The authors would like to thank the members of the Oregon Department of Transportation (ODOT) Research Section and Technical Advisory Committee for their advice and assistance in oversight of this research effort. This project was jointly funded by ODOT and by the Oregon Transportation Research and Education Consortium (OTREC). The authors would like to thank these sponsors for funding this research project.

2.8. **References**

AASHTO. (2004). A Policy on Geometric Design of Highways and Streets (5th Edition). Washington, D.C.: AASHTO.

AASHTO. (2010). Highway Safety Manual. Washington, D.C.: AASHTO.

Avelar, R. E. (2010, August 16). Effectiveness of Curve Advisory Speed Signs. A Characterization of Road Operations in Western Oregon. Retrieved November 08, 2010, from Scholars Archive at OSU: http://hdl.handle.net/1957/17673

Bonneson, J. A., Pratt, M. P., & Miles, J. (2009). Evaluation of Alternative Procedures for Setting Curve Advisory Speed. Transportation Research Record 2122 , 9-16.

Brambor, T., Roberts Clark, W., & Golder, M. (2006). Understanding Interaction Models: Improving Empirical Analyses. Political Analysis , 63-82.

Chowdhury, M. A., Warren, D. L., Bissell, H., & Taori, S. (1998). Are the Criteria for Setting Advisory Speeds on Curves Still Relevant? ITE Journal. February , 32-45.

Courage, K. G., Bastin, H. E., Byington, S. R., Cook, A. R., Ferro, W. N., Freeman, R. L., et al. (1978). Review of Usage and Effectiveness of Advisory Speeds. ITE Journal. September, 43-46.

Dixon, K. K., & Avelar, R. E. (2011). SPR 685: Safety Evaluation of Curve Warning Speed Signs. Salem, OR: ODOT.

Dixon, K. K., & Rohani, J. W. (2008). SPR 641: Methodologies for Estimating Advisory Curve Speeds on Oregon Highways. Salem, OR: Oregon Department of Transportation.

Elvik, R., & Vaa, T. (2004). "Handbook of Road Safety Measures.". Oxford, U.K.: Elsevier.

FHWA. (2009). Manual on Uniform Traffic Control Devices. Washington, D.C.: U.S. Department of Transportation.

Fox, J., & Weisberg, S. (2011). An {R} Companion to Applied Regression, Second Edition. Thousand Oaks, CA: Sage. Retrieved from http://socserv.socsci.mcmaster.ca/jfox/Books/Companion

Iwasaki, M., & Tsubaki, H. (2006). Bivariate Negative Binomial Generalized Linear Models for Environmental Count Data. Journal of Applied Statistics , 909-923.

Lyles, R. W. (1982). Advisory and Regulatory Speed Signs for Curves: Effective or Overused? ITE Journal. August, 20-22.

Pratt, M. P., Bonneson, J. A., & Miles, J. D. (2011). Measuring the Non-Circular Portions of Horizontal Curves: An Automated Data Collection Method using GPS. TRB 90th Annual Meeting (pp. Paper No.: 11-2625). Washington, DC: Transportation Research Board.

Samaniego, F. J. (1976). A Characterization of Convoluted Poisson Distributions with Applications to Estimation. Journal of the American Statistical Association, 475-479.

The R Development Core Team. (2009). R: A Language and Environment for Statistical Computing. Retrieved from http://www.R-project.org

Wackerly, D. D., Mendenhall III, W., & Scheaffer, R. L. (2008). Mathematical Statistics with Applications. 7th Edition. Toronto, Canada: Thomson.

Winkelmann, R., & Zimmermann, K. (1991). A New Approach for Modeling Economic Count Data. Economics Letters 37 , 139-143.

3. How Far Are Current Advisory Speeds from being Optimal? An Analysis Based on Safety Performance

Raul E. Avelar and Karen K. Dixon

Transportation Research Record ISSN 0361-1981

Transportation Research Board

The National Academies

500 Fifth Street, NW

Washington, DC 20001

Paper presented at the 91st Annual Meeting, January 2012, Washington DC. Pending publication in the Journal Transportation Research Record.

How Far Are Current Advisory Speeds from being Optimal? An Analysis Based on Safety Performance

Raul E. Avelar[1*]
Karen K. Dixon[2]

*Corresponding Author
1) Raul E. Avelar, MSc, Doctoral Candidate
Graduate Research Assistant, School of Civil and Construction Engineering
Oregon State University
Owen Hall 220,
Corvallis, OR, 97331
Phone: 541- 602- 9115
Fax: 541- 737-3052
e-mail: avelarr@engr.orst.edu

2) Karen K. Dixon, PhD, P.E.
Associate Professor, School of Civil and Construction Engineering
Oregon State University
Owen Hall 220,
Corvallis, OR, 97331
Phone: 541-737-6337
Fax: 541-737-3052
e-mail: karen.dixon@oregonstate.edu

Word Count: 6491 words + (250 x 4 Tables and Figures) =7491 total
Originally submitted on: August 1, 2011
Presented at TRB 2012 Annual Meeting
Re-submitted for publication on: March 15, 2012

ABSTRACT

Posting advisory speed signs at sharp horizontal curves to provide the driving public with a safe speed is a practice well established in the United States. The operational effectiveness of these signs has long been questioned in the current literature. The authors of this paper recently developed a function to model the expected safety effect of these signs. The function stems from a statistical analysis on crash data from 2-lane rural highways in the state of Oregon.

In general, that research effort found that advisory speed signs tend to enhance safety. However, the authors also determined that advisory speed signs may not be displaying the value with the greatest potential safety benefit. Since the derived function proved meaningful from the engineering and human factors perspectives, these authors then extend the use this function to compute and recommend the theoretically “optimal” advisory speed. A new posting procedure resulted from this effort. The authors compared the expected performance of advisory speeds from the proposed procedure to the speeds derived from current posting guidelines. A comparable performance suggests that current guidelines are close to the hypothetically “optimal” advisory speed. In general, both the current and new computational methods performed better than speeds determined by the ball bank indicator method.

This paper also presents a field validation analysis of the engine function of the new posting method. The results confirmed the meaningfulness of the function, and therefore, of the potential benefit for determining safety-based advisory speeds with the method proposed in this paper.

Keywords: advisory speed, safety, Side Friction Demand, optimal advisory speed, ASCF

3.1. **Introduction**

The authors of this paper have recently proposed a new crash modification function (CMF) to account for advisory speeds in their recently completed effort for the Oregon Department of Transportation (ODOT) (Dixon & Avelar, 2011). The authors coined this CMF the “Advisory Speed Crash Factor” or ASCF. The ASCF models how the displayed advisory speed relative to the speed limit and the associated side friction demand jointly associate with the likelihood of crashes. A recent paper by these authors (Avelar & Dixon, 2011) discusses a plausible human factors interpretation of the ASCF and establishes some of its basic mathematical properties. Because the main objective of the current paper is to use the proposed ASCF concept to develop a new posting procedure, it is necessary to provide a brief overview of that paper as presented in the section following the literature review.

This paper also further defines the mathematical properties of the ASCF. The authors only highlighted key issues as they pertain to the derivation of a basic equation for an “optimal” advisory speed.

The main section of this paper focuses on the proposed procedure (named the OSU method) and compares the resulting advisory speeds to advisory speeds from currently established procedures.

This paper includes a section on the robustness and field validation of the ASCF function. The material in this section is presented as a review of the relationship between the ASCF function and its meaningfulness for the proposed engineering application.

The authors performed all statistical procedures summarized in this paper using an open source statistical package (The R Development Core Team, 2009), (Venables & Ripley, 2002), and (Fox & Weisberg, 2011) but similar analyses can be performed with comparable software.

3.2. Background

The practice of posting advisory speed signs is well established in the United States. The procedures to determine advisory speeds have been evolving since the 1930s, and the practice has been standardized since 1948. The *Manual on Uniform Traffic Control Devices* (MUTCD) states that advisory speeds shall be determined by an "engineering study that follows established engineering practices" (*4* Section 2C.08). The document mentions three commonly accepted such practices: the use of a ball bank indicator (the most widely implemented), geometric design equation, and the use of an accelerometer. The thresholds for the ball bank method have been continually updated through subsequent editions of the MUTCD (FHWA, 2009).

There is a wide variety of advisory speed-posting thresholds currently in use in the United States. ODOT has recently adopted the thresholds suggested by the latest edition of the MUTCD. Previously, Oregon used more conservative thresholds (Dixon & Avelar, 2011).

3.3. Literature Review

A recent research effort (Bonneson, Pratt, & Miles, 2009) performed at the Texas Transportation Institute (TTI) for the Texas Department of Transportation observed that there were considerable inconsistencies for advisory speed posting procedures. This shortcoming appeared linked to the ball-bank and accelerometer approaches. Ultimately the TTI team recommended the use of the design speed equation approach, which yields more consistent values. The TTI team modified the approach to also incorporate a speed variable.

A recent study by Dixon and Rohani (2008) suggests other sources of variation, since they found that a large proportion of curve sites in the state of Oregon do not comply with the state policy. Various authors argue that such lack of consistency results in poor adherence to advisory speeds (Bonneson, Pratt, & Miles, 2009), (Courage, et al., 1978), (Lyles & Taylor, 2006),(Chowdhury, Warren, Bissell, & Taori, 1998), (Lyles, 1982).

In an operational evaluation, Chowdhury et al. (1998) argued that posting criteria are not adequate, since modern vehicles can generate side friction values from 0.65 to 0.90 before skidding out. Such vehicle performance amply exceeds the side friction demands associated with the ball bank indicator thresholds. Along those lines, Lyles and William in their report “Communicating Changes in Horizontal Alignment” (2006) argue that advisory speed signs are largely ineffective if the goal of the signs is that drivers adhere to the posted speed. They report that practitioners and the driving population perceive advisory speeds to be too low. This was also operationally verified by Avelar (2010).

In the area of currently accepted safety modelling (AASHTO, 2010), Elvik and Vaa (2004) suggest a flat CMF for advisory speeds ranging from 0.71 to 0.87, depending on crash severity.

This literature review found only one paper by Ritchie (1972) suggesting that advisory speeds may, contrary to expectation, incite drivers to higher speeds. The author speculates that overconfidence may result from availability of information about the “sharpness” of curves immediately downstream, as the plaques convey.

3.4. The Safety Effect of Advisory Speed Signs

Recent work by Oregon State University (OSU) researchers found a link between advisory speed signs and their hypothetical long term safety benefit (Avelar & Dixon, 2011). The findings of the Oregon research effort do not necessarily contest current literature, which has repeatedly documented poor adherence. On the contrary, the authors of this paper deem a safety improvement possible, despite poor operational compliance, if these signs are successful in conveying meaningful information about the severity of downstream horizontal alignments. Drivers may then adjust their driving thus reducing their chances to be in a crash.

The authors proposed the ASCF function to model the safety impact of advisory speed signs. The function is directly derived from a statistical analysis performed on a probability sample of 210 directional horizontal curve sites representative of rural two-lane two-way state highways in Oregon. The data included geometric and signage features collected from field visits for a previous work by Dixon and Rohani (2008), as well as the crash record for the years 2000 through 2004 at the study sites. The authors proposed a full statistical model for non-intersection crashes, that is, excluding turn, rear and angle crash types. The data set included curves with radii ranging from 100 to 2150 ft, and deflection angles ranging from 1.5º to 200º. The next sub-sections sumarize the highlights of that work and further advances regarding the ASCF function.

3.4.1. **Model Selection**

Since crash data is random by nature, modelling techniques must be appropriately based on their stochastic variability. The authors applied a step-wise selection procedure based on the Akaike Information Criterion (AIC) to select a statistical model considering both the Poisson and Negative Binomial (NB) specifications for fitting a Generalized Linear Model (GLM). If the variance to mean ratio in the model is close to one, then two model specifications are adequate: the classical Negative Binomial (NB2) and the simpler Poisson. A ratio larger than one indicates Poisson-overdispersion and in that case only the NB2 specification is appropriate. Since a goodness-of-fit evaluation from the regression output indicated no evidence of Poisson-overdispersion, both candidate specifications are equally adequate to describe the data. After some consideration, the authors endorsed the Poisson specification for its simplicity and because it allowed an alternative goodness-of-fit assessment. Equation 3-1 shows the resulting full model.

Equation 3-1: Full Model

$$E(\#Crashes) = 0.1554 \times AADT^{0.931} \times CurveLength^{-0.956} \times \exp[-0.282(LaneWidth) + 0.892(Angle) + 0.001(Radius) + 0.002(Angle \times Radius) - 0.004(AdvSpdPresent \times Radius) - 1.211(AdvSpdPresent \times Angle) + 4.026(AdvSpdPresent) + \{5.799(SFD) + 0.024(ASD) - 0.553(ASD \times SFD)\}]$$

Where:

#Crashes	=	Total non-intersection crash frequency (no units);
AADT	=	Annual Average Daily Traffic (vpd);
CurveLength	=	Length of the Curve (ft);
LaneWidth	=	Width of travel lane (ft)
Radius	=	Horizontal Radius (ft);
Angle	=	Horizontal Curve Central Angle (Radians)
SFD	=	Side Friction Demand at Advisory Speed (no units);
ASD	=	Advisory Speed Differential, defined as speed limit minus posted advisory speed (mph); and
AdvSpdPresent	=	Indicator variable equals to one when advisory speed signs are present, otherwise the value is zero.

All variable coefficients Equation 3-1 satisfied at least a 0.95 level of confidence, except Radius, Angle and ASD. The authors retained these coefficients because the model includes statistically significant interactions for their variables (confidence levels of 0.995 or better). Based on the magnitudes of Variance Inflation Factors (VIFs), the authors determined that the standard errors in the final model were stable. The result is said to balance a minimum level of multicollinearity with the meaningfulness of the predictors from the engineering standpoint. Further details on the scope of application and statistical modeling can be found in references (Dixon & Avelar, 2011) (Avelar & Dixon, 2011) and (Dixon & Rohani, 2008).

3.4.2. **Interpretation of the Full Model**

Although the proposed model specification is relatively simple, there is some complexity in the model interpretation emerging from the use of interaction terms among the covariates. However, the inclusion of interaction terms was crucial to reducing the model entropy (per the AIC statistic), increasing the goodness of fit, and ultimately, to developing the ASCF function.

Some predictors are inevitably interrelated in this case, even without modelling interactions. For instance, the horizontal radius and the deflection angle determine the curve length, and thus these three variables are correlated. It is no simple task to isolate the effect for any of these variables from the full model because it includes them simultaneously. However, characterizing such behaviour is not the focus of this research. The authors interpret the inherent complexity in the model as a necessary mathematical way around the very probable case of non-linear underlying structures. Linear models are useful and powerful tools as far as they reasonably fit real world data. The actual relationship between crash occurrence and the relevant covariates, however, is likely not the convenient linear combination of relatively independent terms. Covariates that are expected to have more direct effects on crash occurrence shall be accounted for, but their simple interpretation becomes more challenging, as noted above. Further details on marginal effects for a model with interactions may be found in a previous work by these (Avelar & Dixon, 2011) and in Brambor et al. (2006).

3.4.3. **The Advisory Speed Crash Factor**

Equation 3-2 represents the functional form of the ASCF. Basically, the ASCF is a multiplicative factor applied to the “baseline” number of crashes, which is determined by the rest of variables in the statistical model. This is the reason why the ASCF is referred to as a sub-model throughout this paper.

Equation 3-2: Functional Form of the ASCF

$$ASCF = exp[5.799(SFD) - 0.553(ASD \times SFD) + 0.024(ASD)]$$

The concept of the ASCF is analogous to what existing literature refers to as a crash modification function (CMF). Two variables are involved in the ASCF functional form: the Advisory Speed Differential, or ASD (defined as the speed limit minus the advisory speed) and the Side Friction Demand associated with the advisory speed, or SFD (AASHTO, 2004). In the case of sites not displaying advisory speeds, both the ASD and the SFD were computed using an advisory speed of 5 mph below the speed limit.

The ASCF proved a useful tool to estimate the safety benefit of the advisory speed signs in Oregon. These signs may be responsible for an average of 27% crash reduction at curve sites (Avelar & Dixon, 2011). The Oregon study indicates that advisory speeds are, in general, safety enhancing elements at horizontal curve sites. Such results confirm the safety benefit associated with the signs, as long time assumed by the transportation community. To a certain extent, the results also abide current posting practices, despite of well documented consistency issues in the case of the ball bank indicator (Bonneson, Pratt, & Miles, 2009), (Lyles, 1982).

A closer examination of the mathematical properties of the ASCF function suggests an opportunity to develop a new computational posting procedure based on safety performance. The next section briefly explores such properties and their potential use for a posting procedure.

3.5. **Mathematical Properties of the ASCF**

The two variables that constitute the ASCF function are not mathematically independent. Both variables include the advisory speed in their formulation, though the ASD also includes the speed limit, while the SFD incorporates the radius and superelevation. For posting purposes, the authors considered the speed limit, radius, and superelevation as fixed parameters.

After applying a natural logarithm transformation, the ASCF can be expressed as a third degree polynomial representation of the advisory speed, as shown in Equation

3-3. This equation results from re-expressing Equation 3-2 as a polynomial of *Adv.Speed* when expressing ASD and SFD in terms of Speed limit, Advisory Speeds, radius and superelevation.

Equation 3-3: Advisory Speed Univariate Parameterization of ln(ASCF)

$$ln(ASCF)_{(Adv.Speed)} =$$

$$(\beta_1 \times SpLim - \beta_2 \times SE - \beta_3 \times SE \times SpLim) + (-\beta_1 + SE \times \beta_3) \times (Adv.Speed) + \left(\frac{\beta_2 + SpLim \times \beta_3}{15 \times R}\right) \times (Adv.Speed)^2 - \left(\frac{\beta_3}{15 \times R}\right) \times (Adv.Speed)^3$$

Where:

β_1	=	ASD coefficient from the ASCF function ($\frac{1}{mph}$);
β_2	=	SFD coefficient from the ASCF function (no units);
β_3	=	ASD x SFD coefficient from the ASCF function ($\frac{1}{mph}$);
SpLim	=	Speed Limit (mph);
Adv.Speed	=	Advisory Speed (mph);
R	=	Radius (ft); and
SE	=	Superelevation (no units);

Equation 3-3 directly links the advisory speed to a factor associated on the expected number of crashes. Most important is the known mathematical relationships of polynomials of the second or higher order to their local maximum and minimum values. Such local extremes are referred to as “optimal” values in the operations research literature.

3.6. The Theoretically “Optimal” Advisory Speed

If two different potential advisory speed values are compared using Equation 3-3, the “safer” advisory speed would be the one associated with the smaller ASCF value. This observation leads to the following question: Is there an advisory speed such that the ASCF has a practical minimum value? From this point on, this particular advisory speed value is referred to as the optimal advisory speed.

A relatively simple application of univariate calculus imposes the convexity and extreme point conditions on Equation 3-3 if an optimal advisory speed actually exists. These conditions can be expressed as:

$$\frac{\mathbf{d^2}}{\mathbf{d(AdvSpeed)^2}} \boldsymbol{ln(ASCF)}_{(\boldsymbol{AdvSpeed})} > 0;$$

$$\text{and } \frac{\mathbf{d}}{\mathbf{d(AdvSpeed)}} \boldsymbol{ln(ASCF)}_{(\boldsymbol{AdvSpeed})} = 0.$$

The convexity is independent of the radius and the curve superelevation. Mathematically, it only requires the advisory speed be lower than the speed limit and that both variables have positive values. This condition holds for all advisory speed and speed limit candidate values. Therefore, the optimal advisory speed exists for virtually every 2 lane, 2 way rural highway situation.

There are two points satisfying the extreme point condition, but only the result shown in Equation 3-4 also achieves the convexity condition as discussed above. Equation 3-4, therefore, is the closed functional form of the theoretically optimal advisory speed.

Equation 3-4: Theoretically Optimal Advisory Speed

$$AdvSpeed_{Optimal} = \frac{-2\left(\frac{\beta_2 + SpLim \times \beta_3}{15R}\right) + \sqrt{\frac{4(\beta_2 + SpLim \times \beta_3)^2}{225R^2} + \frac{4\beta_3 \times (SE \times \beta_3 - \beta_1)}{5R}}}{-\frac{2\beta_3}{5R}}$$

It is important to note that the solution for Equation 3-4 depends on the coefficient estimates determined empirically. The Oregon State University posting method, presented in the next section, results in values directly applicable to Oregon rural highways. The authors later demonstrate that this equation tends to agree more with the national guidelines for posting signs than with the historically conservative Oregon policy values.

3.7. The Oregon State University Posting Method

In order to propose a posting procedure based on Equation 3-4 the authors addressed relevant shortcomings inherent to the process of translating a purely theoretical result into a specific engineering application. In this section, the shortcomings are discussed and the solutions outlined. The emerging procedure is coined "The OSU method", named after the Oregon State University, the institution of affiliation for the authors.

The first shortcoming lies in the functional form of Equation 3-4. There is a mathematical singularity when the radius of the curve approaches zero. This mathematical caveat is verified when testing the equation at small radii curves. Large SFDs can be expected for sharp curve (smaller radii) locations. Because of modern vehicle performance, SFDs of 0.5 or more are not unfeasible for many passenger cars, but these larger SFDs would introduce a safety concern of other vehicle types such as trucks and trailers.

The authors then implemented a practical solution to this issue: If the side friction demand resulting from Equation 3-4 exceeds an acceptable threshold (e.g. 0.23, 0.25 or 0.3), then the preferred advisory speed shall be the largest speed that does not exceed that threshold.

The second issue of concern is the role of the regression coefficient estimates Equation 3-4. The posting application of the ASCF coefficients is limited by the fact that Equation 3-1 does not only account for these three ASCF terms, but also includes an indicator variable for the presence of advisory speeds. This means that Equation 3-1 assigns a different baseline of crashes to curves without advisory speeds than it does to posted curves. This makes sense in safety evaluation, where the ASCF is an effect of the advisory speed on expected crashes when comparing similar curves.

For the ASCF to accommodate the case of no-advisory speed needed (which occurs if the recommended advisory speed is within 5 mph of the posted speed limit), the authors repeated the statistical estimation of the function coefficients after removing the indicator variable for advisory speed from Equation 3-1. Doing this forces the only advisory speed coefficients remaining in the equation (i.e. the three ASCF coefficients) to account for as much variation associated with advisory speeds as structurally possible. The cost of this procedure, naturally, is a reduced goodness of fit. However, the authors advocate for the modified model because the meaning of the coefficients is more appropriate for a posting procedure; in that case two decisions are being made explicitly: the appropriate advisory speed value, and if such advisory speed should be posted. Conversely, the coefficients from Equation 3-1 are estimated discounting that the effect of the later decision is accounted for somewhere else in the model. The coefficients resulting from the reduced model are shown in Equation 3-5.

Equation 3-5: ASCF from Reduced Model

$$ASCF = exp[3.98(SFD) - 0.399(ASD \times SFD) + 0.065(ASD)\ ]$$

The authors are aware that these coefficients differ from those shown in Equation 3-2, as well as do the advisory speeds resulting from the two sets of coefficients. Even so, the authors deem each set useful for differentiated applications, Equation 3-2 for safety performance evaluation and Equation 3-5 for the proposed posting procedure.

The third and final issue with Equation 3-4 is the simplest to solve. Since posted advisory speeds are multiples of 5 mph, the new procedure shall recommend the advisory speed as such multiple of 5 value with the smallest ASCF possible, which occurs in the vicinity of the optimal advisory speed.

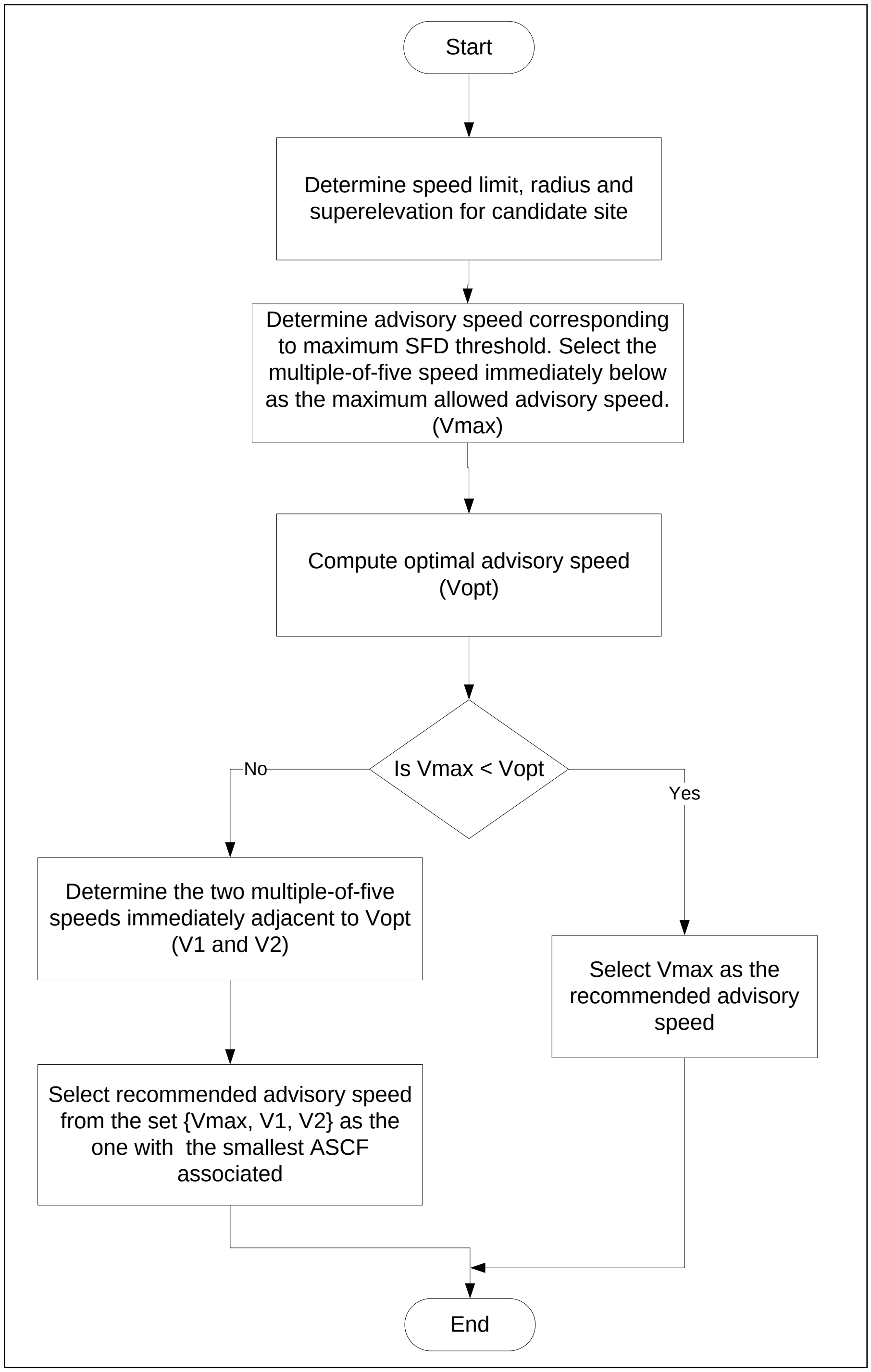

Figure 3-1: Logical Steps to the OSU Posting Method

The logical steps to implement the proposed posting procedure are represented in Figure 3-1.

3.8. Relationship with Current Posting Criteria

The authors computed the OSU method advisory speed for the entire available Oregon state-wide sample using a maximum SFD of 0.23. Similarly, the authors also computed the theoretical MUTCD 2009 values for the sample of sites and compared the performance of these values to the current advisory speeds. This section reviews these comparisons.

Both computational methods yielded larger values than currently posted advisory speeds in Oregon. The OSU method recommended, on average, higher advisory speeds. This observation can be summarized by comparing the raw averages: 42.69 mph for the current plaques, 44.95 mph for MUTCD and 45.16 mph for OSU. This result is not surprising, since a previous study identified the historic Oregon advisory speed policy as among the most conservative across the United States (Dixon & Rohani, 2008). It is interesting to note, however, that the OSU and the MUTCD trends are more similar to each other than they are to the historic Oregon policy.

When the authors contrasted the advisory speeds from the three methods to their associated SFDs, they observed that the current Oregon values were smaller than those obtained using the two computational methods (0.101 for the current plaques, 0.121 for MUTCD, and 0.124 for OSU).

When comparing how the associated SFD varied by curve radius, the authors observed that the three sets of speeds tended to exhibit larger SFDs at smaller radii. On average, the MUTCD and OSU speeds result in SFDs 0.03 above the current values all across the radii range, as also suggested by the raw averages.

Figure 3-2 shows a comparison of posting methods using the contour map of the ASCF function (a higher number of crashes correspond to the higher points in this surface).

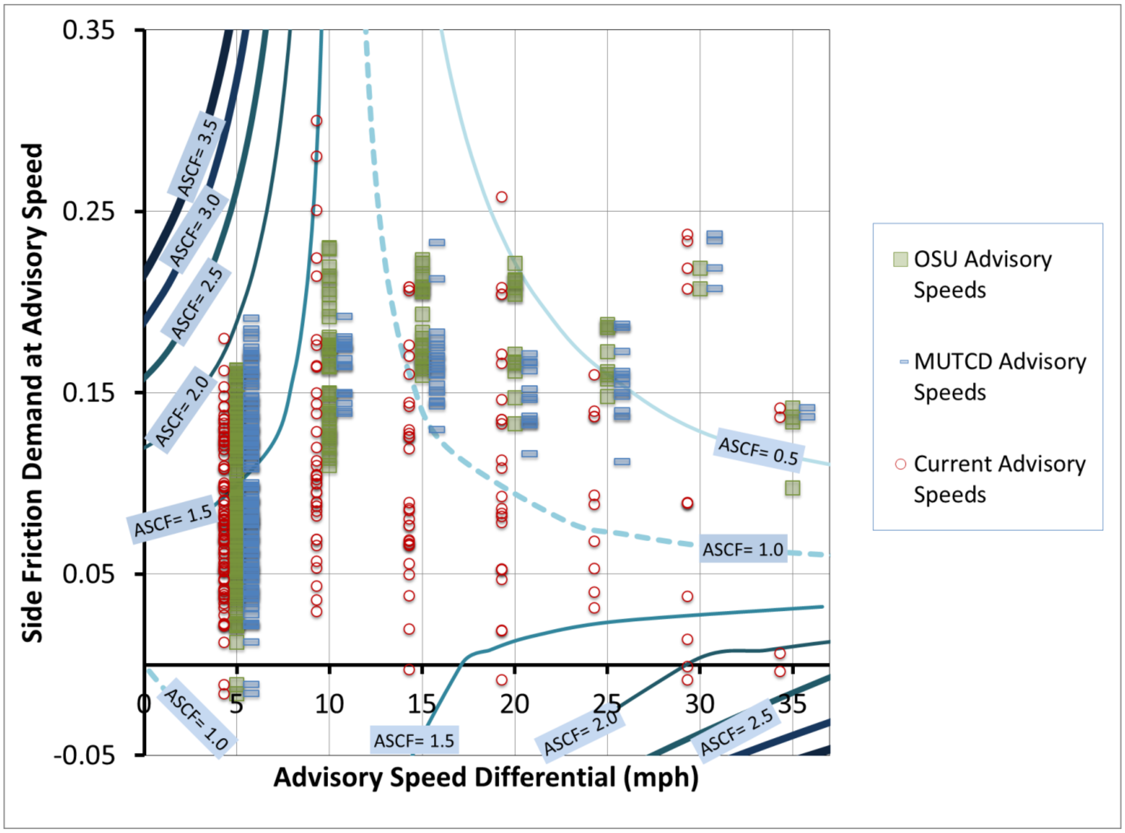

Figure 3-2: Comparison of Posting Methods over the ASCF Contour Map

It is important to notice that OSU advisory speeds do not land along the diagonal of symmetry for the surface (as they would be expected) precisely because these speeds were calculated using Equation 3-5 but the contour correspond to the Equation 3-2 coefficients for the reasons exposed when deriving the OSU method. Current advisory speeds are notably more dispersed than any of the two computational methods. It is also obvious that current advisory speed tend to favor low advisory speeds that are coupled with lower SFDs, and as a result, they fall closer to the “horizontal ASCF hill” that is located along the ASD axis. Advisory speeds from the MUTCD method tend to fall in a roughly horizontal line when they are explicitly posted (i.e. ASD>5mph). This trend is probably reflecting that this method mostly ponders SFD as a criterion disjoint from the corresponding ASD to certain extent. Finally, though OSU speeds tend to favor larger SFDs but this trend also draws very close to the MUTCD set. Though this comparison is somehow informative, the authors consider that the posting methods should better be contrasted to the theoretical scenario when advisory speeds are not present.

Figure 3-3 displays the theoretical safety performance as it relates to the Advisory Speed Differential (Speed Limit minus Advisory Speed). The Absolute ASCF or AASCF is the ratio of the ASCF at the advisory speed to the ASCF if the advisory speed was set just below the speed limit. This reference ASCF is particularly meaningful for advisory speeds close to the speed limit. Figure 3-3 demonstrates that regardless of the posting criterion, lower advisory speeds tend to be more beneficial.

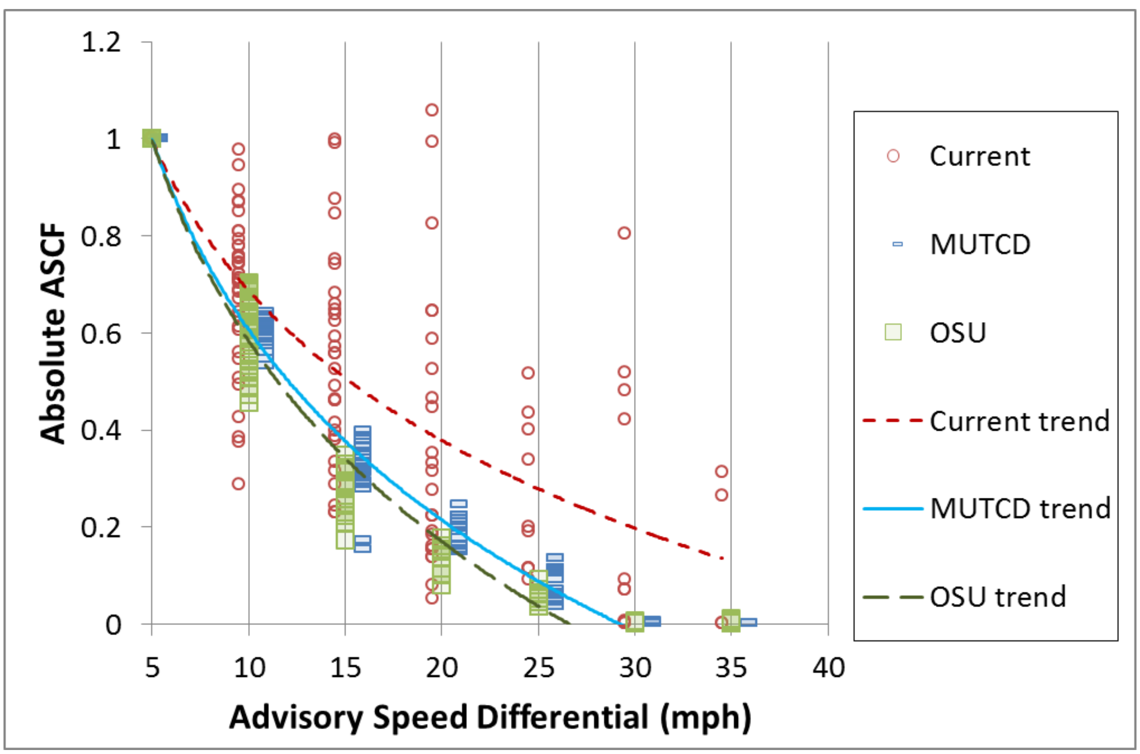

Figure 3-3: Absolute ASCF by Posting Method vs. Curve Radius

The trend is less distinct for the case of currently posted speeds, as they relate to more disperse AASCF values as the ASD increases. Interestingly, as in Figure 3-2, both the OSU and MUTCD criteria do not exhibit excessive variation. This observation resonates with previous work that suggested consistency issues may be associated with the use of the Ball Bank indicator method (Bonneson, Pratt, & Miles, 2009), (Lyles & Taylor, 2006).

Finally, the trends in Figure 3-3 suggest that both the MUTCD and the OSU criteria are expected to have a safety performance better than the currently posted speeds. Although the trend lines are very comparable, the OSU criterion appears to improve its safety performance at the fastest rate as the advisory speed differential increases.

Given these comparisons, it is not surprising how closely the OSU and the MUTCD methods performed. It is possible to map both constituent elements of the ASCF directly to the current posting guidelines. Table 2C-5 of the MUTCD 2009 encourages the inclusion of advisory speed and other signage, such as chevrons, based on the difference between the advisory speed and the speed limit (the ASD value in this analysis). At certain thresholds, their postage becomes mandatory. It is also possible to theoretically establish a cause-effect relationship between the Ball-Bank indicator angle and the SFD through the articulation of vehicle dynamics and road geometry (the original basis for the ball-bank application).

3.9. Discussion of Results and their Scope

The authors recognize that, similar to determining speed limits, posting criteria for advisory speeds are affected by technical and social trends. The authors expect that Equation 3-4 incorporates such elements implicitly through the use of ASCF empirically determined coefficients.

The authors rely on the fact that the statistical analysis was performed based on a probability sample and believe that the coefficients in this paper are not biased towards particular site characteristics, and that they represent a balanced average of factors such as the various levels of laxity in posting advisory speeds, severity of law enforcement at different jurisdictions, current vehicle fleet, curve sharpness, proportion of crashes by type, severity or conditions, among others. The authors recognize that operating speeds upstream of horizontal curves are influential on traffic operations at the curves. The authors expect, however, that operating speeds are roughly accounted for in the ASD by the speed limit, as operating speed would rise or fall to a significant extent as a response to higher or lower speed limits. In this regard the authors consider that the fact that advisory speeds obtained from the OSU method positively correlates with speed limit, as verified in a sensitivity analysis, is an indication that the OSU method is sensitive to traffic operations prevailing upstream the curve, as has been suggested by other researchers (Bonneson, Pratt, & Miles, 2009), (Bonneson J. A., 1999).

3.10. Robustness of the ASCF Function: Field Validation Analysis

This section presents the field validation analysis of the full-model and the ASCF sub-model, and is provided as supplemental evidence of the substance behind the ASCF model.

3.10.1. Field Validation Based on a New Sample of Sites

During July of 2011, the authors collected another independent sample consisting of 44 new curve sites so as to field validate both the full model and the ASCF sub-model. These sites were selected randomly from the state-maintained rural highways in Oregon including a regional subset distributed across four counties. This new sample comprised a wide variety of geometric and operational characteristics: radii ranging between 110 through 1800 ft, superelevations between 1% and 15%, and AADTs between 474 and 6160 pcph. The data set also included six sites without speed plaques and three sites that were located at 45 mph speed zones.

The researchers obtained crash records for the period 2003 to 2007 and identified a total of 29 crashes at the validation sample sites. The largest number of crashes at a particular location was five. The authors could not locate any recorded crashes at 27 of the sites.

3.10.2. Overall Goodness-of-fit

Some literature cautions that traditional goodness of fit criteria may be misleading for count models where the mean is predicted as a small value in combination with a small sample size (Lord & Miranda-Moreno, 2007). Due to this concern, the authors developed an alternative goodness-of-fit test metric so as to relax the assumption of large sample sizes that the Maximum Likelihood Estimation methods rely upon.

The regression model is the parameterization of the expectation of a random “response” variable conditioned to the values of a vector of covariates. Statistical theory (Wackerly, Mendenhall III, & Scheaffer, 2008) relates the conditional, joint, and marginal expectations of random variables as shown in Equation 3-6.

Equation 3-6: Conditional, Marginal and Joint Probabilities Relationship for Random Variables

$$P\left(Y = y, \vec{X} = \vec{x}\right) = p(y, \vec{x}) = p_{\vec{x}}(\vec{x}) \times p(y|\vec{x})$$

Where:

y	=	predicted variable;
$\vec{x}$	=	vector of predictors;
$p(Y = y, X = \vec{x})$	=	joint probability of y and $\vec{x}$;
$p_{\vec{x}}(\vec{x})$	=	marginal probability of $\vec{x}$; and
$p(y|\vec{x})$	=	conditional probability of y given $\vec{x}$.

In the frame of this proposed test, every data point is equally weighed. It is simple then to obtain the joint probability of both the response variable and the vector of predictors. The marginal probability of y, the response variable, can be obtained in turn by integrating the joint probability over all the available realizations of $\vec{x}$, the vector of predictors.

This logic is valid without any assumptions regarding the relationships between the variables, and it may be applied to any given conditional probability distribution, such as Equation 3-1.

Finally, it is possible to predict the expected frequencies for values of Y by substituting the Poisson probability function in Equation 3-6 and solving as described, by integration, for the marginal distribution of 'y'. This marginal distribution is then used to predict the frequency of sites with 'y' crashes, for a sample of size of *n*. Equation 3-7 shows this result.

Equation 3-7: Expected Frequency of Sites with "Y" Crashes in the Validation Sample

$$E.F._{(y)} = \sum_{i=1}^{n} \frac{e^{\left[y\vec{\beta}.\vec{x}_i - \left(\exp(\vec{\beta}.\vec{x}_i)\right)\right]}}{y!}$$

Where:

$E.F.(y)$ = Expected Frequency of sites with "y" crashes.

This equation may be used to assess the overall goodness of fit of the model without the need to mandate any assumptions about the sample size or the size of the predicted mean. In fact, the concern about a low count in the response variable is now removed, because the new count variable is in this context the number of sites with a particular number of crashes, as opposed to evaluating Equation 3-1, where the corresponding count is the number of crashes. Table 3-1 shows the results of the goodness of fit test just outlined. The resulting p-value supports the hypothesis of the model adequately fitting the validation data set.

Table 3-1: Goodness-of-fit Test over the Observed Distribution of Crashes

Observed Number of Crashes	***Actual Frequency of Sites***	***Expected Frequency of Sites***
0	27	30.3398
1	9	9.9078
2	6	2.5815
3 and more	2	1.1709
Total	**44**	**44**
	Chi-Squared Statistic	**5.5649**
	p-value	**0.1348**

3.10.3. **Validation of the ASCF**

The authors developed and performed a GLM estimation for a partition of the vector of covariates in order to find the statistical significance of the predicted values for the ASCF and the associated crash baselines.

The analysis revealed that both partition coefficient estimates were statistically different from zero (p-values of 0.012 and $<2\text{x}10^{-16}$ respectively). The estimation found no significant evidence of Poisson-overdispersion (p-value of 0.09 for a 54.812 residual deviance on 42 degrees of freedom, for a dispersion parameter estimate of 1.3), which is also evident at an aggregate level from Table 3-1.

The authors computed a global estimate of the probability of a type I error. A very small p-value of $2.03\text{x}10^{-11}$ from a Hotelling's T^2 test (which considers simultaneously both the partition coefficients) increases the confidence on the validity of the full model. This p-value represents the probability of both the baseline and ASCF terms being as significant under the assumption that they were significant in the original sample only by chance (this is the default assumption, the null hypothesis).

Additionally, it was possible to estimate the statistical power of this analysis, since it is testing specific coefficient expectations, which implies a single point alternative hypothesis. The probability that the analysis would result in a type-II error was found as a p-value of 0.084. This value was computed from a Hotelling's T^2 test, which considers both the partition coefficients simultaneously. The corresponding statistical power of the validation is 91.6%. The statistical power is the probability that this analysis rejects the null hypothesis when both the baseline and ASCF terms are in fact as found in the original analysis (this is the alternative hypothesis).

Similarly, both type-I and type-II errors can be obtained for the ASCF partition alone. In this case, the probability of a type-I error was 0.0057, which indicates that it is unlikely that the ASCF sub-model effect may be attributed to chance only. However, the statistical power in this case is moderate, 71.7%, which indicates the need of a larger sample to increase the confidence on the actual ASCF coefficients.

3.10.4. **Final Remarks on the Validation Analysis**

Based on the field validation analysis, the authors are confident about the relevance and validity of the model as a safety performance function. Adequate goodness of fit on a second independent sample of curve sites indicates a good predictive power.

This confidence also extends to partitioning the model in baseline crashes versus the ASCF sub-model. Although this further analysis deems the ASCF contribution to the full model statistically significant (i.e. its coefficients are statistically different from zero), a mild statistical power for the given sub-model indicates that such a result may not be almost certainly expected as are the overall fit and predictive power of the full model. However, the authors embrace the postulate of an actual ASCF effect, considering the favorable evidence in the modelling and validation samples (both rejecting the hypothesis of a null ASCF), as well as the plausible human factors articulation of such an effect, as described in a previous work by these authors (Avelar & Dixon, 2011).

3.11. Conclusions and Recommendations

The main objective of this paper is to develop a procedure to post advisory speed plaques directly based on their expected safety performance. Such a procedure is based on the main criterion of the Advisory Speed Crash Factor. The ASCF describes, to the authors' satisfaction, how safety performance is statistically related to the two covariate functions associated with the advisory speed: the Advisory Speed Differential and the Side Friction Demand.

The authors derived a closed-form equation to determine the theoretically optimal advisory speed. Such a theoretical optimal is thought to balance the human factors effects that the authors induce underlie the ASCF: Drivers adjust their behaviour considering and balancing the information the ASD and SFD variables carry jointly. The ASD is thought to indicate how much slower drivers should be navigating the curve while the SFD is thought to indicate the level of discomfort the driver will experience for a given advisory speed.

The authors identified and addressed the issues naturally expected from deriving an engineering application from a theoretical concept. The resulting procedure is the OSU method. They then contrasted this newly developed method with both the MUTCD recommended values as well as the currently displayed advisory speeds in Oregon. Both the OSU method and the MUTCD produced advisory speed values that are believed to perform better than currently posted speeds. In that comparative analysis, it became apparent that advisory speed values based on a computational method (either the OSU or MUTCD) offer, in general, more consistent values than actual advisory speeds that most likely have been determined by the ball bank indicator method. As a result, the authors share the opinion of researchers who encourage the use of computational alternatives (Bonneson, Pratt, & Miles, 2009). The authors deem the safety-performance-based OSU formulation a viable alternative among other computational methods already available in the literature.

The close performance of the OSU method and the MUTCD criterion is not surprising. It is possible to link the ASCF components to the MUTCD posting guidelines in a meaningful way. This finding suggests that MUTCD procedures yield values that are almost optimal, if indeed there is an “optimal” advisory speed under the current conditions of generalized driver understanding of the signs.

The authors performed a field validation analysis in order to test the robustness of the ASCF function. The analysis verified the predictive power of the function over the number of crashes of an independent sample of curve sites. As a consequence, the authors recommend two direct engineering applications stemming from the ASCF function: for safety assessment, as previously demonstrated in the case of Oregon rural highways, and the determination of advisory speed values for new sites, by using the OSU method, as outlined in this paper.

Finally, the authors recommend future work to explore the link of the ASCF to field operational data. Specifically, future research should explore how the operating speed relates to the components of the ASCF bivariate function. The authors also recommend future research exploring alternative analysis tools to verify these results, as well as calibrating the OSU method using data from other states because general driver awareness and understanding of the signs probably varies significantly across jurisdictions.

Acknowledgements

The authors would like to thank the members of the Oregon Department of Transportation (ODOT) Research Section and Technical Advisory Committee for their advice and assistance in oversight of this research effort. This project was jointly funded by ODOT and by the Oregon Transportation Research and Education Consortium (OTREC). The authors would like to thank these sponsors for funding this research project.

3.12. References

1. Dixon, Karen K. and Avelar, Raul E. *SPR 685: Safety Evaluation of Curve Warning Speed Signs. Final Report.* Salem, OR : Oregon Department of Transportation, July 2011.

2. Avelar, Raul E. and Dixon, Karen K. *Modelling the Safety Effect of Advisory Speed Signs: A Bivariate Multiplicative Factor on Number of Crashes based on the Speed Differential and the Side Friction Demand.* [CD-ROM] Indianapolis, IN : Transportation Research Board, 2011.

3. The R Development Core Team. *R: A Language and Environment for Statistical Computing.* [Online] 2009. Version 2.10.1 (2009-12-14). http://www.R-project.org. ISBN 3-900051-07-0.

4. Venables, W. N. and Ripley, B. D. *Modern Applied Statistics with S. Fourth Edition.* New York : Springer, 2002. ISBN 0-387-95457-0.

5. Fox, John and Weisberg, Sanford. *An {R} Companion to Applied Regression, Second Edition.* Thousand Oaks, CA : Sage, 2011.

6. FHWA. *Manual on Uniform Traffic Control Devices.* Washington, D.C. : U.S. Department of Transportation, 2009.

7. Bonneson, James A., Pratt, Michael P. and Miles, Jeff. Evaluation of Alternative Procedures for Setting Curve Advisory Speed. In *Transportation Research Record: Journal of the Transportation Research Board*, No. 2122, Transportation Research Board of the National Academies, Washington, D.C., 2009, pp. 9-16.

8. Dixon, Karen K. and Rohani, Joshan W. *SPR 641: Methodologies for Estimating Advisory Curve Speeds on Oregon Highways.* Salem, OR : Oregon Department of Transportation, 2008. Technical Report. SPR 641.

9. Lyles, Richard W. and Taylor, William C. *Communicating Changes in Horizontal Alignment.* Washington, D.C. : Transportation Research Board, 2006. NCHRP Report 559.

10. Chowdhury, Mashrur A., et al. *Are the Criteria for Setting Advisory Speeds on Curves Still Relevant?* s.l. : ITE Journal, 1998. pp. 32-45.

11. Avelar, Raul E. *Effectiveness of Curve Advisory Speed Signs. A Characterization of Road Operations in Western Oregon*. Scholars Archive at OSU. [Online] 16 August 2010. [Cited: 08 November 2010] http://hdl.handle.net/1957/17673.

12. AASHTO. *Highway Safety Manual.* Washington, D.C. : AASHTO, 2010.

13. Elvik, R. and Vaa, T. *Handbook of Road Safety Measures.* Oxfort, U.K. : Elsevier, 2004.

14. Ritchie, Malcolm L. *Choice of Speed in Driving Through Curves as a Funcion of Advisory Speed and Curve Sign.* s.l. : Human Factors, 1972. pp. 533-538.

15. Silvey, S. D. *Multicollinearity and Imprecise Estimation.* Journal of the Royal Statistical Society. Series B (Methodological), 1968 pp. 539-552.

16. Brambor, Thomas, Roberts Clark, William and Golder, Matt. *Understanding Interaction Models: Improving Empirical Analyses.* s.l. : Political Analysis, 2006. pp. 63-82.

17. AASHTO. *A Policy on Geometric Design of Highways and Streets (5th Edition).* Washington, D.C. : AASHTO, 2004.

18. *Side Friction Demand and Speed as Controls for Horizontal Curve Design.* Bonneson, James A. 1999, Journal of Transportation Engineering, pp. 473-480.

19. Lord, Dominique and Miranda-Moreno, Luis F. *Effeects of Low Sample Mean Values and Small Sample Size on the Estimation of the Fixed Dispersion Parameter of Poisson-gamma Models for Modeling Motor Vehicle Crashes: a Bayesian Perspective.* [CD-ROM] Washington, DC : TRB, 2007.

20. Wackerly, Dennis D., Mendenhall III, William and Scheaffer, Richard L. *Mathematical Statistics with Applications. 7th Edition.* Toronto, Canada : Thomson, 2008.

4. Improving the Practice of Posting Advisory Speeds: A Methodology to Mitigate Ball Bank Indicator Inconsistencies by Using a Safety Performance Criterion

Raul E. Avelar and Karen K. Dixon

Journal of Transportation of the Institute of Transportation Engineers ISSN: 2162 1616

1627 Eye Street, NW, Suite 600
Washington, DC 20006

Currently under consideration for publication.

Improving the Practice of Posting Advisory Speeds: A Methodology to Mitigate Ball Bank Indicator Inconsistencies by Using a Safety Performance Criterion

Raul E. Avelar1*
Karen K. Dixon2

*Corresponding Author
1) Raul E. Avelar, MSc, Doctoral Candidate
Graduate Research Assistant, School of Civil and Construction Engineering
Oregon State University
Owen Hall 220,
Corvallis, OR, 97331
Phone: 541- 602- 9115
Fax: 541- 737-3052
e-mail: raul.avelar@lifetime.oregonstate.edu

2) Karen K. Dixon, PhD, P.E.
Associate Professor, School of Civil and Construction Engineering
Oregon State University
Owen Hall 220,
Corvallis, OR, 97331
Phone: 541-737-6337
Fax: 541-737-3052
e-mail: karen.dixon@oregonstate.edu

Submitted on February 17, 2012 to be considered for publication in the Journal of Transportation of the Institute of Transportation Engineers.

ABSTRACT

Posting advisory speed signs at sharp horizontal curves is a practice well established in the United States. The intent of these signs is to aid the driving public in selecting appropriate speeds to negotiate such curves. The authors recently completed an assessment of advisory speed safety in the state of Oregon, a study that suggests that updating to the latest posting guidelines may be beneficial in terms of safety performance. The authors also observed unwarranted variability of advisory speed values when these values were determined using the ball bank indicator posting method (BBI).

Since the BBI is a straightforward and widely accepted tool, it is likely that practitioners may be reluctant to stop using the BBI in spite of this well documented variability in results. This paper outlines an analysis of BBI data to develop a methodology to help mitigate this undesirable variability in BBI readings. For the purposes of this paper, this proposed methodology is referred to as 'the Hybrid OSU Posting Method' because it uses the BBI in combination with the Advisory Speed Crash Factor (ASCF), which is the engine function for the OSU posting method previously proposed by these authors. The ASCF is a safety criterion to characterize safety performance of advisory speed signs. Therefore, the researchers expect this methodology will result in advisory speeds associated with an improved safety performance.

This research uses 3114 BBI readings from a sample of 425 horizontal curves at two-lane rural highways in the state of Oregon. The authors used half the available BBI data to develop a methodology and reserved the other data for testing the proposed methodology. The results indicate that despite the variability inherent to the BBI, the advisory speeds resulting from the Hybrid OSU method are more consistent than those from the traditional BBI method, but less consistent than the OSU method. Accordingly, the results indicate that the expected safety performance of the Hybrid OSU method is better than the traditional BBI method, but not as good as the computational OSU method.

Keywords: advisory speed, ball bank indicator, safety, body roll angle, Side Friction Demand, optimal advisory speed, OSU method, Hybrid OSU method.

4.1. Introduction

Following a review of current literature on the topic of advisory speeds and a brief description of the data available for this research effort, this paper consists of two main parts: Part one deals with an in depth analysis of the physics involved in a vehicle negotiating a curve, and how such analysis relates to quantities involved in the ball bank indicator reading (BBI) and the advisory speeds that stem from accepted methodology based on this instrument. Since scarce information about the influence of body-roll angle in using the BBI is available, the authors performed an assessment on horizontal curve data to gain a better insight on how this angle behaves and affects the variability of the BBI reading.

The second part of this paper reviews the development of a methodology to mitigate the well-known variability of the BBI as a way of confidently making advisory speed decisions based on expected safety performance. This methodology is then compared to the computational OSU method and the advisory speeds posted in the sample data. The improved performance of the Hybrid OSU method (i.e. the proposed methodology) is explained by it being based on a 'smooth' estimate obtained from several BBI data points for a broad range of speeds, as opposed to current BBI procedures which are based only on the BBI readings that are at or around the advisory speed that will ultimately be recommended.

4.2. Literature Review

This literature review focuses on published literature that addresses determining appropriate advisory speed values and assessing their effectiveness. This effectiveness is generally presented in terms of expected speed reduction or long term safety impact.

4.2.1. A Brief History of Current Practices

The practice of posting advisory speeds dates back to the 1930s, but standard procedures became available as late as 1948. Currently, the reference document in the

United States for any type of signage is the Manual on Uniform Traffic Control Devices (MUTCD) (FHWA, 2009). This document recognizes three accepted procedures to determine advisory speed recommended values: estimated values identified using the BBI (this is the most widely implemented approach), calculated values based on the geometric design equation from “the Green Book” (A Policy on Geometric Design of Highways and Streets) (AASHTO, 2004), and values determined by using an accelerometer.

Currently in the United States, there are several available speed-posting thresholds used by agencies. Until 2010, Oregon used a 13-10-7 degree threshold (for less than 30 mph, 35 to 55 mph, and greater than 55 mph values respectively). In 2010, they adopted the thresholds suggested in the latest edition of the MUTCD. In the 2009 edition of the MUTCD, BBI thresholds of 16-14-12 degrees now correspond to speed thresholds of up to 20 mph, up to 30 mph, and above of 30 mph, respectively.

4.2.2. **Driver Response to Advisory Speeds**

There are various studies that concentrated directly on measuring curve speeds and comparing these values to the posted advisory speeds. This difference is expected to range between 7 to 10 mph (Chowdhury, Warren, Bissell, & Taori, 1998), (Koorey, et al., 2002), and (Lyles & Taylor, 2006). However, for the case of Oregon and its known history of using more conservative thresholds, a probability sample suggests that the average such differential is likely 13.8 mph for that state, as found by Avelar (2010).

Lyles and Taylor (2006) argue that if the intent of these signs is for drivers to adhere to the suggested speed, then the signs are largely ineffective. They also report that both practitioners and the driving population in general perceive the posted speed to be too low.

From the Human Factors point of view there are research works with conflicting results. On the one hand Zwahlen (1987) performed a study on 40 drivers on a driving loop for which curves were posted at advisory speeds. The drivers were equipped with eye scanners and this information was contrasted with the driving task parameters. Although the drivers consistently fixated their sight to the warning signs, the author did not find any correlations between values such as the driver speed and the displayed advisory speed. The author also did not find evidence of a difference between the two runs of each driver, nor the status of a familiar and unfamiliar driver. Zwahlen concluded that advisory speeds add very little information to the drivers, and thus posting and maintaining them should be of low priority. On the other hand Ritchie (1972) suggests that advisory speeds may be associated with higher operating speeds, since the additional information they convey may give drivers confidence about speed selection thresholds over the posted speed.

4.2.3. **Advisory Speed Consistency Issues**

For a recent study in Oregon by Dixon and Rohani (2008), the project team conducted field visits for sites with posted advisory speeds across the state. This effort verified that the actual posted speeds differed from recommended speeds based on the threshold values in use by Oregon at the time of the study. A study by Bonneson, Pratt and Miles (2009) suggested that a main reason for this observed difference between posted and expected advisory speeds may be due to the lack of consistency of results when using the BBI. Various authors argue that such lack of consistency could explain to a great extent the observed lack of adherence to advisory speeds (Bonneson, Pratt, & Miles, 2009) and (Lyles, 1982).

Recently, Avelar and Dixon (2012) proposed a function to estimate the expected safety performance of advisory speeds, and found that when comparing different posting criteria, curve locations that were expected to perform better in terms of safety were also the more consistent, both in the variability of the posted values, as well as in the expected safety performance itself. In general, their results agree with the conclusions of Bonneson et al. in that computational methods should be preferred for their enhanced consistency, if compared to the ubiquitous BBI method. Finally, Avelar and Dixon developed a new recommended computational methodology, named the

OSU posting method that performed slightly better than a computational version of the MUTCD 2009 thresholds.

4.3. Available Data

The data utilized for this research includes geometric characteristics for 425 curves, located at 166 randomly selected sites, with a total of 3114 BBI records and their corresponding speed runs. The source of this data is from a study performed for the state of Oregon by Dixon and Rohani (2008).

Dixon and Rohani selected two large random samples of roads in Oregon: 80 state-maintained, and 90 county-maintained rural highway sites. At least two curves were surveyed at each site for data collection, the number of curves in a site depending on the how the curves were located within the sampling scheme and in relation to each other. It is important to mention that the samples from that research work are actually probability samples, and thus are representative of the prevailing conditions across the state of Oregon. More details about the probability structure of the state-maintained sample are available at a subsequent effort by Avelar (2010). Dixon and Rohani instrumented a vehicle with both a manual and a digital BBI in an effort to reproduce the advisory speeds corresponding posting different criteria, those of the 2009 version of the MUTCD (FHWA, 2009).

4.4. Part One: The Physics of the Ball Bank Indicator and the Side Friction Demand

To fully understand the dynamic environment associated with the BBI, Figure 4-1 shows a schematic of the forces and the angles affecting a BBI-equipped vehicle.

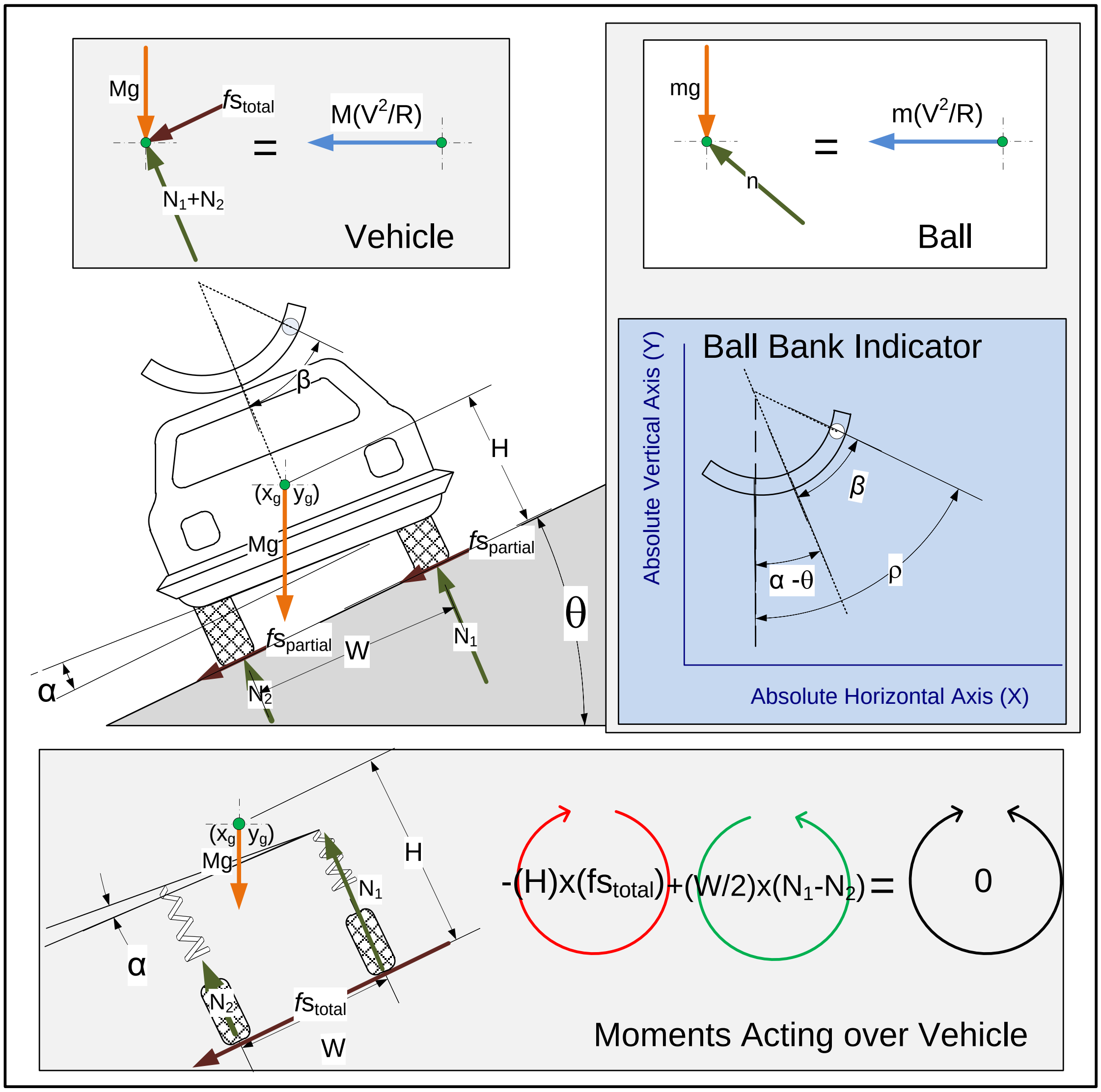

Figure 4-1: Geometry and Dynamics of the BBI

It is important to notice that ρ, the ball equilibrium angle measured from an inertial frame of reference, does not depend on the vehicle or road geometry, but that β, the BBI reading, does deviate from ρ as a function of the superelevation angle (θ) and the vehicle roll angle (α).

Equation 4-1 shows the basic relationship between the relevant angles when considering only the schematic for the BBI.

Equation 4-1: Relationship between the BBI and Vehicle Dynamics

$$\beta = \rho - \theta + \alpha$$

Where:

β	=	Ball Bank angle, measured from the BBI dial (degrees);
ρ	=	Equilibrium angle of the ball, measured from the vertical, to the radial (degrees);
θ	=	Superelevation angle, measured from the horizontal to the pavement surface (degrees); and
α	=	Vehicle roll angle, measured from the vertical to the vehicle symmetry plane (degrees).

In addition, if one uses the information in the free-body diagram, it is easy to demonstrate that $Tan(\rho) = \frac{V^2}{g.R}$, where V is the speed, R radius and g the local earth gravitational field. It is worth noting that $Tan(\theta) \stackrel{\text{def}}{=} e$, where e is the superelevation rate depicted as a ratio and as commonly used in highway design.

An analysis on the forces required by a vehicle to traverse a horizontal curve yields a definition for the side friction demand (SFD):

Equation 4-2: Side Friction Demand

$$SFD \stackrel{\text{def}}{=} \frac{V^2}{g.R} - e$$

This relationship derives from the single-point-mass analysis of the forces over the vehicle as shown in the central scheme of Figure 4-1. It represents the ratio of the forces necessary to achieve the dynamic equilibrium shown in Figure 4-1. In other words, the SFD is the ratio of the lateral force required on the surface of the road (i.e.

the friction force provided by the tires) to the normal force generated over the banked surface.

It is important to notice that the SFD is a simplified quantification of the dynamic requirements of the circular movement of a vehicle. Although the SFD is not influenced by the amount of vehicle roll, the friction in the tires is not necessarily uniform and very likely exhibits some distribution that depends on the geometry and weight distribution of the vehicle. A similar case occurs for the normal forces generated by the superelevated surface. The rolling angle is direct evidence of a significant difference between the Side Friction Supply (SFS) available for the tires at both sides of the vehicle. This occurs because the maximum SFS should be proportional to the normal force in every tire, so it follows that the normal forces at each side of the vehicle necessarily differ in order to create a moment that prevents the vehicle from overturning outside of the curve.

Finally, it is possible to relate the rotational equilibrium shown in the lower part of Figure 4-1 to the vehicle roll angle. When combining the information available from the three vector diagrams in Figure 4-1, and under the assumption of equally stiff linear-elastic suspensions at both sides of the vehicle, it is relatively straightforward to arrive to the following relation:

Equation 4-3: Relationship between Body-Roll Angle, Vehicle Dynamics, and Vehicle Characteristics

$$Tan(\alpha) = \frac{2 \times H \times M}{K \times W^2} \times \left(\frac{V^2}{R} Cos(\theta) - gSin(\theta) \right)$$

Where:

α	=	Vehicle roll angle, measured from the vertical plane to the vehicle transversal symmetry plane (degrees);
K	=	Stiffness constant of linear-elastic suspension springs (lb/ft);
M	=	Vehicle mass (lb.s^2/ft);
H	=	Vehicle mass center height (ft);
W	=	Vehicle width, as measured from tire to tire (ft);

V = Vehicle speed (ft/s);
θ = Superelevation angle, (degrees); and
g = local gravitational field (ft/s^2)

The number of unknown variables in the emerging relationship makes it impractical to explicitly account for this effect in most situations. There are some important observations that are noteworthy about the rolling angle:

1. It is directly proportional to both vehicle mass and height of the center of mass,
2. It is directly proportional to the square of the vehicle speed,
3. It is inversely proportional to the suspension stiffness and squared vehicle width,
4. It is inversely proportional to the superelevation, and
5. It is inversely proportional to the horizontal radius.

Despite these complex relationships, the rolling angle has been treated as an insignificant quantity, if compared to the rest of elements that influence the BBI reading. Standard procedures do not consider this angle explicitly, in part because of its expected insignificance, but also because a procedure directly measuring it would likely be very challenging. However, Equation 4-3 demonstrates that the significance of the distortion introduced by this angle to the BBI reading can be expected to peak when the next set of conditions confluence: (1) when the tested speed is high; (2) at curves with small radii and which are poorly superelevated; (3) when the BBI-instrumented vehicle is heavy and with a high center of mass (i.e. S.U.V. type vehicles), (4) when the vehicle has a narrow frame, and (5) when the vehicle has a soft suspension relative to the vehicle mass (i.e. a typical relationship for new suspensions).

Though a large α is not generally desirable, in practice the value for this angle is expected to be toward the outside of the curve, which means that the BBI reading is a conservative estimate of the SFD, on average.

As a result, an assessment of these various vehicle dynamic relationships helps to identify several important points: (1) that the BBI reading does not directly translate into a corresponding SFD but both quantities are closely related; (2) that the SFD is determined by the geometry of the curve, the tire and pavement conditions, and the kinetic parameters of the vehicle; and (3) that the BBI reading is a measure of the dynamic equilibrium as perceived in the cabin of the motor vehicle and is subject to other factors in addition to those mentioned above. Specifically, the BBI reading depends on the suspension stiffness, vehicle width, the location of the vehicle's center of mass, and a distinctively different relationship with speed and superelevation, as demonstrated in Equation 4-3. All of these additional factors determine the body roll angle, which is a systematic deviation in the BBI reading. The next section focuses on explicitly evaluating to what extent the premise of a negligible body roll angle holds for the data available from Oregon.

4.4.1. **Investigating the Body Roll Angle influence over the Ball Bank Indicator**

In general, it is well known that for higher advisory speed conditions, the BBI tends to be more sensitive to small distortions caused by road surface inconsistencies or small steering jolts. Equation 4-3 also shows that when other contributing factors are equal, the higher speeds are associated with systematically higher body-roll angles. It is expected then that in addition to more sensitivity to random driving surface distortions, the BBI reading also diverges systematically from the SFD at higher readings. This section will use the previously derived relationships to estimate the expected body-roll angle using the Oregon-based data.

As a first step, the authors assessed the level to which the BBI readings are influenced by the body-roll angle. Solving for alpha in both Equation 4-1 and Equation 4-3 and combining the results, one obtains the following relationship:

$$\beta - \rho + \theta = \left\{\frac{2.H.M}{K.W^2}\right\}.\left(\frac{V^2}{R}.Cos(\theta) - g.Sin(\theta)\right)$$

This relationship incorporates the assumption that $\alpha \cong Tan(\alpha)$, a reasonable simplification for small angles. For the purposes of this assessment, an angle is considered small if it does not exceed 10 degrees, a value which would be excessive for the body roll angle that is typically assumed to range from 1 to 3 degrees.

Since $\hat{\rho} = Atan\left(\frac{V^2}{g.R}\right)$, and $\theta = Atan(e)$, there is only one unknown factor in the above relationship as depicted in the curly brackets. An important observation about this factor is that it depends only on the vehicle fixed characteristics (i.e. mass, geometry, and suspension stiffness). From this point forward, this term will be referred to as the vehicle index factor (VIF).

For the Oregon study, the research team acquired all of the BBI data using only one vehicle commonly used by the Oregon Department of Transportation for advisory speed curve assessments. As a result, the VIF should be a constant value for the available data set. In addition, a single driver obtained all the data so it is expected that an estimate of the VIF derived from the sample should be relatively free of random noise.

Upon inspection of the BBI data, it is apparent that the manual BBI readings appear to consistently yield lower readings than those obtained using the digital version of the BBI. In order to explicitly account for the two different types of BBI, the researchers performed the estimation of the VIF via an ordinary least squares regression (OLS) of the BBI Reading as shown in Equation 4-4.

Equation 4-4: Ordinary Least Squares Estimation of the VIF

$$E(\beta|\hat{\rho},\theta,V,R,Type.M) = \gamma_1.\left(\frac{V^2}{R}.Cos(\theta) - g.Sin(\theta)\right) - \gamma_2.Type.M + \gamma_3.\rho - \gamma_4.\theta$$

Where:

Type.M	=	Indicator variable with a value of 1 for manual BBI readings, zero otherwise;
γ_1	=	First regression coefficient. This coefficient is such that $\gamma_1 = \widehat{\text{VIF}}$;
γ_2	=	Second regression coefficient. This is $\Delta\widehat{BBI_{Manual}}$, the average deviation of the manual BBI with respect to the digital BBI;
γ_3, γ_4	=	Third and fourth regression coefficients, not subject to estimation; instead, they were set equal to 1.0, as of Equation 4-1;
		All other variables as previously defined.

The resulting VIF regression estimate and its corresponding standard error are shown in Equation 4-5.

Equation 4-5: Vehicle Index Factor Regression Estimate

$$\widehat{\text{VIF}} = (0.368 \pm 0.0283)\frac{deg}{ft/_{s^2}}$$

Figure 4-2 shows the body-roll estimate (alpha) resulting from combining the newly obtained $\widehat{\text{VIF}}$ and Equation 4-3.

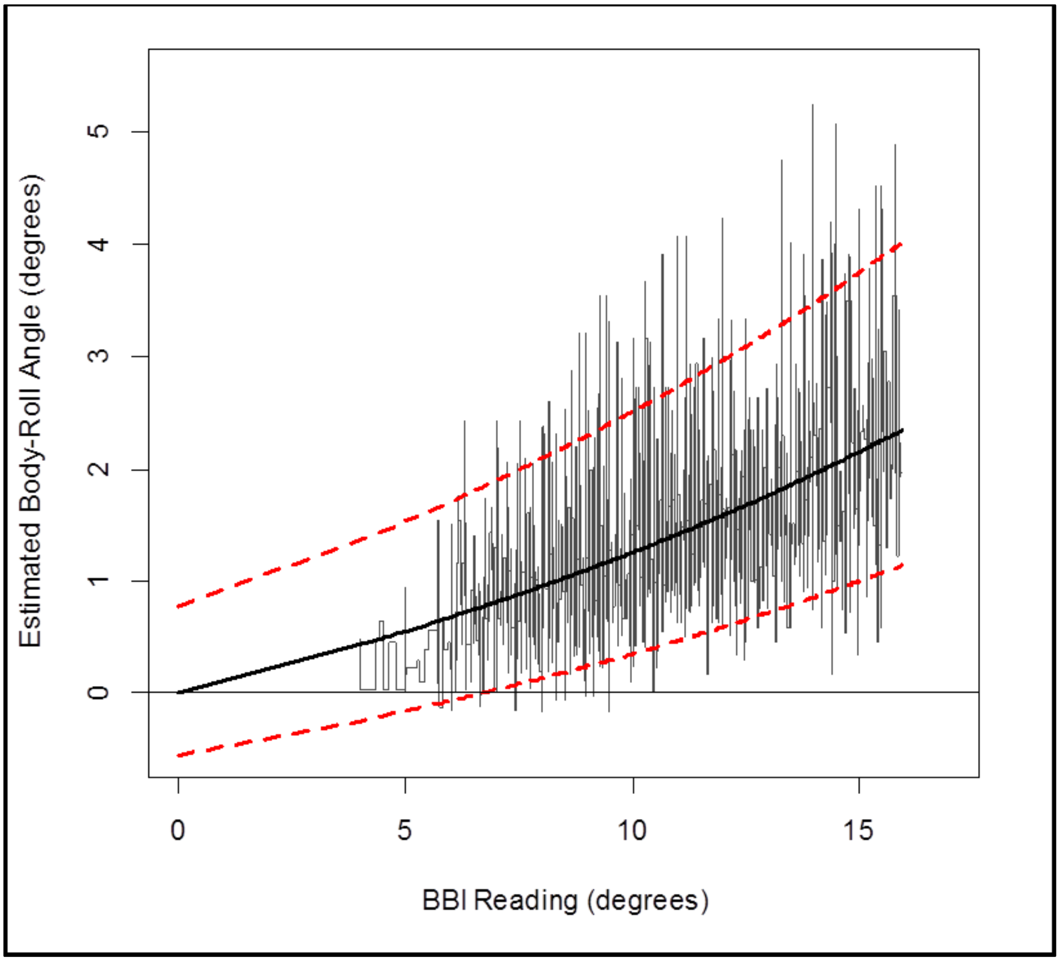

Figure 4-2: Estimated Body-Roll Angle vs. BBI Reading

The estimates are shown by their corresponding BBI reading in gray. A black trend line is provided to show the estimated average body-roll angle. Finally, two dashed lines that correspond to a 95% confidence level depict the upper and lower boundaries around the estimated average. In other words, approximately 95% of the body-roll angle estimates are contained by the region delimited by the dashed lines.

It is important to note, as shown in Figure 4-2, that although the mean body-roll angle behaves as expected, increasing BBI readings that range from zero up to 15 degrees experience a great deal of variation around the mean body-roll angle (generally zero up to 2 degrees). Furthermore, inspection of Figure 4-2 suggests that the body-roll angle range of variation is actually larger than the expected mean body-roll angle for BBI readings smaller than 6 or 7 degrees (i.e. where the lower limit dashed line crosses the BBI axis); however, the body-roll angle is expected to be significant when the BBI reading exceeds 9 degrees (i.e. generally where the estimated body-roll angles are exclusively positive values). In the extreme region to the right of Figure 4-2, where the BBI readings are around 16 degrees, the average body-roll angle is expected to be approximately 2 degrees, but it is also expected that this angle would typically vary between 1 and 4 degrees. This variation can have a significant impact on the BBI reading (between 6% and 25% of the BBI reading could correspond to the body-roll angle at this extreme region).

Figure 4-2 suggests that in some rare instances, the test vehicle is likely to have had body roll angles directed toward the center of the curve rather than away from the center of the curve, as implied by the expected vehicle dynamics (depicted in Figure 4-1). This relationship is represented by negative values in Figure 4-2. Body roll angles toward the center of the curve, however, are physically possible in superelevated curves if either the speed is very low or the superelevation is too large in comparison. Equation 4-3 mathematically captures this unexpected condition in the subtraction inside the last parenthesis. This difference is negative whenever the projection over the superelevated surface of the centripetal acceleration, a speed-dependent quantity, is small compared to the projection of the weight of the vehicle. This analysis suggests that a few runs in the Oregon study might have met this condition (i.e. whenever the estimated body roll angle falls below the zero horizontal line in Figure 4-2). In these rare cases, the BBI underestimates the SFD. For the vast majority of the BBI readings from the Oregon sample, the average body roll angle was larger at larger BBIs resulting in a large BBI as an overrated estimate of the SFD. This over estimated value would result in advisory speeds that are conservative, if one compares them with advisory speeds resulting from a computational method based on the SFD (e.g. the curve dynamics formula method suggested in the Manual on the MUTCD, or the OSU posting method proposed by Avelar and Dixon (2012)).

Because the alpha estimates are heteroscedastic, the researchers used a statistical package (R Development Core Team, 2011) to parameterize the average and boundary lines shown in Figure 4-2. Equation 4-6 shows the empirical relationship obtained for the line representing the mean in Figure 4-2.

Equation 4-6: Empirical Relationship between the Body-Roll Angle and the BBI Reading

$$E(\hat{\alpha}|\beta) = 2.0 \times \left(e^{(0.0485\times\beta)} - 1\right)$$

Where:

$\hat{\alpha}$	=	body-roll angle estimate (degrees); and
β	=	Ball-bank indicator reading (degrees)

Since this analysis found that the body-roll angle may be exacerbating the known variability problem associated with the BBI, the next section uses the empirical relationship to mitigate this variability, resulting in a BBI-based but more consistent advisory speed that are more likely associated with improved safety performance.

4.5. Part Two: Mitigation Strategy for Using the BBI -- The Hybrid-OSU Posting Method

Previous research recommends determining advisory speeds using more consistent computational alternatives rather than the more variable BBI method. Such works offer evidence of the expected posting variability inherent to the BBI method (Dixon & Rohani, 2008), (Bonneson, Pratt, & Miles, 2009) and (Bonneson J. , Pratt, Miles, & Carlson, 2007). Recent work by these authors (Avelar & Dixon, 2012) suggests that a likely consequence of high variability in posted values is an inconsistent safety performance. Additionally, the analysis in the previous section suggests that the body-roll angle may systematically increase with the BBI reading, resulting in a posted advisory speed associated with relatively low SFDs, which, according to the results of (Avelar & Dixon, 2011), could also be associated with a reduced safety performance.

Regardless, the simplicity of operation and interpretation of the BBI makes this equipment option an attractive alternative to practitioners. An additional consideration when using a computational method is that the available site information (i.e. site plans, aerial photos, etc.) may be accurate enough without the need for a site visit, but practitioners accustomed to the use of the BBI may feel a site visit is preferable to estimated conditions applied to a computational approach.

The authors, therefore, consider that a mitigation strategy to the BBI method is necessary, as many practitioners are likely to continue to use a posting method that requires field visits and the use of the BBI. This enhanced strategy must incorporate procedures to address the known BBI variability. Such an enhanced procedure can help to minimize the amplitude and number of data collection runs required for each curve location and to maximize the quality of the information obtained from each run.

Currently, the BBI method uses sequential data collection runs that attempt to limit the BBI angle to a predetermined threshold based on consistently increasing 5 mph interval speed values until identifying values directly above and below the designated thresholds. In order to increase consistency across the advisory speed range, the new methodology does not directly derive the advisory speed from a single series of BBI readings. Instead, it uses several BBI readings from runs across a wide range of speeds. Such a strategy would also benefit from the advantage of incorporating the information from multiple BBI readings at different speeds, as opposed to determining the advisory speed based on the last two or three runs and discarding readings that resulted in values that were too low (but could still provide meaningful information about the road, expected data variability, and the BBI reaction to the surface). However, it is of particular importance that the range of test runs should include run tests at the advisory speed that will be ultimately recommended, as these runs would serve as field verification of the recommended advisory speed.

To achieve the objectives previously outlined, the proposed methodology uses an explicit formulation of the BBI as a function of the run speed, so as to estimate the required parameters from all the data collected in all of the field test runs.

Based on relationships in Equation 4-1 and Equation 4-2, if the approximations $C_1 \times Tan(\rho) \cong \rho$, and $Tan(\theta) \cong \theta$ are deemed reasonable, then:

$\beta \cong C_1 \times \left(\frac{V^2}{g.R}\right) - e + \alpha.$

The constant, C_1, merits additional discussion. The approximation $Tan(x) \cong x$ applies to small angles, and as such, it is used throughout this paper for angles that are known to range across small values. However, for the case of ρ, its values could extend to values as large as 30 degrees for a curve with a radius equal to 150 ft at a speed of 35 mph. The constant C_1 is then an adjustment that the authors considered necessary. Through the application of an OLS procedure, the authors estimated this constant at a value of 0.98 for the range of ρ available from the sample. The authors found that linearity is still very strong at this range. The adjustment to the two quantities (i.e. $Tan(\rho)$ and ρ) systematically explains 99.98% of the variation in between (R-squared of 0.998).

Because the only two pieces of information available when performing a test run around a curve are the BBI reading and the speed, the previous expression can be adapted to perform an estimation of the other variables that are unknown to the personnel in the test vehicle:

Equation 4-7: Linear Relationship between the BBI and the Squared Run Speed

$$\beta \cong \left(\frac{C_1}{g.\grave{\hat{R}}}\right) \times (V^2) - \acute{\hat{e}} + \hat{\alpha}$$

Where,

$\grave{\hat{R}}$	=	Grave dynamic estimate of horizontal curve radius; and
$\acute{\hat{e}}$	=	Acute dynamic estimate of curve superelevation;

$\hat{\alpha}$ = Empirical estimate of α, as of Equation 4-6.
All other variables as previously defined.

First, to determine the best fit for the available BBI data, the authors estimated the vector where both quantities are components of the paired vector $\begin{bmatrix} \grave{\hat{R}} \\ \acute{\hat{e}} \end{bmatrix}$, which dynamically approximates the horizontal radius and the superelevation.

From statistical theory, a relationship between β and V^2 can be determined, as shown in Equation 4-7, by defining the OLS regression of β on V^2. The regression can then be defined as:

$$E(\beta|V^2) = \vartheta_0 + \vartheta_1(V^2) + \vartheta_2\hat{\alpha}.$$

Where,

ϑ_0, ϑ_1 = OLS regression coefficients from local estimation; and
ϑ_2 = constant offset factor on the empirical $\hat{\alpha}$, determined by a global optimization;
All other variables as previously defined.

From this relationship and Equation 4-7 it is possible to establish that

$\vartheta_1 \stackrel{\mathrm{m}}{=} \left(\frac{C_1}{g \times \grave{\hat{R}}}\right)$, and $\vartheta_0 \stackrel{\mathrm{m}}{=} \left(-\acute{\hat{e}}\right)$.

Therefore, $\begin{bmatrix} \grave{\hat{R}} \\ \acute{\hat{e}} \end{bmatrix} = \begin{bmatrix} \left(\frac{C_1}{g \times \vartheta_1}\right) \\ -\vartheta_0 \end{bmatrix}$

It is important to envision the estimated quantities jointly as a vector instead of as independent approximations to the radius and the superelevation. By definition, they are biased quantities, but their biases are negatively correlated. In other words, the more $\grave{\hat{R}}$ overestimates R, the more $\acute{\hat{e}}$ underestimates e. Using OLS procedures, this is a necessary condition so as to minimize the squared errors. To confidently determine good estimators of R and e, a large number of test runs would be necessary, but that is not the case for this research.

This resulting vector can then be applied to the second step in the methodology: determining the optimal advisory speed based on the Advisory Speed Crash Factor (ASCF) formula recently proposed by Avelar and Dixon (Avelar & Dixon, 2012). This function emerged from an effort evaluating the safety effect of advisory speed signs. The authors used a generalized linear regression model to characterize the relationship between crash data to geometry, road operations and signage characteristics of a sample of horizontal curves in Oregon. The ASCF is a factor emerging from this analysis that accounts for the safety effect of advisory speeds, after controlling for other important elements, such as radius, lane width, curve length, and traffic intensity, among others.

Denoting the components of $\begin{bmatrix} \grave{\hat{R}} \\ \acute{\hat{e}} \end{bmatrix}$ as estimated above, Equation 4-8 shows the optimal advisory speed as a function of a set of BBI readings:

Equation 4-8: Optimal Advisory Speed based on Dynamic-equivalent Estimates

$$AdvSpeed_{Optimal} = \frac{-2\left(\frac{\varphi_2 + SpLim \times \varphi_3}{15\grave{\hat{R}}}\right) + \sqrt{\frac{4(\varphi_2 + SpLim \times \varphi_3)^2}{225\grave{\hat{R}}^2} + \frac{4\beta_3 \times \left(\acute{\hat{e}} \times \varphi_3 - \varphi_1\right)}{5\grave{\hat{R}}}}}{-\frac{2\varphi_3}{5\grave{\hat{R}}}}$$

Where:

φ_1	=	ASD coefficient from the ASCF function ($\frac{1}{mph}$);
φ_2	=	SFD coefficient from the ASCF function (no units);
φ_3	=	ASD x SFD coefficient from the ASCF function ($\frac{1}{mph}$);
$SpLim$	=	Speed Limit (mph); and
$AdvSpeed_{Optimal}$	=	Advisory Speed (mph);

All other variables as previously defined.

Upon development of Equation 4-8 for computing the optimal advisory speed, this relationship can then be used to apply the OSU posting method, as it was described in greater detail at a previous work (Avelar & Dixon, 2012).

4.5.1. **Summary of Proposed Methodology**

This section reviewed in detail the development of the proposed Hybrid-OSU. Though the initial analysis may appear onerous, upon automation of the statistical estimation (using a spreadsheet or any portable device, such as a programmable calculator), the practitioner only needs to obtain and input a minimum of four readings for the BBI and associated speeds.

Figure 4-3 shows a graphic summary of the proposed methodology. The next section focuses in testing the performance of the methodology on the available data.

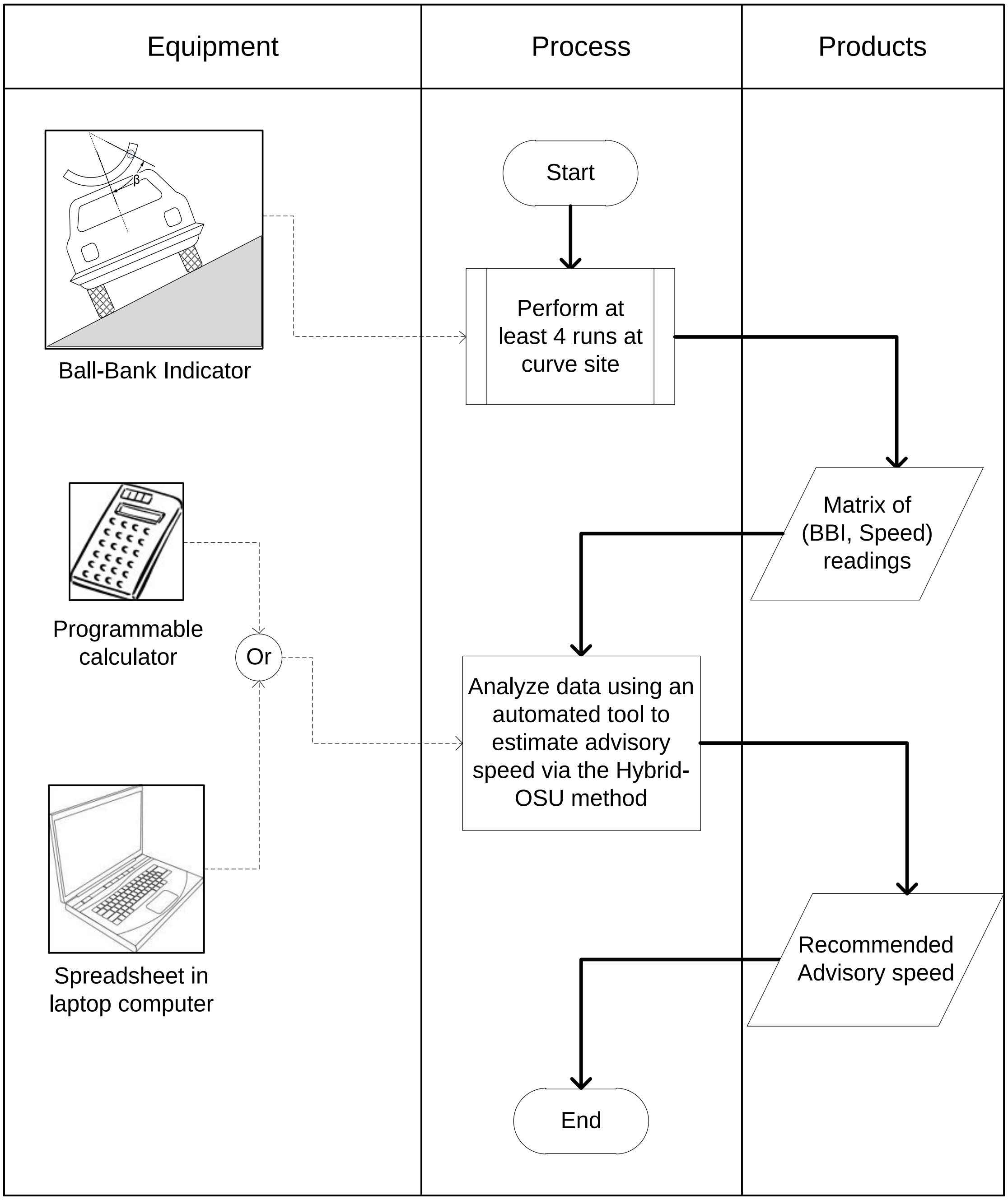

Figure 4-3: Schematic for the Hybrid-OSU Posting Method

4.6. Calibration and Validation of Proposed Methodology

As previously indicated, the Oregon sample is comprised of substantial BBI data collected at numerous sites. The offset value for ϑ_2 -the empirical $\hat{\alpha}$ coefficient- was not defined as 1.0 intentionally, so as to use it as a global calibration parameter. Additionally, the researchers treated the maximum allowable SFD for the Hybrid OSU method as another global calibration parameter, allowing it to vary independently from the fully computational OSU method maximum SFD. The authors performed a calibration of the methodology for state-maintained rural roads Oregon.

Table 4-1 shows the parameters resulting from the calibration process. These values were such that the trend of the OSU method was approximated by the Hybrid OSU method with none of the 90 state maintained sites exceeding the desired maximum SFD of 0.23 by more than 0.015.

Table 4-1: Maximum SFD and Global Calibration Parameter Estimates for the H-OSU Method

Parameter	**Value**
Maximum Recommended SFD	0.23
Maximum SFD used in Hybrid OSU method	0.15
Empirical $\hat{\alpha}$ offset value	-1.0

Figure 4-4 shows the expected safety performance, as of the Absolute ASCF criterion, for the calibration data set. As briefly discussed above, the ASCF criterion is a multiplier on the expected number of crashes. The Absolute ASCF is such multiplier referenced to the hypothetical scenario of removing the advisory speed plaque. Therefore, smaller Absolute ASCFs mean expectedly better safety performances. The differences among the trend are obvious: the faster decaying (better performing) trend corresponds to the OSU method. This relationship is not surprising since this is the method based on geometry information directly measured from the field.

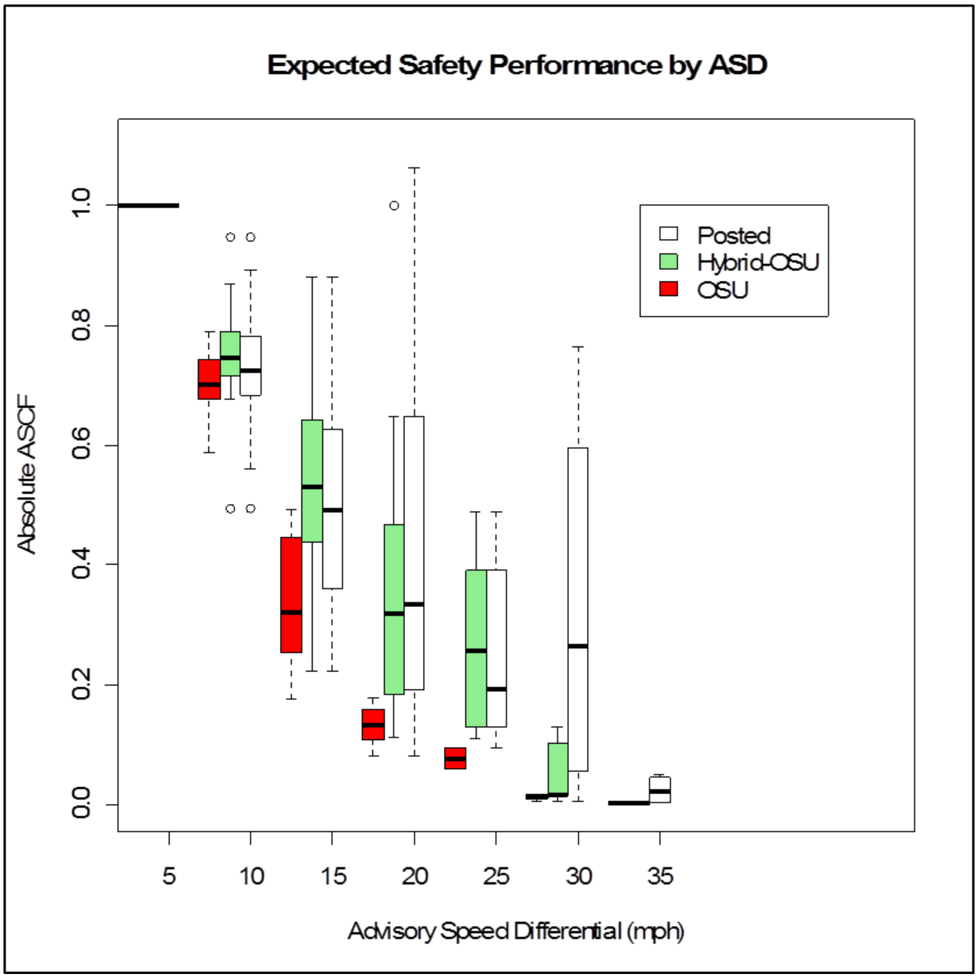

Figure 4-4: Expected Safety Performance by Posting Method (Calibration)

The second best performing is the Hybrid OSU method, as its trend roughly lies between the other two. As previously indicated, this hybrid method is based off of actual ball bank indicator readings. Finally, the actual posted advisory speeds also show a decaying trend line, and thus still can be expected to enhance safety. This is the set of advisory speeds that would be expected to have the poorest performance.

It is also noticeable that the most consistently performing method (i.e. the one with the least variation) is the OSU method, followed by the H-OSU method.

Using the same parameters from Table 4-1, the researchers repeated the computation of the OSU and Hybrid OSU method's advisory speeds, as well as the Absolute ASCF (AASCF), the corresponding measure of safety effectiveness. Figure 4-5 depicts a similar relationship for the county-maintained sites.

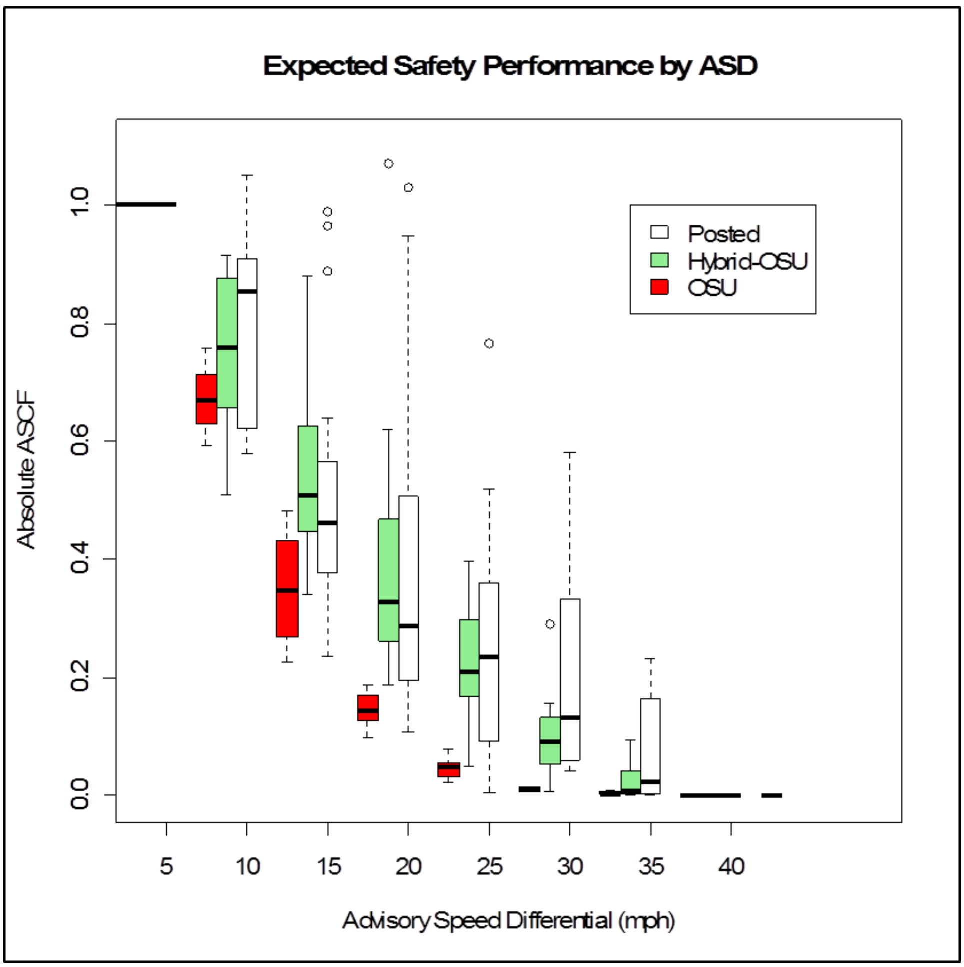

Figure 4-5: Expected Safety Performance by Posting Method (Validation)

Since the conclusions that one can derive from both figures are the same, the authors deemed the calibrated Hybrid OSU method as consistently validated on the second data set.

Finally, Figure 4-6 shows the SFD based on posting method for the validation data set. One relevant observation is that, similar to previous evaluations, the OSU method is the one that delivers advisory speeds associated with a more consistent SFD. The second most consistent in terms of SFD is, again, the Hybrid OSU method.

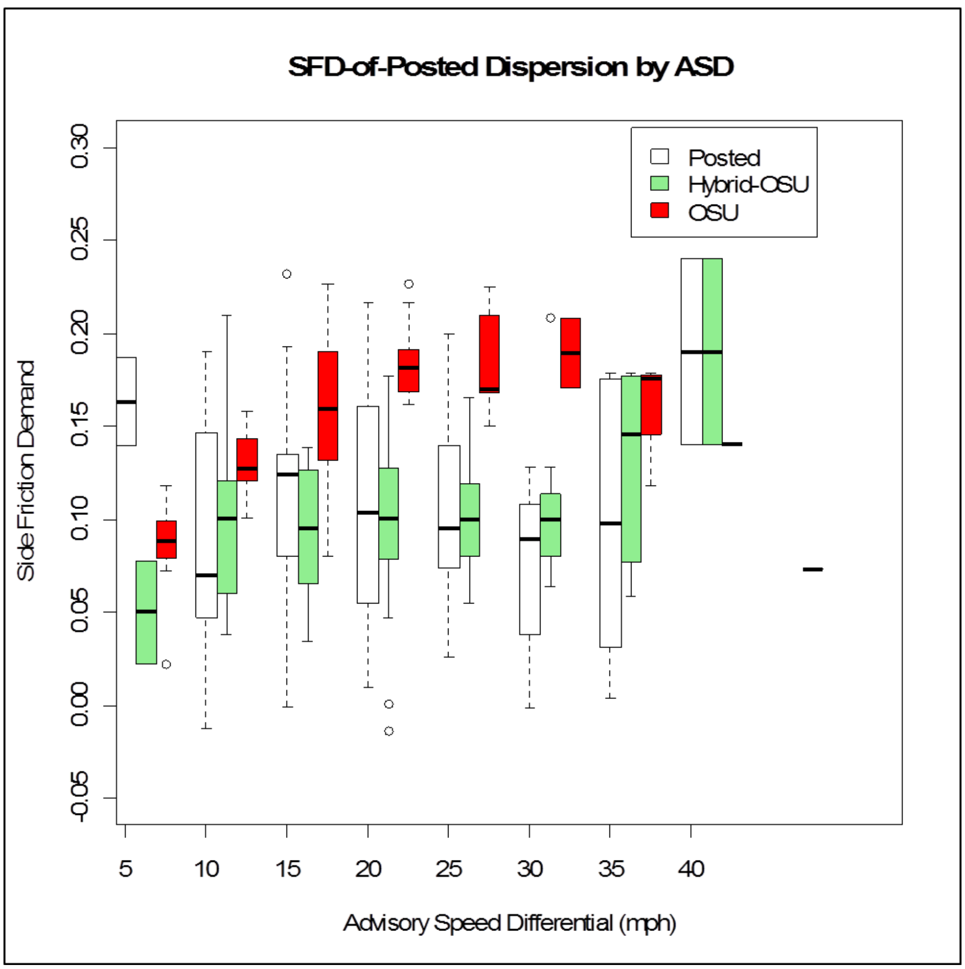

Figure 4-6: Actual Side Friction Demand by Posting Method (Validation)

This figure has another noticeable characteristic: the trends are quite different: the OSU method SFD climbs steadily from an average of about 0.1 for sites without posted signs, up to an average of about 0.2 for sites posted 20 mph below the speed limit. The SFD value appears similar for advisory speed differentials (ASDs) of 25 and 30 mph, and then drops to 0.15 for curves posted at an ASD of 35 mph. The data set only included one site with an ASD=40 mph (represented by a SFD of 0.215) and one site with an ASD=45 mph (a SFD value of 0.05). In contrast, the Hybrid OSU method slowly increases starting from 0.05 at ASD=5 mph, leveling off at 0.11, and remaining roughly flat until ASD=35 mph. This method includes two sites posted at ASD=40 mph with SFDs of 0.215 and 0.24 respectively. Finally, the trend of the posted advisory speeds begins to decline in value and increase in variability. The authors verified that in order for the Hybrid OSU method to follow the trend of the OSU method, it would allow some of the sites with high SFDs to exceed the desired maximum SFD of 0.23.

Finally, it is worth noting that the Hybrid OSU performance, as depicted in the validation assessment (Figure 4-5 and Figure 4-6), is based on the estimates that result from all the BBI readings available at each curve. The number of these BBI readings varied from 3 up 16 per site. The authors verified via several replications that such a performance is achievable when randomly selecting only 4 readings from every site. Therefore, the use of the Hybrid OSU method is recommended in conjunction with at least 4 runs and at least 3 different speeds. The use of this level of BBI assessment will minimize the bias associated with estimating $\begin{bmatrix} \grave{\hat{R}} \\ \hat{e} \end{bmatrix}$ from a limited range.

4.7. Conclusions

This paper reviews the development of a thorough analysis of the dynamics involved in determining the optimal advisory speed based on the BBI, an instrument widely used for advisor speed assessment but also know to result in a large variability in readings for the same or similar facilities. An analytical evaluation of the body roll angle emerges from the analysis in this paper including an observation that this angle can be expected to peak, on average, around a value of 2 degrees. However, the same evaluation indicated that when evaluating the expected variability around the body roll angle average, a systematic deviation of the BBI readings larger or equal to 9 degrees begins to emerge. Under some conditions, the body roll angle may be expected to reach values up to 4 or 5 degrees, a portion that is, in fact, significant when compared to expectedly maximum BBI readings of 15-16 degrees. The assessment concluded with the construction of an empirical model that can explicitly account for this effect. Ultimately, the authors used the body roll angle as an additional degree of freedom in the calibration process of the Hybrid OSU method, the mitigation methodology that was the ultimate goal of this paper.

The authors then expanded the mathematical relationships that emerged from the dynamics analysis in an effort to link the BBI readings to the concept of the optimal advisory speed, a measure that represents the best expected safety performance as proposed by these authors in a previous publication (Avelar & Dixon, 2012). The authors labeled this emerging methodology as the Hybrid OSU method, a method that basically includes two steps: (1) using as many BBI readings as available from a site to obtain dynamics-equivalent regression estimates of the horizontal radius and superelevation, and (2) using the dynamics-equivalent estimates to compute the optimal advisory speed, as proposed in (Avelar & Dixon, 2012).

To demonstrate performance of the newly developed methodology, the authors applied the procedure to two random Oregon-specific data sets. The authors calibrated the methodology using one of the samples, and subsequently validated the procedure with the other sample. In general, it is expected that the new methodology performs better than the traditional BBI method in terms of consistent SFDs and expected safety improvements. The authors argue that the reason for the improvement is that, as opposed to the traditional BBI method, the proposed methodology is statistically efficient: the more BBI readings available, the more accurate the estimated parameters, thus the more consistent the resulting advisory speed.

Noteworthy is the fact that the Hybrid OSU method requires additional computational efforts, but such efforts have the potential to be easily automated, so practitioners will likely have a computational tool readily in the field when using this new BBI based method (e.g. a laptop computer, a programmable calculator, a smart phone, etc.)

Although the Hybrid OSU method performed better than the traditional BBI method, this analysis also demonstrated that whenever the horizontal radius and superelevation are available or easily obtainable, the recommended method would be the OSU method as proposed in a previous work. This method is the one that yields the more consistent sets of SFDs and the one theoretically associated with the larger reduction in expected number of crashes.

The authors conclude that the Hybrid OSU method is a feasible alternative to the traditional BBI method for practitioners who would prefer using the BBI or for locations where it is not possible or reliable to obtain information about the radius and superelevation of a curve.

4.8. **Bibliography**

AASHTO. (2004). A Policy on Geometric Design of Highways and Streets (5th Edition). Washington, D.C.: AASHTO.

AASHTO. (2010). Highway Safety Manual. Washington, D.C.: AASHTO.

Avelar, R. E. (2010, August 16). Effectiveness of Curve Advisory Speed Signs. A Characterization of Road Operations in Western Oregon. Retrieved November 08, 2010, from Scholars Archive at OSU: http://hdl.handle.net/1957/17673

Avelar, R. E., & Dixon, K. K. (2011). Modelling the Safety Effect of Advisory Speed Signs: A Bivariate Multiplicative Factor on Number of Crashes based on the Speed Differential and the Side Friction Demand. 3rd International Conference on Road Safety and Simulation, September 14-16, 2011, Indianapolis, USA. 3rd International Conference on Road Safety and Simulation. Indianapolis, IN: Transportation Research Board.

Avelar, R. E., & Dixon, K. K. (2012). How Far are Current Advisory Speeds from being Optimal? An Analysis Based on Safety Performance. Washington D.C.: Transportation Research Board.

Bonneson, J. A. (1999). Side Friction Demand and Speed as Controls for Horizontal Curve Design. Journal of Transportation Engineering, 473-480.

Bonneson, J. A., Pratt, M. P., & Miles, J. (2009). Evaluation of Alternative Procedures for Setting Curve Advisory Speed. Transportation Research Record 2122, 9-16.

Bonneson, J., Pratt, M., Miles, J., & Carlson, P. (2007). Development of Guidelines for Establishing Effective Curve Advisory Speeds. Springfield, VA: FHWA.

Carlson, P. J., Burris, M. W., Black, K., & Rose, E. R. (2005). Comparison of Radius-Estimating Techniques for Horizontal Curves. Transportation Research Record (1918), 76-83.

Charlton, S. G., & De Pont, J. J. (2007). Curve Speed Management. Land Transportation New Zealand Research Report 323. Waterloo Quay, Wellington, New Zealand: Land Transportation New Zealand.

Chowdhury, M. A., Warren, D. L., Bissell, H., & Taori, S. (1998). Are the Criteria for Setting Advisory Speeds on Curves Still Relevant? ITE Journal. February, 32-45.

Courage, K. G., Bastin, H. E., Byington, S. R., Cook, A. R., Ferro, W. N., Freeman, R. L., . . . Zogby, J. J. (1978). Review of Usage and Effectiveness of Advisory Speeds. ITE Journal. September, 43-46.

Dixon, K. K., & Avelar, R. E. (2011). SPR 685: Safety Evaluation of Curve Warning Speed Signs. Salem, OR: ODOT.

Dixon, K. K., & Rohani, J. W. (2008, January). SPR 641: Methodologies for Estimating Advisory Curve Speeds on Oregon Highways. Salem, OR: Oregon Department of Transportation. Retrieved April 13, 2009, from Oregon Department Of Transportation: http://www.oregon.gov/ODOT/TD/TP_RES/docs/Reports/2007/SPR_641.pdf

Eccles, K. A., & Hummer, J. E. (n.d.). Safety Effects of Fluorescent Yellow Warning Signs at Hazardous Sites in Daylight Curves. Washington, DC: Transportation Research Board.

Elvik, R., & Vaa, T. (2004). "Handbook of Road Safety Measures.". Oxford, U.K.: Elsevier.

FHWA. (2009). Manual on Uniform Traffic Control Devices. Washington, D.C.: U.S. Department of Transportation.

Fox, J., & Weisberg, S. (2011). An {R} Companion to Applied Regression, Second Edition. Thousand Oaks, CA: Sage. Retrieved from http://socserv.socsci.mcmaster.ca/jfox/Books/Companion

Gates, T. J., Carlson, P. J., & Hawkins Jr., H. G. (2004). Field Evaluations of Warning and Regulatory Signs with Enhanced Conspicuity Properties. Transportation Research Record 1862, 64-76.

Glennon, J., Newman, T., & Leisch, J. (1985). Safety and Operational Considerations for Design of Rural Highway Curves. Washington, D.C.: Federal Highway Administration.

Kanellaidis, G. (1995). Factors Affecting Drivers' Choice of Speed on Roadway Curves. Journal of Safety Research, Vol. 26(Spring 1995), 49-56.

Koorey, G., Page, S., Stewart, P., Gu, J., Ellis, A., Henderson, R., & Cenek, P. (2002). Curve Advisory Speeds in New Zealand. Lambton Quay, Wellington, New Zealand: Transfund New Zealand.

Lyles, R. W. (1982). Advisory and Regulatory Speed Signs for Curves: Effective or Overused? ITE Journal. August, 20-22.

Lyles, R. W., & Taylor, W. C. (2006). Communicating Changes in Horizontal Alignment. Washington, D.C.: Transportation Research Board.

ODOT. (2006). Traffic Manual and the ODOT Sign Policy and Guidelines. Salem, OR: Oregon Department of Transportation.

R Development Core Team. (2011). R: A language and environment for statistical computing. Vienna, Austria: R Foundation for Statistical Computing. Retrieved from http://www.R-project.org/

Ritchie, M. L. (1972). Choice of Speed in Driving Through Curves as a Function of Advisory Speed and Curve Sign. Human Factors, 533-538.

Venables, W. N., & Ripley, B. D. (2002). Modern Applied Statistics with S. Fourth Edition. New York: Springer.

Winkelmann, R., & Zimmermann, K. (1991). A New Approach for Modeling Economic Count Data. Economics Letters 37, 139-143.

Zegeer, C. V., Stewart, J. R., Council, F. M., Reinfurt, D. W., & Hamilton, E. (1992). Safety Effects of Geometric Improvements on Horizontal Curves. Transportation Research Record, 11-19.

Zwahlen, H. T. (1987). Advisory Speed Signs and Curve Signs and Their Effect on Driver Eye Scanning and Driving Performance. Transportation Research Record (1111), 110-120.

Zwahlen, H. T., Russ, A., & Schnell, T. (2003). Driver Eye Scanning Behavior While Viewing Ground-Mounted Diagrammatic Guide Signs before Entrance Ramps at Night. Washington, D.C.: Transportation Research Board.

5. Additional Content not Included in Manuscripts

This chapter consists mostly of material that the author initially developed to be included in the three manuscripts heretofore presented, but that was excluded from the final versions due to the space constraints of the conferences and journals.

Additionally, this chapter includes some discussions and materials derived from the more relevant comments of reviewers to the manuscripts and the corresponding clarifications that this author crafted in response. Particular emphasis was given to observations and responses that are important but that did not make it to the final version of the manuscripts due to space constraints.

Finally, this chapter includes additional materials that this author developed in areas of this work that were not extensively addressed in the manuscripts.

5.1. Overview of the Data Used in this Work

This section presents a brief summary of the data used in this dissertation, particularly focusing on the modelling data set and the most relevant variables that were included in the various analyses of this work.

5.1.1. Probability Sample of Oregon Curve Sites

As previously described, chapter 2 is based on a probability sample of curve sites that is representative of the state of Oregon. This probability sample was available from a previous work by Dixon and Rohani (2008). These researchers intended to study 32 corridors selected from each ODOT region that comprise the state of Oregon. In total, they selected 160 corridors, half of which were collected from state-maintained highways and the other half from county-maintained highways. Figure 5-1 shows a schematic of the sampling procedures followed by Dixon and Rohani.

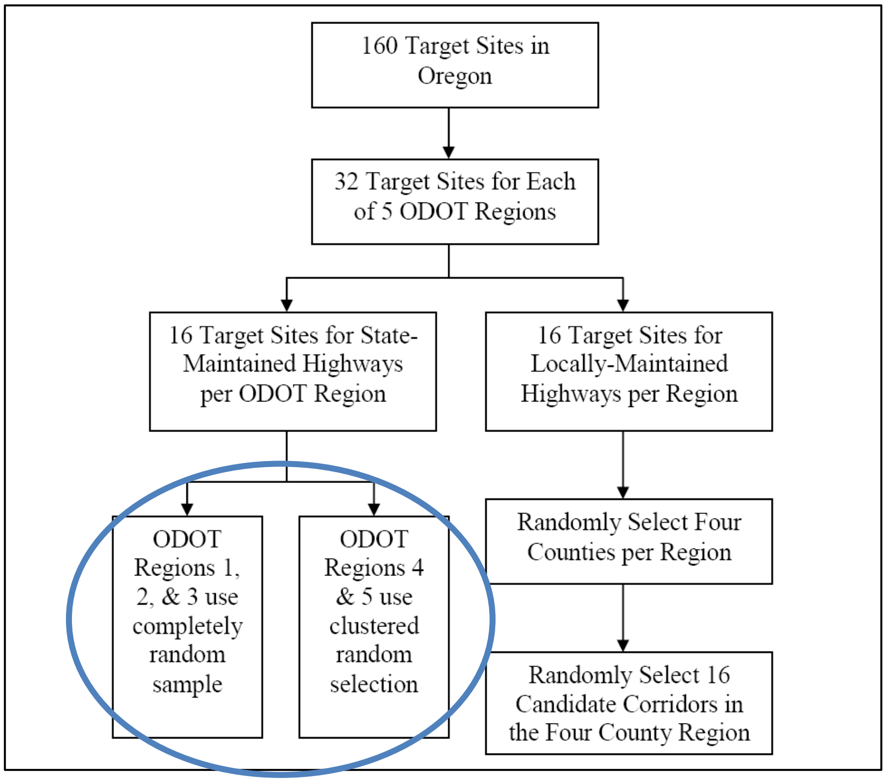

Source: Avelar, 2010

Figure 5-1: Probability Structure of Sampling Procedure by Dixon and Rohani

The 210 curve sites used in chapter 2 are located along the 80 corridors randomly selected through the procedure in the left branch of the sampling scheme, showed circumscribed by an ellipse in Figure 5-1. The rest of sites collected by Dixon and Rohani were used for the validation effort presented in chapter 4 (i.e. 90 curve sites coming from the 80 corridors at locally-maintained highways, shown in the right branch of Figure 5-1).

As can be inferred from this figure, the sampling procedure was such that each county had equal weights (in the case of the locally-maintained sites) regardless of its size and constitution. Similarly, in the case of state-maintained roads, the sampling procedure equally weighted each ODOT region. However, the weights of the second sampling stage within regions 1, 2, and 3 clearly differed from the weights used for regions 4 and 5. Obtaining analytical forms of the overall probability structure and the sampling errors of this tree-like, multi-stage sampling scheme is not a simple task. As an example, previous work by this author presents the analytical forms and estimates of such sampling errors for a sub set of sites from the state-maintained sample (Avelar, 2010). Figure 5-2 shows the geographic distribution of such a sub-sample, which is still statistically representative of state-maintain roads in ODOT regions 1, 2 and 3.

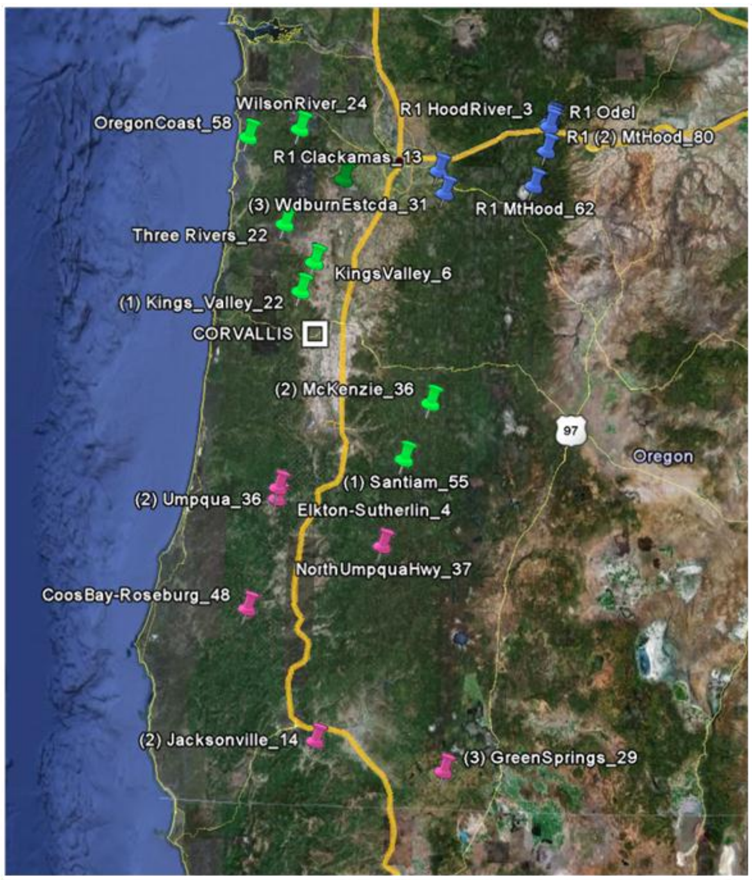

Figure 5-2: Geographic Distribution for a Double-sample of State Maintained Sites

Table 5-1 shows the functional classification of the samples obtained by the schematic shown in Figure 5-1. When comparing the state-maintained and county-maintained samples, a shift toward facilities that prioritize mobility is evident in the state maintained sites.

Table 5-1: Functional Classification of Selected Sites

State-Maintained Highways				
Local and Minor Collector	Major Collector	Minor Arterial	Principal Arterial	Total
0	11	38	31	80
County-Maintained Highways				
Local and Minor Collector	Major Collector	Minor Arterial	Principal Arterial	Total
12	64	10	0	86

Noteworthy to mention is that the methods heretofore proposed were adequate to be used at county maintained highways as well, given that the effort in chapter 4 validated such site transferability for the tools presented in this dissertation.

5.1.2. **Site Characteristics at State-maintained Roads**

This section presents a brief summary of site characteristics at the modelling sample (i.e. state-maintained sites).

In order to convincingly study the effect of advisory speeds, a sample covering a wide range of geometric conditions, including different parameter configurations is required. Figure 5-3 shows the range of advisory speed presence as it relates to the horizontal radius. A difference between the two sets of sites becomes apparent (i.e. sites with posted advisory speeds tend to have smaller radii than sites without these signs).

Regardless, a differentiation between the advisory speed presence and radius effects is still feasible, given that most of the radius bins include sites with posted advisory speeds and sites without them.

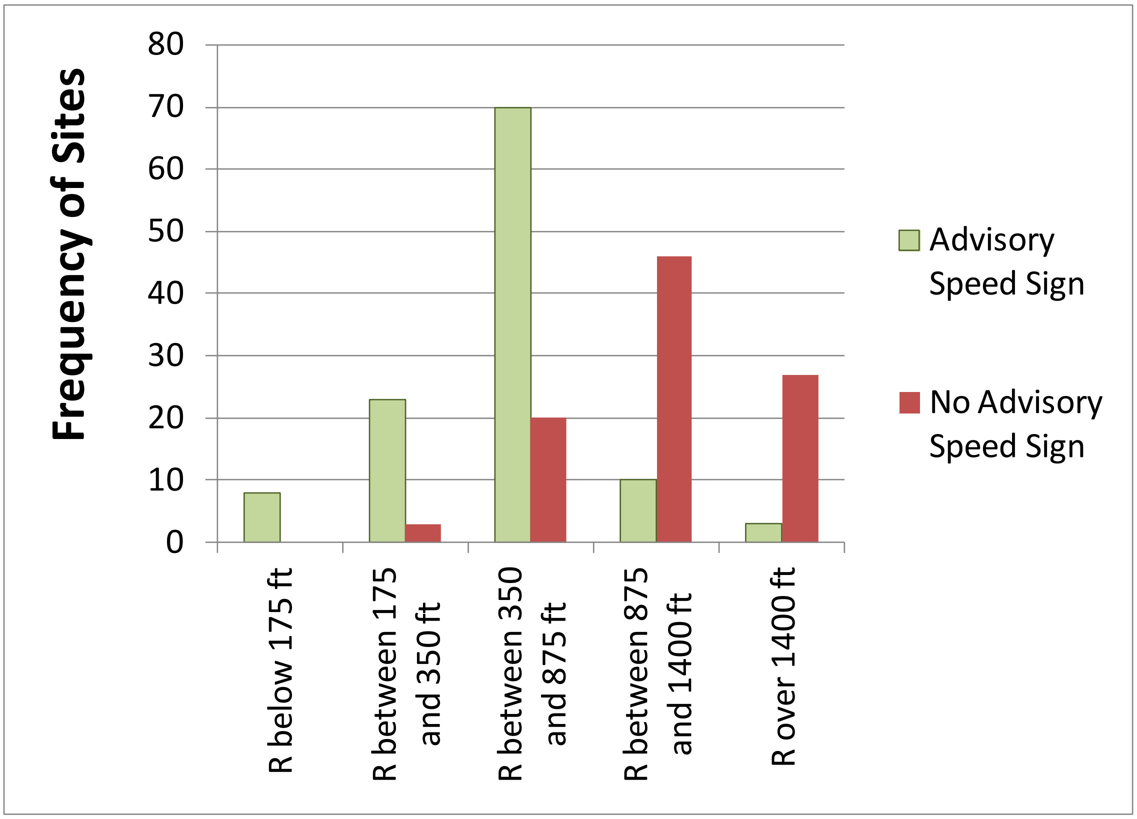

Figure 5-3: Site Frequency by Radius and Advisory Speed Presence

However, as the radius becomes smaller, the ability to discern between these effects quickly diminishes. In the extreme case, such a contrast is not possible for the bin with radii smaller or equal to 175 ft, since that bin only contains sites displaying advisory speed signs.

Similar to Figure 5-3, Figure 5-4 shows that a meaningful contrast between sites displaying advisory speed signs and sites without these signs is feasible when accounting for curve length.

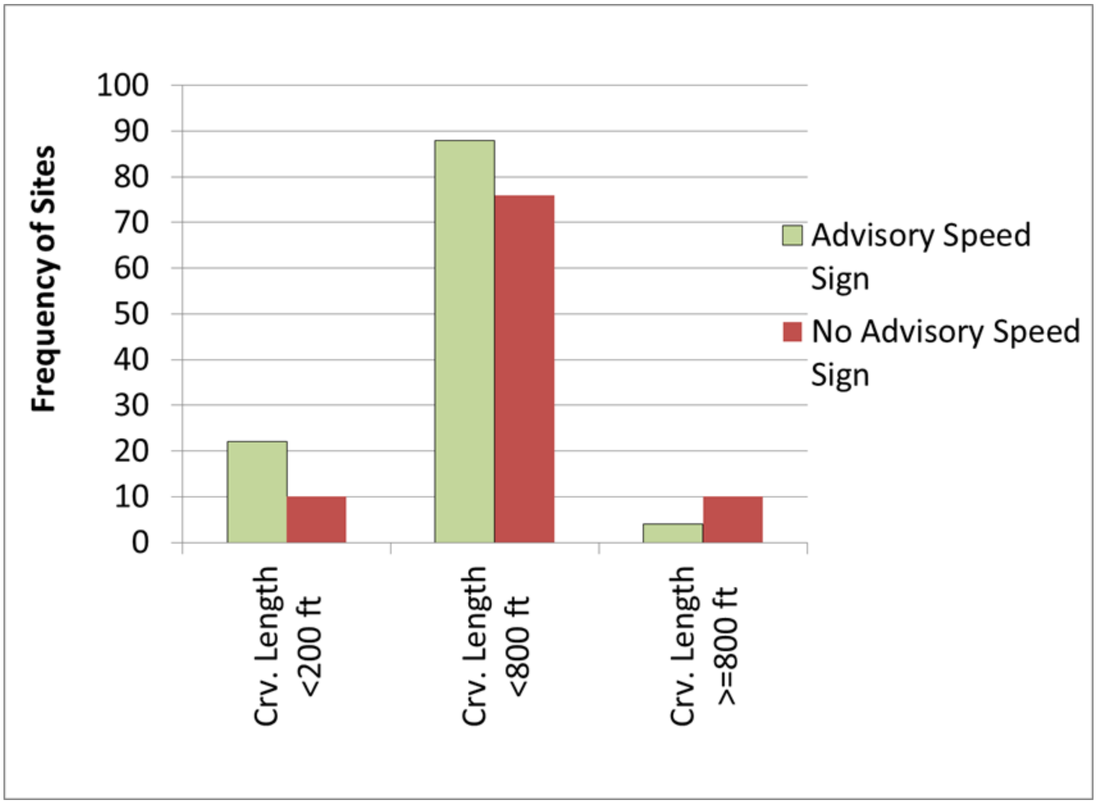

Figure 5-4: Site Frequency by Curve Length and Advisory Speed Presence

Finally, Figure 5-5 shows that the sample includes a relatively wide range of AADTs, ranging from 106 vpd up to 13,700 vpd, a desirable characteristic for the work in this dissertation. This figure shows that a meaningful contrast between the presence and the absence of advisory speeds can be performed for a wide range of traffic intensities.

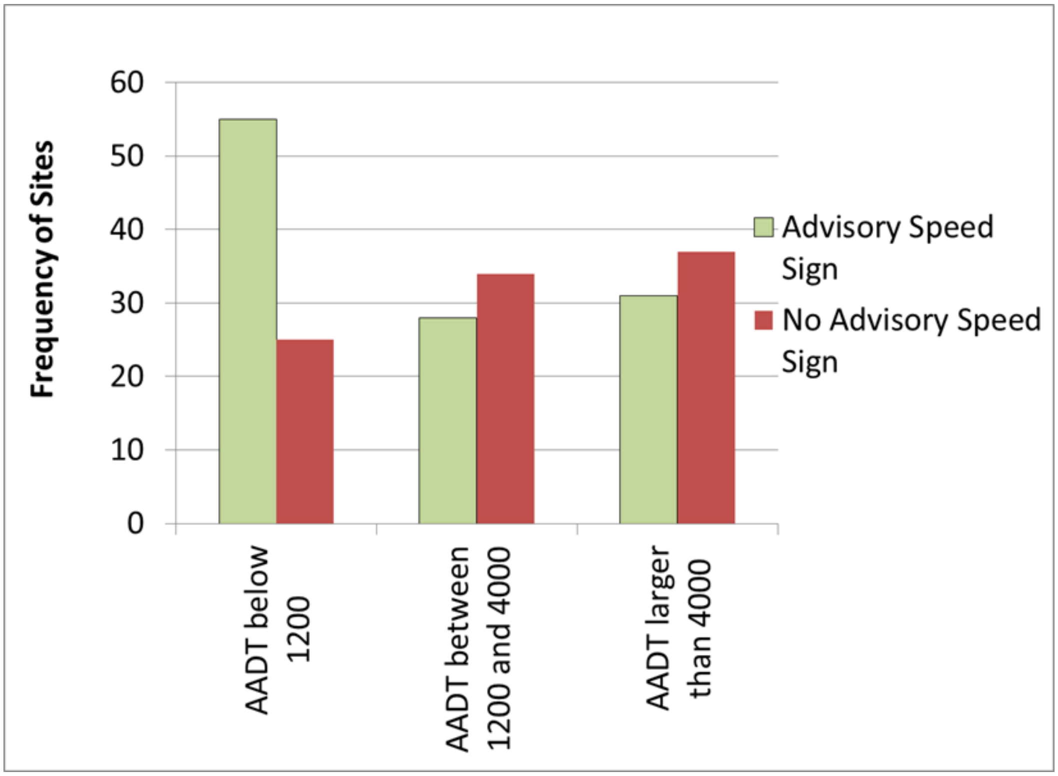

Figure 5-5: Site Frequency by AADT and Advisory Speed Presence

Because the core of this dissertation lies on characterizing the relationship between crash history and the data described in this section, the following section presents crash data characteristics at the state-maintained sample sites.

5.1.3. **Crash Data Characteristics at State-maintained Sites**

This author supplemented the data available from Dixon and Rohani's work with the corresponding 5-year crash history at every site for the period of 2000-2004. Since this dissertation is based on a probability sample, the range of such additional data is necessarily representative of the safety profile of curve sites for the state of Oregon. The crash frequency in the modelling sample of 210 directional curves totaled 207 crashes, ranging from the most common value of zero (125 sites did not exhibit any record of crashes) up to 11 crashes at one particular site. The actual distribution of crashes is shown in Table 5-3 later in this chapter.

Figure 5-6 shows a sample site with relatively intense traffic volume. As a result, crash frequency is relatively high, but the safety of this curve is also influenced by the presence of an intersection. The severity level of crashes is moderate.

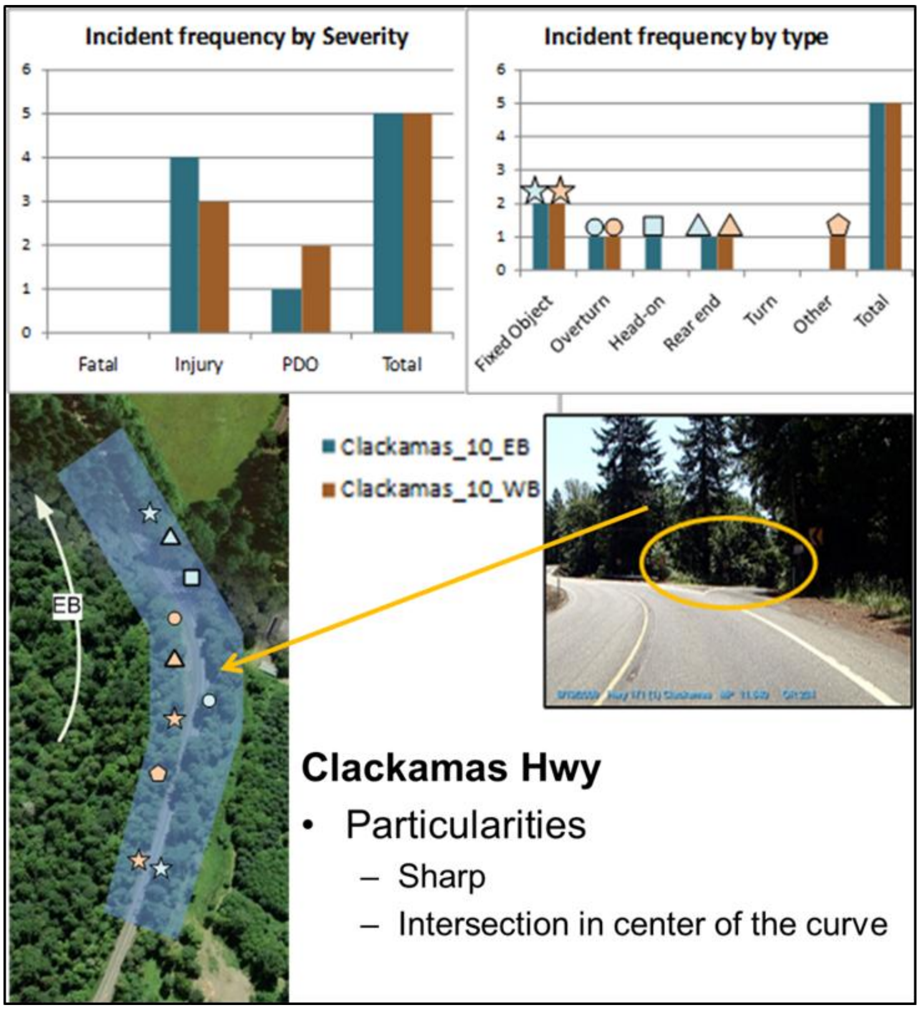

Figure 5-6: Data Characteristics at a Sample Site (Clackamas Hwy MP 10)

In contrast, Figure 5-7 shows a site with lower traffic intensity and low crash frequency but one that is clearly prone to speeding crash occurrence. Since this site includes a compromising combination of vertical and horizontal alignments, it is not surprising to observe that the severity of crashes at this location is significantly increased.

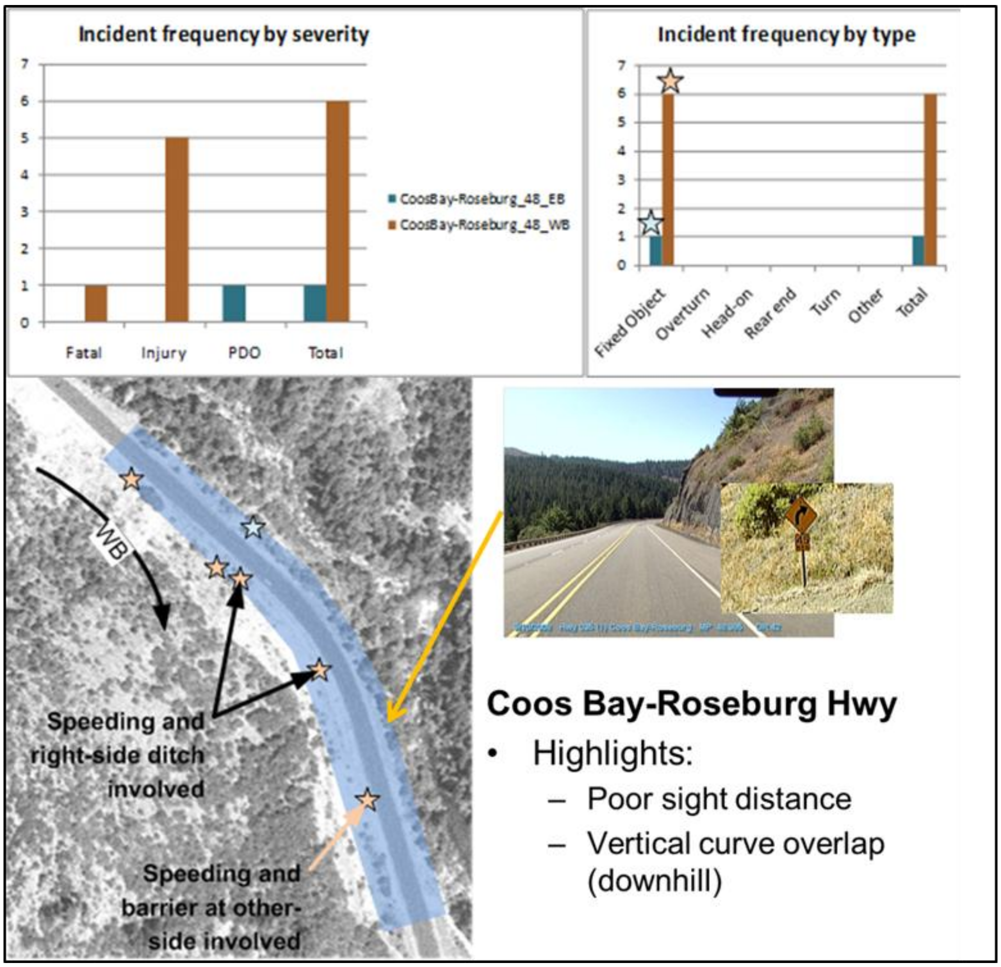

Figure 5-7: Data Characteristics at a Sample Site (Coos Bay-Roseburg Hwy MP 48)

Figure 5-8 displays a curve at a highway with high traffic intensity but with a more forgiving geometry. Although the crash frequency is high, in this case the severity of crashes is moderate.

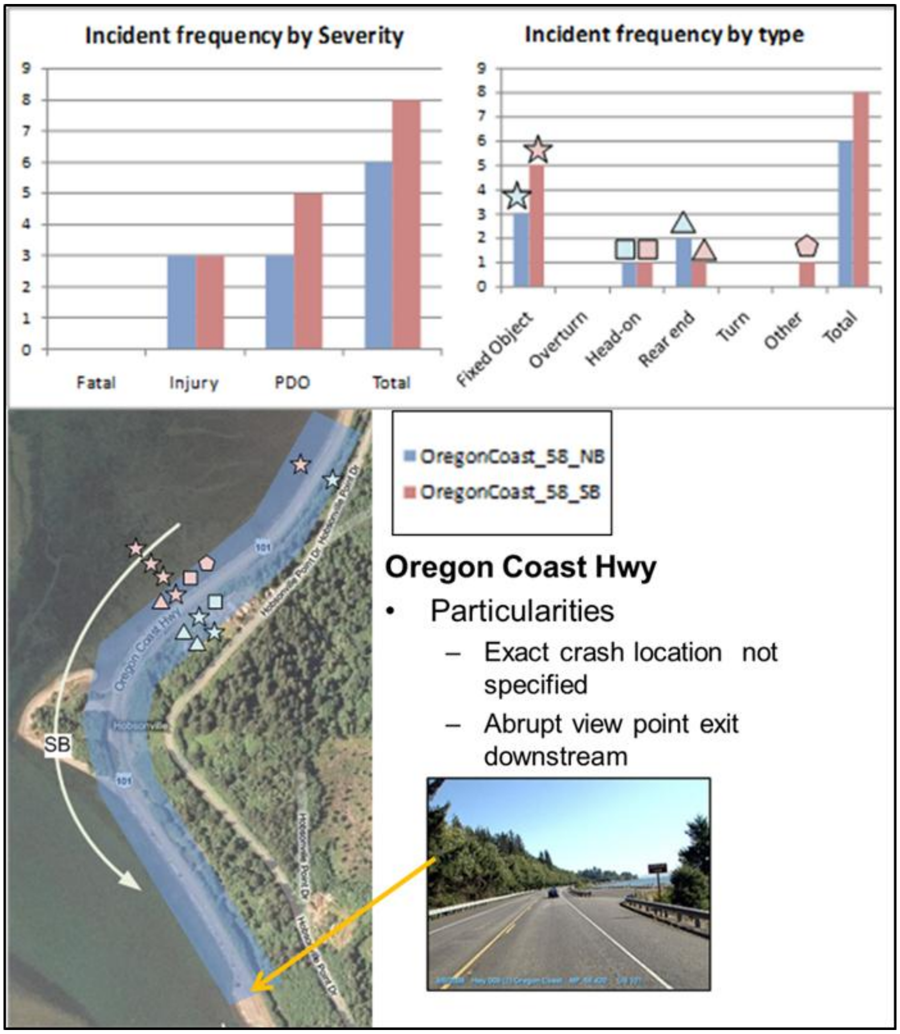

Figure 5-8: Data Characteristics at a Sample Site (Oregon Coast Hwy MP 58)

However, it is clear that there is some anomaly regarding the reported location of crashes at this curve. It is very unlikely that most reported crashes actually occurred at a single point location that incidentally had an integer milepost, as displayed in the figure. Such circumstances, among others discussed in the next section, required a degree of filtering in the data before any modelling work, as presented in chapter 2.

5.2. Crash Data Filtering Prior to the Modelling Effort

Before performing the statistical analysis, it was necessary for the author to filter the crash data so as to exclude crashes unlikely to be associated with curve geometry and signage, the main focus of this research. In order to draw meaningful comparisons, this author compiled all the crashes that occurred along 2-mile corridors from which the study curves were selected, in addition to the crashes associated with the curve locations. These crashes served as a baseline to compare the study site crashes to characteristics of crashes in the site surroundings. Figure 5-9 shows the 1104 crashes at the 2-mile corridors depicted by severity levels.

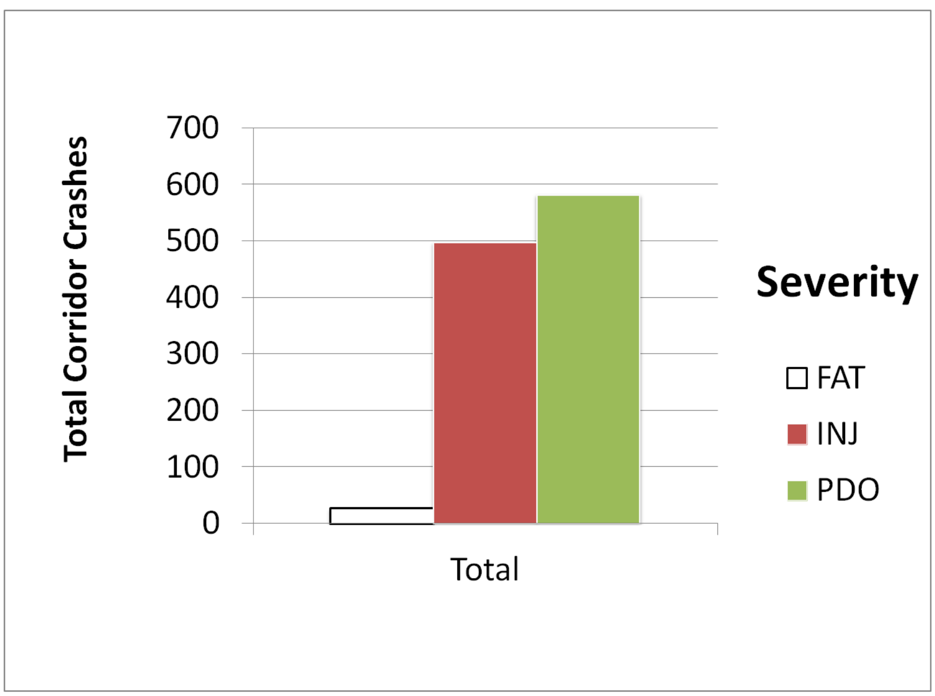

Figure 5-9: Total Crashes in Set of 2-mile Corridors by Severity

In general, this author expected that the crashes at the curve locations would exhibit characteristics that are clearly different from those of the 2-mile corridor baseline.

Figure 5-10 shows the proportions of crash severities by their relative locations within the 2-mile corridors (In Study Curve vs. Out of Study Curve) relative to the corresponding global proportions (the proportions that may be obtained from the totals presented in Figure 5-9). The chances of crashes resulting in fatality at the study curves roughly double the overall chances of fatality crashes in the 2-mile segment. Similarly, the chances of crashes resulting in injuries are about 15% larger than the corresponding global chances at the 2-mile corridors.

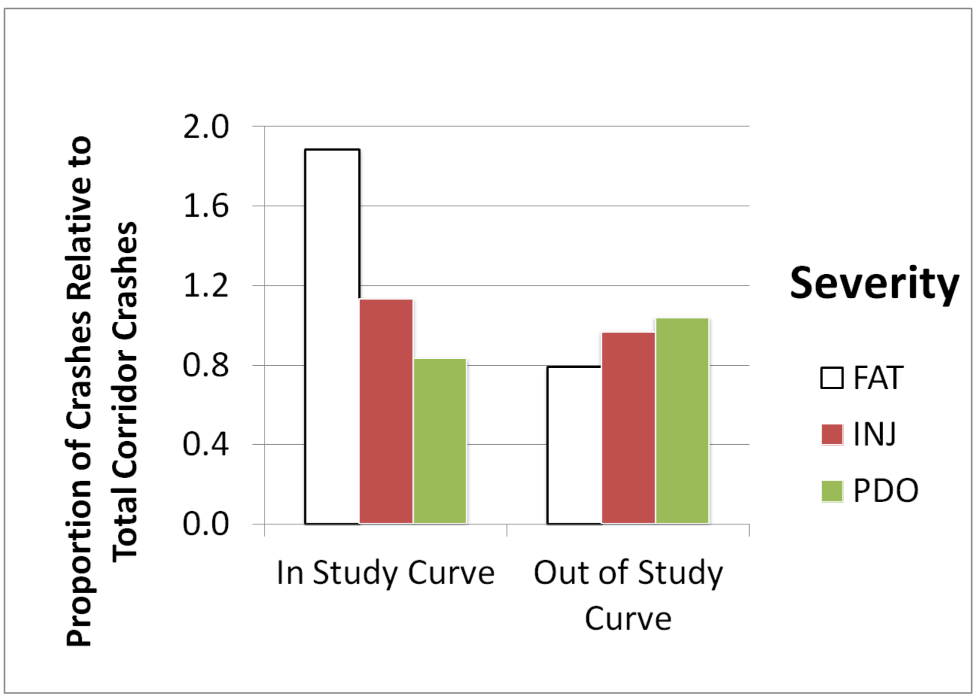

Figure 5-10: Proportion of Crashes by Different Severities Relative to Total Crashes in 2-mile Corridors

Along this line of comparison, this author expected that the chances of run-off-road crashes (ROR) would likely be large when compared to the overall chances of ROR crashes in the segments. However, ROR crashes are ubiquitous, and no clear rule to filter the data based on this characteristic is available. This author then turned again to examining the differences between the 2-mile segments and the study curves.

Figure 5-11 shows the ratio of the proportions of ROR and non-ROR crashes to the corresponding proportions of ROR and non-ROR crashes from the 2-mile corridors (these ratios are obtained in the same way that are the proportions in Figure 5-10).

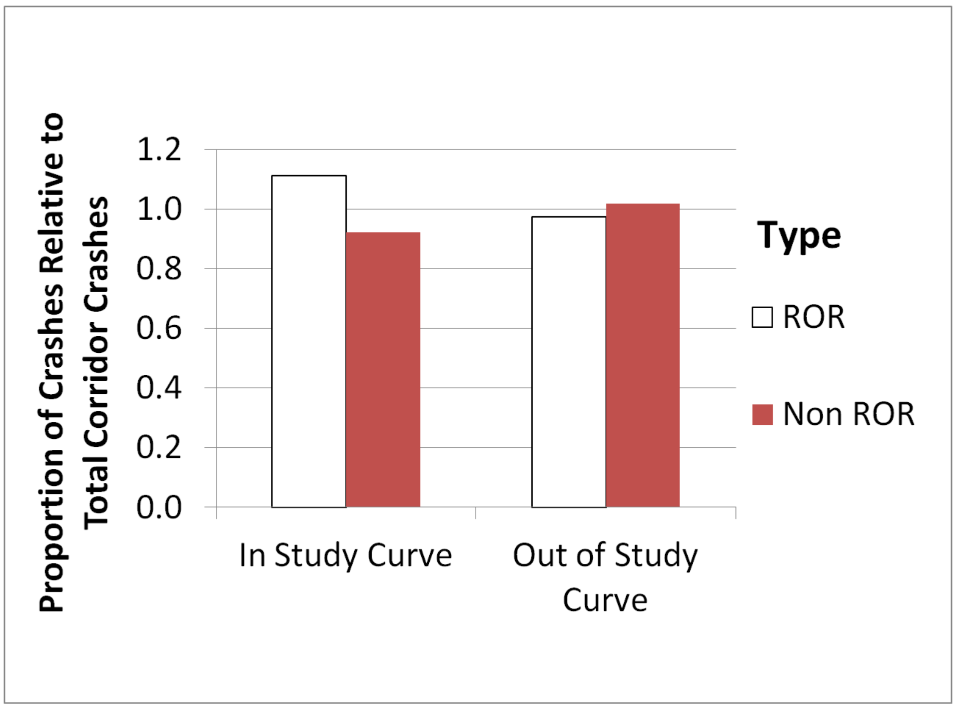

Figure 5-11: Proportions of ROR and non-ROR Crashes Relative to Total Corridor Crash Proportions

It is apparent from this figure that the chances of observing ROR crashes at the study curves are slightly larger than one would expect if the chances were uniform in the 2-mile corridors. Conversely, the chances of observing non-ROR crashes at the study curves are around 0.9 of the chances that one would expect in the 2-mile corridors. These differences, however, are minimal and may not be statistically significant.

It is well known that crashes reported as angle, rear-end and turn collisions are most likely associated with intersections or driveways. Figure 5-12 shows the expected ROR and non-ROR proportions for these kinds of crashes only. The chances of non-ROR crashes are the same at study curves, as well as outside of them (i.e. this type of crashes occurs uniformly within the corridors). However, this figure differs very clearly from Figure 5-11 when looking at the ROR crashes: the chances of observing ROR intersection-like crashes in the study curves are remarkably smaller than the chances at the whole corridor (about 60% of the corridor chances). This difference clearly suggests different mechanisms influencing crash occurrence, and provided this author with a sound reason to exclude the intersection-like crashes from the analysis.

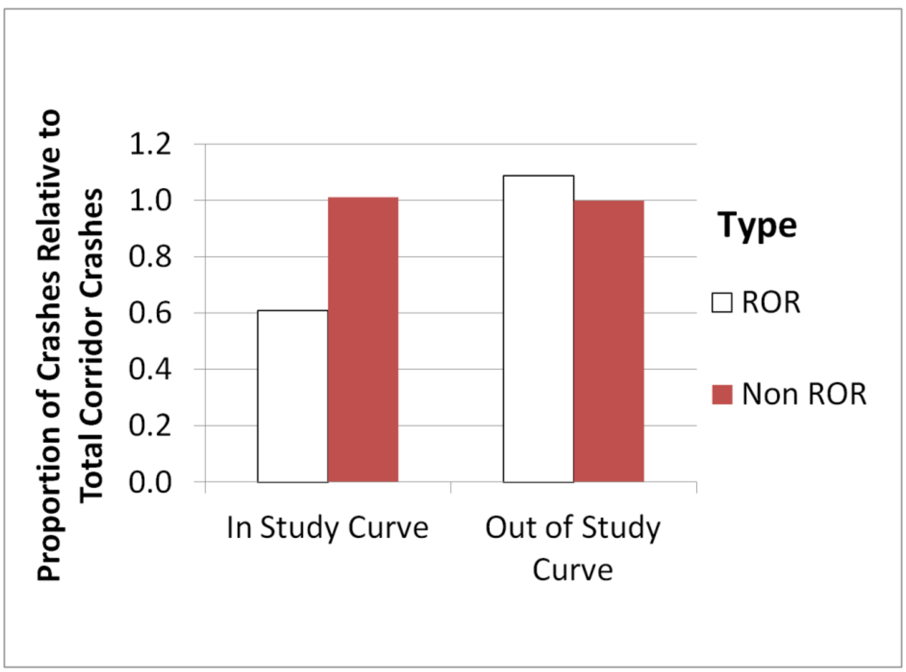

Figure 5-12: Proportions of ROR and non-ROR Intersection-like Crashes Relative to Total Segment Crash Proportions

Figure 5-13 shows the relative proportions after removing the intersection-like categories of crashes. Although the curve relative proportion of ROR crashes remains almost unchanged (about 110% of the corridor proportion), the proportion of non-ROR crashes is further reduced from around 90% to 80% of the corridor proportion.

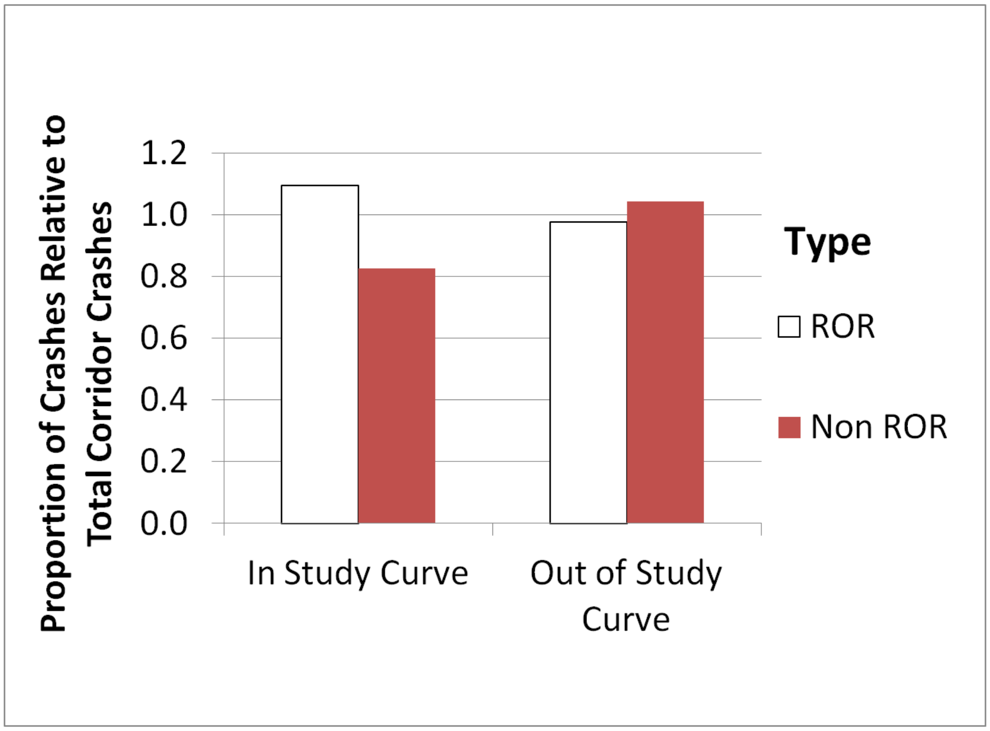

Figure 5-13: Expected Proportions of ROR and non-ROR Crashes Relative to Corridor Crashes, after Removing Intersection-like Crashes

Finally, this author performed a second filtering of the crash data. Some of the crash records exhibited mile posts recorded as whole-numbers. At some 2-mile corridors, several crashes appeared concentrated at the exact-mile locations, a very unlikely trend from a statistical point of view. Since some of the exact mile posts were located within the boundaries of a few study curves, this author faced the problem of discerning "round-up" mileposts from those that were truly located at exact mile posts. Although high density clusters of crashes at exact mileposts were easily identified as round-ups, and thus removed from the data set, such a distinction was not clear at locations with few crashes but with one or two crashes at exact mileposts. To overcome this difficulty, this author compared the on-site characteristics of the remaining crash records with exact mileposts (identified as “possibly curve located” at this point) to the records already identified as curve located.

Because the site sample corresponds to a probability sample, this author expects that the geometry, signage and crash distributions observed from the sample are statistically representative of the regional average distributions (previous work by Avelar (2010) used this feature to characterize the road operations at curve sites in the western region of Oregon). Although the horizontal radius is a natural choice to compare the two sets of crashes, the number of possible curve located crashes was too small and the range of horizontal radii too wide to perform such a comparison. Instead, this researcher used the presence of advisory speeds and the two sets of crashes to create the contingency table shown in Table 5-2.

Table 5-2: Number of Crashes by Location and Advisory Speed Sign Presence

	With Advisory Speeds	Without Advisory Speeds	Grand Total
Curve Located	71	47	**118**
Possibly Curve Located	17	24	**41**
Grand Total	**88**	**71**	**159**

A Pearson’s chi-squared homogeneity test with Yates’ continuity correction yielded a test statistic of 3.5845 on 1 degree of freedom. This corresponds to a p-value of 0.058, which is mildly suggestive of heterogeneity among the variables in the table. This circumstance, in turn, suggests that including the sites with possibly imprecise mileposts may exacerbate the model bias when accounting for advisory-speed associated variables as predictors. It is clear that the distribution of crashes by presence of advisory speed signs is different for crashes where milepost values were rounded to integer values. Because of this potential for furthering bias, this author did not include the 41 possible curves affected by this rounding in the subsequent analysis. This statistical test was performed on the statistical computing language R (The R Development Core Team, 2009). This author performed no further filtering of the data before proceeding to the statistical analysis.

5.3. Robustness of Selected Model (Material Supplemental to Sections 2.6 and 3.10)

Subsection 5.3.1 is an extension of material already presented in section 3.10. Subsection 5.3.2 briefly presents an additional effort of this author to account for structural correlation in the response variable. This effort expands on what was already presented in section 2.6. Finally, subsection 5.3.3 presents a brief analysis and interpretation of the role of curve length in the model. This variable coefficient is anomalous at first sight, but this author found the apparent anomaly being unfounded after a closer look at its ramifications. This subsection expands on the concern of a reviewer of the second manuscript.

5.3.1. Development of the Overall Goodness of Fit Test introduced in Section 3.10.2

The test proposed in section 3.10.2 is based on the closed form of the probability function of number of sites, given a particular number of crashes. This is a formulation alternative to looking at the conditional distribution of crashes, given the covariates, which is a goodness of fit point of view based on the log-likelihood function from regression diagnostics. This alternative test was developed in order to avoid the requirement of assuming normality of the regression goodness-of-fit estimates, which relies on the law of large numbers. This formulation is justified precisely because the available validation sample can hardly be called ‘large enough’ (only 44 sites).

The marginal probability of the total number of crashes is required in order to determine the expected distribution of number of sites given a particular number of crashes in a sample of n sites. In order to arrive at the required distribution, this author first defined the available sample as a theoretical population of sites from which a census was obtained. Even under the assumption of a known population, the number of crashes would vary randomly if the sites were to be studied under the same conditions in subsequent occasions. The distribution of the total number of crashes at this theoretical population would then be linked to the range of predictor variables. The total distribution would emerge through an aggregating function of all the conditional probabilities, as estimated through the regression model formulation.

In the simple case of a bivariate joint distribution, the relationship to the marginal and conditional probabilities can be easily articulated as shown by Wackerly, Mendenhall and Scheaffer (2008). The fact that in this analysis such variables are also seen as a response/explanatory pair is merely incidental.

Let the i-th observed realization of the vector of predictors $\vec{X}$, from now defined as $\vec{x}_i$, be mapped 1 to 1 to a scalar field Z. Even when the values of vector $\vec{X}$ could be fixed at will, the realizations at hand depend on the characteristics of the sites in the sample (the population of this test), which were selected at random. Because of this feature, let Z be a random variable in the context of this test. This artifice allows a dimensionality reduction for the proposed test (a bivariate situation from this point on). Any functional form *f(.)* that maps $\vec{X}$ over the domain of Z would be adequate at this point. The relationship that links the marginal, conditional and total probabilities of Y and Z is shown in Equation 5-1.

Equation 5-1: Joint Probability Function as Related to the Marginal and Conditional Probabilities of Two Random Variables

$$P\big(Y, Z = f(\vec{x})\big) = p_{Y,Z}\big(Y, Z = f(\vec{x})\big) = p_Z\big(Z = f(\vec{x})\big) \times p\big(Y \big| Z = f(\vec{x})\big)$$

Where:

$\vec{X}$	=	vector of predictors;
$\vec{x}$	=	particular realization of the vector of predictors $\vec{X}$;
Y	=	predicted variable;
Z	=	scalar field, mapped from the observed realizations $\vec{x}$ of the vector of predictors $\vec{X}$;
$f(.)$	=	link function between Z and $\vec{x}$;
$p_{Y,Z}\left(Y, Z = f(\vec{x})\right)$	=	joint probability of Y and Z;
$p_Z\left(Z = f(\vec{x})\right)$	=	marginal probability of Z; and
$p\left(Y \middle| Z = f(\vec{x})\right)$	=	conditional probability of Y given Z.

Let every realization of $\vec{x}$ be equally probable under the scheme of Equation 5-1. This is because the test is over the whole theoretical population, thus:

$$P(S \ni \vec{x_i}) = 1 \; \forall \; 0 \leq i \leq n$$

Where S represents the total census of the population of available sites and n is the total number of sites in the theoretical population of sites.

In this case, it may be assumed that the marginal sampling probability of a value of Z is simply $\frac{1}{n}$ prior to obtaining the census data from the population. Additionally, let *f(.)*, the link function between Z and the vector of predictors be the exponential function of the internal product $\vec{\beta}.\vec{X}$, where $\vec{\beta}$ is the vector of coefficients from Table 2-1. Incidentally, the relation $Z = \hat{Y}$ is true in this case. The conditional probability of Y given Z is then simply a Poisson distribution with parameter equal to the predicted number of crashes, as of the GLM presented in chapter 2.

Equation 5-2 shows the total joint probability function of Y and Z. This equation results from re-expressing Equation 5-1 as just discussed, using the relations:

$p_Z\left(Z = \exp(\vec{\beta}.\vec{x})\right) = \frac{1}{n}$, and

$p\left(Y \middle| Z = \exp(\vec{\beta}.\vec{x})\right) \sim Poisson\ (\lambda = Z = \exp(\vec{\beta}.\vec{x}))$.

Equation 5-2: Joint Probability Function of y and $\vec{x}_i$

$$p(Y,Z) = \left(\frac{1}{n}\right) \times \left(e^{-\left(\exp(\vec{\beta}.\vec{x})\right)} \times \frac{\exp(\vec{\beta}.\vec{x})^{y}}{y!}\right)$$

Where:

Y	=	predicted variable;
$\vec{x}$	=	a realization of the vector of predictors;
$\vec{\beta}$	=	the vector of regression coefficients;
Z	=	$\exp(\vec{\beta}.\vec{x})$; and
n	=	number of sites in the sample (test population).

To perform a goodness-of-fit test, this author required $p_Y(Y = y)$, the marginal probability of Y, be known. This marginal probability is obtained, by definition, when integrating over all the domain of Z, which to this point has been assumed as a scalar field only.

Though in general defining $D_Z = \mathbb{R}$ holds for an infinite population of sites, in the particular case of this test, the population of Z is a fixed finite collection of values depending on the particular realizations of $\vec{x}$, available from the sample at hand. Let the ordered Z variable be mapped 1:1 to an integer auxiliary variable W with domain $D_W = \{1 \leq i \leq n | i \in \mathbb{Z}\}$.

If $p(y,W)$ is known, then, $p_Y(Y = y) = \int_{D_W} p(Y,W)dW$. Since W is a subset of subsequent integers, it follows that dW=1, so

$\int_{D_z} p(Y,W)dW = \sum_{i=1}^{n} p(y,W_i)$.

Since $W_i \overset{1:1}{\leftrightarrow} Z_i$, it follows that,

$\sum_{i=1}^{n} p(y,W_i) = \sum_{i=1}^{n} p(y,Z_i)$.

After replacing $Z_i = \exp\left(\vec{\beta}.\vec{x_i}\right)$ in the above expression, and noting that $D_Z \overset{1:1}{\leftrightarrow} D_{\vec{X}}$, Equation 5-3 emerges as the marginal probability of Y in terms of the available realizations of the vector of covariates $\vec{X}$.

Equation 5-3: Marginal Probability Function of Y

$$p_Y(Y=y)=\sum_{i=1}^{n}p\big(y,Z_i=\exp(\vec{\beta}.\vec{x}_i)\big)=\sum_{i=1}^{n}\left(\left(\frac{1}{n}\right)\times\left(e^{-\left(\exp(\vec{\beta}.\vec{x}_i)\right)}\times\frac{\exp(\vec{\beta}.\vec{x}_i)^y}{y!}\right)\right)$$

Finally, this author performed a chi-squared goodness-of-fit test by comparing the observed frequencies of sites with different values of Y (number of crashes) to the expected frequencies as of Equation 5-3, assuming that the whole population of n is surveyed. Again, it is important to point out that repeatedly surveying the population would yield different results, but such results should align with the predicted values from Equation 5-3.

The expected frequency of Y crashes is simply $n\times p_Y(y)$, which can be translated into Equation 5-4 by use of Equation 5-3.

Equation 5-4: Expected Frequency of Sites with "y" Crashes for a Set of Crash Realizations from the Available Sample

$$E.F._{(y)}=\sum_{i=1}^{n}\left(e^{-\left(\exp(\vec{\beta}.\vec{x}_i)\right)}\times\frac{\exp(\vec{\beta}.\vec{x}_i)^y}{y!}\right)$$

Where:

$E.F._{(y)}$ = Expected frequency of sites with y crashes.

It is easy to show that Equation 5-4 is equivalent to Equation 3-7, as it was briefed in Chapter 3.

Since Chapter 3 already showed the results of the proposed goodness-of-fit test applied to the OSU method validation sample (i.e. Table 3-1, with n=44), this section concludes by demonstrating the application of the proposed test to the original sample of 210 sites. This result is shown in Table 5-3.

As with the validation sample presented in section 3.10.2, there is no evidence that the observed distribution of sites by their observed crashes is statistically different from the expected distribution of sites by their predicted crash frequencies as of the proposed Poisson model.

Table 5-3: Goodness-of-fit Test over the Whole Oregon Sample

Crashes	***Observed***	***Expected***
0	125	115.864
1	48	49.149
2	13	21.196
3	6	10.248
4	11	5.522
5	3	3.172
6	2	1.886
>6	2	2.963
Total	**210**	**210**
	Chi-Squared Statistic	**11.441**
	p-value	**0.1205**

An additional, valid observation for Table 5-3 is that, as expected, it coincides with the computer output statistic (i.e. the residual deviance) in that both indicate a satisfactory goodness-of-fit to the data. In this case the residual deviance is based on a large sample (n=210) and thus this author concludes that the model is valid. Nevertheless, this result strengthens the case for the usefulness of the test developed in this subsection.

5.3.2. Assessing the Structural Correlation in the Response Variable (Complementary to Section 2.6)

This section deals with a relevant issue this author recognized in the underlying structure of the data available for this research. A high correlation between the numbers of crashes from each pair of directions of travel emerges from the rough data because every curve site in the study comprises two directions of travel, and each pair contains relevant common factors (e.g. driving population, traffic volume, and horizontal radius) The use of univariate GLMs would be problematic if such correlation is substantial and beyond the explaining power of these statistical models. The assessment for this correlation was already summarized in section 2.6.1. This section presents supplemental tables and figures that were originally intended to be part of that section.

Table 5-4 shows the correlation for the total sample of 105 pairs of crash counts, as well as the corresponding correlation between the pairs of expected number of crashes, as of the regression model.

Table 5-4: Comparison of Sample and Parameter Correlations

Correlation from paired Data	0.698
Correlation from paired Parameters	*0.926*

Although there is a high correlation between the predicted pairs of number of crashes, this author considers that the sample correlation does not compare directly to the correlation of the predicted parameters. The reason is that the sample counts should be understood as realizations of the theoretical Poisson distributions from the statistical model instead. This author considers that the correlation in the sample should be compared to the distribution of correlations that arise from repeated realizations of the theoretical Poisson distributions, instead of comparing it to the raw Poisson parameters.

A synthetic sample of such distribution of correlations was obtained by the technique of static simulation. Every replication consists of the overall correlation obtained from independently generated realizations of the 105 pairs of Poisson variables as of the statistical model. The simulation was replicated two hundred times. Figure 5-14 represents a histogram of this distribution obtained from the synthetic sample.

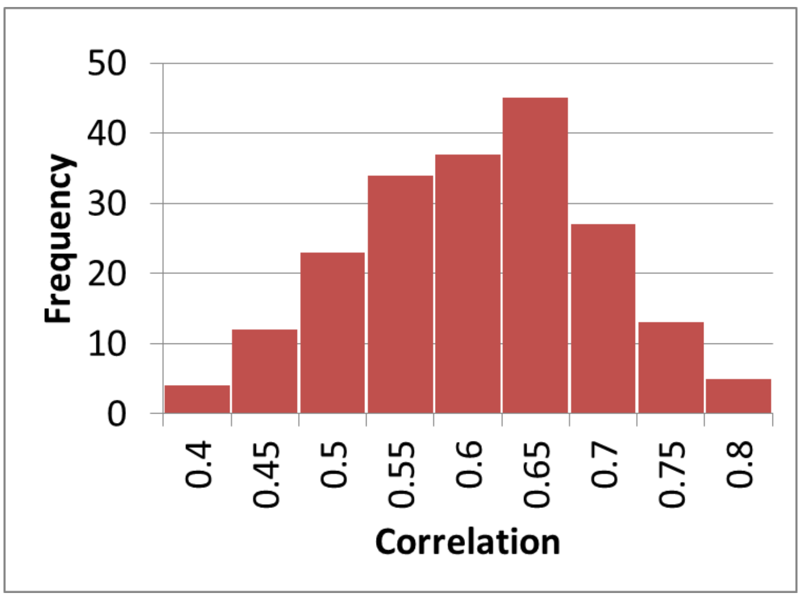

Figure 5-14: Synthetic Sample of Paired-Sites Correlations for Independent Crash Realizations

Figure 5-14 clearly suggests that a normal curve could roughly approximate this distribution. The researchers computed the corresponding parameters in order to assess the statistical significance of the correlation from the crash data. Table 5-5 shows the distribution parameters from the simulations, the actual sample statistic and the corresponding p-values (0.1838 2-sided, and 0.0919 1-sided). Additionally, this table provides an empirical p-value (0.0900), computed from the raw synthetic sample as the proportion of simulated correlations that resulted in values more extreme than 0.698, the sample statistic.

Table 5-5: Distribution of Paired-Sites Correlations for Independent Crash Realizations

Mean	0.581
Standard Deviation	0.088
Sample Statistic	0.698
Z-Statistic	1.3292
2-sided p-value	0.1838
1-sided p-value	0.0919
Empirical p-value	0.0900

From the results presented in Table 5-5, this researcher concludes that the correlation observed between the pairs of directions of travel in the sample is not atypical, and that it is reasonable to expect such a degree of correlation from pairs of truly independent Poisson variables with similar parameters, as of the regression model.

5.3.3. **Dealing with Functionally Linked Covariates: The Case of Curve Length Effect in the Proposed Model**

The statistical model for curve crashes proposed in this dissertation is useful as a predictive tool from the empirical side alone (as it demonstrated predictive power over a new set of sites). This author was initially not interested in interpreting variables other than those pertaining advisory speeds. However, if the model resonates with an underlying causal relationship, it should be robust beyond its fit to the data; in that case, variables related to geometry and exposure effects should behave as expected from the engineering standpoint. However, the complexity added by the interaction terms makes it more challenging to isolate such effects. Although this author never intended the model for studying these variables, as said, such characterization was, in one instance, pointed out by a reviewer of the second manuscript: the effect of Curve Length.

The statistical model presented in this dissertation was fitted over a wide range of curve lengths and angles (Curve length ranging from 44ft to1400ft, and angles from 1.5 to 200 degrees). The coefficient in Table 2-1 corresponding to curve length is negative and statistically significant, a circumstance that seems to challenge the expectedly proportional effect of more crashes at larger curves, as many previous works have suggested. However, this author verified that curve length behaves as expected, although it may not be immediately apparent.

The effect of curve length is not linear (i.e., not available as a single coefficient in the model), as will be demonstrated below, and thus the sign of *ln(CurveLength*) does not convey the entirety of the impact of this variable.

Similar to when a model includes both a quadratic and a linear term for a particular variable, the impact of Curve Length is captured by two coefficient estimates. *ln(CurveLength)* obviously is one of them. However, the length of a curve can be obtained by simply multiplying Radius, Angle and a constant. The units of curve length are the same as radius, and if the angle is given in radians (which is the case in the model), the required constant is simply 1.0. Therefore, the interaction between Radius and Angle, included in Equation 2-1, can be seen as either such an interaction of two geometric parameters, or as another avenue in which Curve Length affects crashes. Equation 2-1 can then be rewritten with two components including Curve Length: a transcendental term and a linear term: $\beta_1.\ln(CurveLength) + \beta_2.CurveLength$

In order to extract the marginal effect of curve length, one requires taking the first derivative of this rewritten Equation with respect to curve length, which results in a marginal effect that is dependent on the curve length variable itself:

$$\frac{\partial}{\partial CurveLength}(lnY) = \frac{\beta_1}{CurveLength} + \beta_2$$

Although the sign of β_1 is indeed negative (-0.956 from Equation 2-1), its partial impact decays as *CurveLength* increases, whereas the second positive coefficient remains unchanged (+0.002, from Equation 2-1). In fact, this overall functional form converges to a positive value (+0.002) becoming a linear effect on the log of crashes as the horizontal radius tends to infinity. In light of the marginal effect just described, and despite the model accounts for *CurveLength* as a "cut" in crashes from the "partial-baseline number of crashes", such a "cut" decreases and converges to an increment in crashes as the curve flattens and converges into a tangent section. Such a trend indicates a positive relationship between crashes and curve length, which is opposite to the conclusion that can be extracted when examining the sign of the *ln(CurveLength)* coefficient alone.

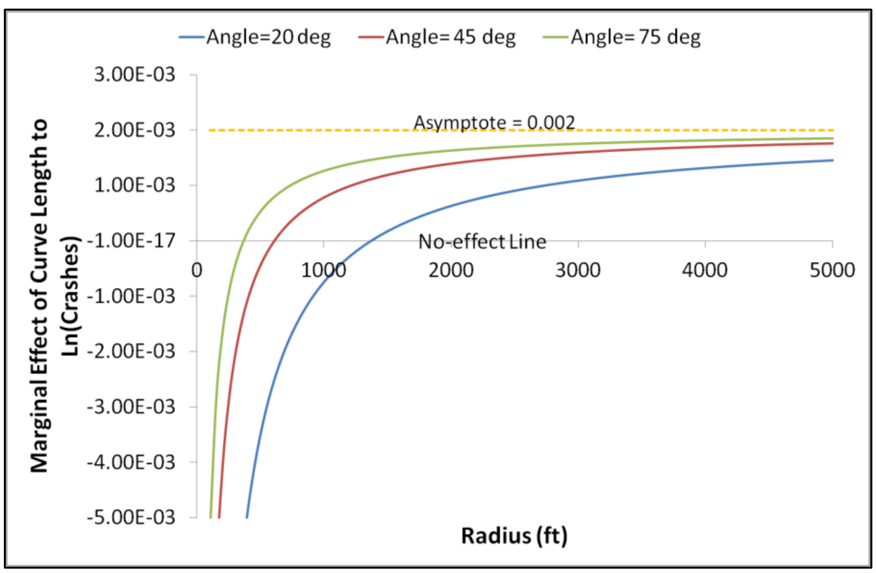

Figure 5-15: Marginal Effect of Curve Length for Different Deflection Angles

Figure 5-15 shows the marginal effect of curve length. A direct relationship between curve length and crashes is obvious. For any given radius, the marginal effect of curve length translates into more crashes at longer angles, which also means longer curves (since the comparison is at any given radius). This can be verified by drawing a vertical line over Figure 5-15 and comparing the relative effects of the angles therein depicted.

According to the described effect, the eventual change of sign into a positive effect is only delayed by the size of the angle, but it is inevitable as the horizontal curve flattens.

5.4. Statistical Significance and Size of Effect of the ASCF and its Constituents

Although the marginal effect of the variables involved in the ASCF were presented and discussed in chapter 2, this author deems it appropriate to present in this section the statistical significance of these marginal effects and a discussion of the ramifications.

As a closure, the last two sub-sections in this section explore the size of the effect and the statistical significance of the ASCF as a joint function of ASD and SFD.

5.4.1. Significance of the Marginal Effect of ASD

Table 5-6 shows the marginal effect of the variable ASD for different levels of SFD. The standard errors were computed using a correspondent version of Equation A-3 (see Appendix A, p.166) applied to the final model selected for this work. Additionally, the statistical significance is shown in the last column.

Table 5-6: Marginal Effect of ASD for Different Values of SFD

SFD	***Marginal Coeff.***	***Std. Err.***	***z-stat***	***p-value***
0.07	-0.015	0.022	-0.689	0.491
0.14	-0.054	0.026	-2.100	0.036
0.21	-0.092	0.033	-2.841	0.004
0.28	-0.131	0.041	-3.194	0.001
0.35	-0.170	0.050	-3.374	0.001
0.42	-0.208	0.060	-3.473	0.001
0.49	-0.247	0.070	-3.532	<0.001

In this table, not only does the marginal effect of the ASD become more beneficial at higher levels of SFD, but it is statistically significant only for values of SFD larger than 0.14. This fact resonates with the trend of the OSU method to propose advisory speeds that are associated with larger SFDs.

5.4.2. **Significance of the Marginal Effect of SFD**

Analogous to Table 5-6, Table 5-7 shows the details of the marginal effect of SFD at different levels of ASD. The same trends described above are present in the case of this marginal effect: This trend demonstrates a beneficial effect (for ASD values larger than or equal to 10 mph), which improves for larger values of ASD; and a limited range for the statistical significance of said marginal effect (ASD values larger than or equal to 15 mph).

Table 5-7: Marginal Effect of SFD for Different Values of ASD

ASD	***Marginal Coeff.***	***Std. Err.***	***z-stat***	***p-value***
5	3.035	1.818	1.669	0.095
10	0.271	1.604	0.169	0.866
15	-2.493	1.724	-1.446	0.148
20	-5.257	2.124	-2.475	0.013
25	-8.021	2.680	-2.993	0.003
30	-10.785	3.315	-3.253	0.001
35	-13.549	3.992	-3.394	0.001

This author considers it important to point out some salient characteristics regarding this marginal effect. First, there is a big difference between the ASD level of 5 mph and the other ASD levels. This resonates with the fact that an ASD of 5 mph corresponds to sites where advisory speed sign posting is not required, as opposed to the rest of ASD levels. The severely detrimental marginal effect of SFD at the 5 mph is associated with a mild statistical significance. Because Figure 3-2 shows that this ASD level had an ample range of SFDs (as nearly half the sites in the analysis did not exhibit advisory speeds) this author speculates that the effect of SFD is simply not meaningful at this level. In contrast, the poor statistical significance at an ASD level of 10 mph is probably due to a modest effect in combination of a small subset of sites available at this level. This is also shown in Figure 3-2. The rest of ASD levels exhibited SFD marginal effects in spite of similarly small subsets of sites; this is possibly due to the increasing size effect of the SFD marginal contribution to explain the overall crashes, as shown in the second column of Table 5-7 (i.e. decreasing values of the marginal effect, thus diverging from 1.0, the level at which the effect is null).

5.4.3. **Effect Size of the ASCF Function**

This section explores the effect size and the trend of the ASCF as it is jointly determined by the SFD and the ASD.

As demonstrated in the previous section, Table 5-8 clearly shows a contrast between the behaviours of the ASCF when the ASD is 5 mph and when the ASD is any other value.

For ASD=5 mph, the ASCF increases with increasing SFD. The opposite is true for other ASD values. Since advisory speeds are present only when the ASD is larger than 5 mph, this author interprets the different behaviour of sites with ASD=5mph as a reflection of the hazardous case of sites not displaying advisory speeds but with dangerously large associated SFDs. In that case, the number of expected crashes increases as the SFD increases.

Table 5-8: Advisory Speed Crash Factor Values

		ASD (mph)						
		5	**10**	**15**	**20**	**25**	**30**	**35**
SFD	**0.07**	1.623	1.535	1.452	1.374	1.299	1.229	1.163
	0.14	2.059	1.440	1.007	0.704	0.493	0.345	0.241
	0.21	2.612	1.351	0.699	0.361	0.187	0.097	0.050
	0.28	3.313	1.267	0.485	0.185	0.071	0.027	0.010
	0.35	4.203	1.189	0.336	0.095	0.027	0.008	0.002

On the other hand, whenever advisory speeds are present (ASD>5 mph), the ASCF makes the case for lower advisory speeds (larger ASDs) associated with higher SFDs.

Finally, the shaded boxes in Table 5-8 indicate the cases when the ASD is on the verge of being null (i.e. very close to being a multiplicative factor of 1.0). However, a better visualization of the shape of this surface is offered in Figure 2-5 and Figure 3-2.

5.4.4. **Statistical Significance of the ASCF Function**

To finalize section 5.4, this author provides a quick review of the statistical significance of the ASCF effect as jointly determined by the SFD and the ASD.

The variance of a linear combination of two or more random variables (as the ASCF is) can be easily formulated from statistical theory (Wackerly, Mendenhall III, & Scheaffer, 2008). Specifically for three variables:

$$
\begin{aligned}
&V(A.\beta_1 + B.\beta_2 + C.\beta_3) = \\
&\qquad A^2.V(\beta_1) + B^2.V(\beta_2) + C^2.V(\beta_3) + \\
&\qquad 2.\langle A.B.Cov(\beta_1, \beta_2) + A.C.Cov(\beta_1, \beta_3) + B.C.Cov(\beta_3, \beta_2)\rangle;
\end{aligned}
$$

which in the case of the ASCF translates into Equation 5-5.

Equation 5-5: ASCF Variance Computation

$$
\begin{aligned}
&V\{ASD.\beta_{ASD} + SFD.\beta_{SFD} + ASD.SFD.\beta_{ASD\times SFD}\} = \\
&\qquad ASD^2.V(\beta_{ASD}) + SFD^2.V(\beta_{SFD}) + ASD^2.SFD^2.V(\beta_{ASD\times SFD}) + \\
&\qquad 2.\langle ASD.SFD.Cov(\beta_{ASD}, \beta_{SFD}) + ASD^2.SFD.Cov(\beta_{ASD}, \beta_{ASD\times SFD}) + \\
&\qquad ASD.SFD^2.Cov(\beta_{ASD\times SFD}, \beta_{SFD})\rangle.
\end{aligned}
$$

It follows then that in order to compute the statistical significance of a particular realization of the ASCF, the covariance structure of the vector of estimates $\begin{bmatrix} \beta_{ASD} \\ \beta_{SFD} \\ \beta_{ASD\times SFD} \end{bmatrix}$ is required. Such covariance structure is easily obtainable from the statistical modeling software (R Development Core Team, 2011). Table 5-9 shows the p-values corresponding to the values previously computed in Table 5-8 when tested under the null hypothesis that ASCF=1.0, and based on the ASCF variance obtained from Equation 5-5.

Table 5-9: P-values Associated with ASCF Values Shown in Table 5-8

		ASD (mph)						
		5	**10**	**15**	**20**	**25**	**30**	**35**
SFD	**0.07**	0.035	0.193	0.397	0.568	0.698	0.795	0.869
	0.14	0.040	0.394	0.989	0.600	0.380	0.261	0.194
	0.21	0.044	0.577	0.589	0.216	0.094	0.049	0.030
	0.28	0.047	0.719	0.367	0.093	0.031	0.014	0.008
	0.35	0.050	0.825	0.252	0.049	0.014	0.006	0.003

In the context of Table 5-9, a small p-value implies an ASCF value statistically different than 1.0. The shaded cells correspond to ASCF values that are not statistically different than 1.0 (at a 5% significance level), which is, in this author's opinion, quite a large range. No advisory speed posted 10 mph below the speed limit, or associated with a SFD smaller than 0.14 is expected to have a clear and unequivocal ASCF effect, regardless of the expected size effect. In contrast, the ASCF should be distinct and easy to notice (i.e. with a statistically significant effect) at sites not displaying advisory speeds (i.e. ASD=5mph) and at sites for which the approximate relation ASD+ (10 x SFD) > 51 holds (i.e. roughly all other not-shaded cells in Table 5-9).

5.5. Validation test for the ASCF and Base sub-model partitions in the proposed Poisson Model

During July 2011, this author collected a new random sample of sites from a database of state maintained rural highways. Because of limited funding and time constraints, the new sampling only included sites from Benton, Linn, Lincoln, Polk and Lane counties, the five located adjacent to each other and in western Oregon. All 61 complete segments of highway in these counties were treated as clusters of different lengths, varying from 0.23 to 80.8 miles. The author performed a weighed random selection, considering both length and average distance from Corvallis, OR. A preliminary list of 21 clusters emerged from this effort. This author used road-view images available from Google.com to identify curves within the 21 segments. This author noted the advisory speed value or lack thereof and the geographic location of horizontal curves with a large enough length and small enough radius so that the horizontal alignment change would be obvious to drivers. After exhausting all segments, this author randomly ordered the list of segments and selected 44 sites. Grade, lane width, shoulder width, superelevation, curve length, relative location of warning and advisory speed signs, and site photographs were obtained at 3 points between the Point of Curvature (PC) and the Point of Tangency (PT) of each curve during field visits. The radius and AADTs were obtained from the ODOT reporting system and aerial photographs available online. Crash history was obtained by using reporting SQL code over available databases from years 2003 to 2007.

Faced with a limited sample size, this author first assessed the overall goodness-of-fit of the original statistical model to the newly collected data set by the procedure demonstrated in 5.3.1. However, in order to validate the ASCF effect, it would have been ideal to fit the whole model again on a new sample, so as to statistically compare the new coefficient estimates with the estimates in the original model. Regardless, this author expected insufficient statistical power to do so over a sample of only 44 sites because there are coefficients barely significant in the original model, even when that model was fit over 210 sites. Unfortunately, this circumstance impedes the validation of particular ASCF coefficients via this ideal path.

The alternative that this author deemed appropriate to address this setback is that of fitting a new Poisson GLM, so to assess the predicting power of both the ASCF sub-model and the corresponding baseline of crashes sub-model, as predictors themselves in a new GLM formulation. The procedure shown in this section, the author expects, permitted him to at least validate the predictive power of the overall ASCF effect over a new but reduced sample of sites.

The proposed ASCF validation is based on the premise that values from both the ASCF and baseline crashes sub-models (obtained using the coefficients of the model introduced in chapter 2) should exhibit predictive power over the crash history at the new sample. This validation, thus, only assesses the predictive power of the two sub-models based on the statistical significance of their marginal contributions in a new regression model.

Let $Y \sim Poisson(\lambda) \wedge \lambda = \exp\left(\vec{\beta}^T . \vec{X}\right)$ specify a model such as that of chapter 2. Let $\vec{X}_{ASCF}$ and $\vec{X}_{Base}$ be a partition of the vector of predictors $\vec{X}$. This partition is such that separates the covariates from both the sub-models of interest in this validation so that $\vec{X} = \begin{bmatrix} \vec{X}_{Base} \\ \vec{X}_{ASCF} \end{bmatrix}$. Then, $\lambda = \exp\left(\vec{\beta}_{Base}{}^T . \vec{X}_{Base} + \vec{\beta}_{ASCF}{}^T . \vec{X}_{ASCF}\right)$.

In the context of the scheme shown above, it is obvious that, in general,

$\widehat{\vec{\beta}_k}^T . \vec{X}_k = \widehat{\vec{\beta}_k^T . \vec{X}_k}$, since the components of $\vec{\beta}_k$ are random variables but the components of $\vec{X}_k$ are directly measurable or deterministically computed from the actual sites in the sample.

If the sub-models $\widehat{ASCF}$ and $\widehat{Base}$ are known for a new sample of sites, then let $Y_v \sim Poisson(\lambda_v) \wedge \lambda_v = \exp\left[offset\langle\widehat{\beta_0}\rangle + \varphi_1 . \widehat{ASCF} + \varphi_2 . \widehat{Base}\right]$ be a new GLM formulation over the validation sample using the sub-models as predictors. In this case

β_0 from the original model is carried out to the new model as an offset value and the estimation is performed without an intercept.

This new modelling effort should provide evidence supporting the original model's coefficients and their statistical significance as a surrogate to a more rigorous validation procedure in the face of a limited validation sample. Even when validating the original set of coefficients may prove challenging, this analysis should suffice in providing convincing evidence of the ASCF effect being statistically significant, given that the original model is valid beyond the modelling data set. That would be the case if, for example, the original model specification reasonably approximates the real underlying process to the crash generation, independently of the particular coefficient estimates originally obtained for the ASCF effect.

When the sub-models stemming from the original model are used as predictors for another meta-model, and if they are approximately unbiased (as both the model and its validation meta-model are based on Oregon probability samples) then it is also expected that: $E(\varphi_1) = E(\varphi_2) = 1.0$ because then:

$$E\left(\widehat{ASCF}\right) = ASCF \quad \wedge \quad E\left(\widehat{Base}\right) = Base.$$

Here, the terms *ASCF* and *Base* are parameters that were initially estimated when fitting the full model. These are the quantities to be verified using the new sample, under the hypothesis of an underlying set of prior parameters, common to both probability samples.

If the validation sample is large enough, then the regression should provide evidence of the only two regression coefficients in this case (i.e. φ_1 and φ_2) not being statistically different than 1.0. If the initial modelling effect yielded meaningful estimates, one would expect that these new coefficients would be statistically different from zero.

5.5.1. **Hypothesis Testing on Regression Output**

The test presented in chapter 3 and expanded in this section assumes that the validation model specification is correct, and that the standard errors are not inflated. This is not necessarily the case because normality is not necessarily achieved for Maximum Likelihood Estimation using a small data set (44 sites in this case). Because of this circumstance, p-values based off the standard normal distribution are expected to be inflated. However, this author verified that the correlation between the predictor variables ASCF and Base is -0.503, which in turn is expected to produce smaller standard errors compared to a regression of truly independent covariates.

Table 5-10: Poisson Regression Model for Validation over new Sample

Term	Estimate	Standard Error	z-value	2-sided p-value	Significance[1]
ASCF	0.8182	0.3236	2.529	0.0115	*
Base	1.2215	0.1318	9.271	$< 2.0\text{x}10^{-16}$	***

[1] *Significance values are as follows:*
° p<0.1; * p < 0.05; ** p < 0.01; and *** p < 0.001

Residual Deviance: 54.812 on 42 degrees of freedom

Proceeding as if these two circumstances balanced out, the simplest tests that can be performed are those directly using the information in Table 5-10.

5.5.1.1. Expected value of the ASCF sub-model

This procedure tests the significance of the ASCF as a predictor in the validation sample. Additionally, it is possible to specify a concrete alternative hypothesis, since a particular value is expected for the corresponding coefficient.

Specifically:

$$H_0: \varphi_{ASCF} = 0$$

$$H_a: \varphi_{ASCF} = 1$$

By using, $\varphi_{ASCF} = 0.8182$ and $Std.Error(\varphi_{ASCF}) = 0.3236$ from Table 5-10, the results of this test are shown in Table 5-11.

Table 5-11: Hypothesis Testing Results for the ASCF Sub-model

Scope	Ho: Phi= 0			Ha: Phi = 1		
ASCF Sub-Model	**Statistic**	**Value**	**1-sided p-value**	**Statistic**	**Value**	**1-sided p-value**
	Z statistic	2.529	0.0057	Z statistic	-0.562	0.2830

Based on the results in Table 5-11, this author rejects the hypothesis of a null ASCF sub-model. However, there is not enough statistical power to embrace the specific alternative hypothesis emerging from the expected values of the ASCF sub-model as estimated from the first modelling effort. A type II error of 0.2830 means that the power of this test is 0.7170. This is the probability of rejecting the null hypothesis if the alternative hypothesis were true. Though is author considers this result offers mild evidence in favor of H_a, he speculates that a larger sample may strengthen the evidence in favor of the specific ASCF coefficients.

5.5.1.2. Simultaneous testing of both sub-models

Because the covariance structure is available from the validation regression model, it is possible to simultaneously test the significance of both sub-models by using the Hotelling's T^2 statistic, and under the assumption of bivariate normality. The corresponding variances of the coefficients are simply the squared standard errors from

Table 5-10. This author obtained the corresponding covariance of +0.0198 from the computer output. Results for the test are shown in Table 5-12.

Table 5-12: Hypothesis Testing Results for Both Sub-models

Scope	Ho: Phi_1 = Phi_2 =0			Ha: Phi_1 = Phi_2 =1		
Both Sub-models	Statistic	Value	p-value	Statistic	Value	p-value
	Hotelling's T^2	89.94	$2.03x10^{-11}$	Hotelling's T^2	5.11	0.084

Based on the results of simultaneous testing both sub-models, this author rejects the hypothesis that both of them have null effects simultaneously. The alternative hypothesis of the coefficients being simultaneously equal to 1 may be embraced with moderate statistical evidence, yet satisfactory to this author. A p-value of 0.084 associated with a type-II error implies that the statistical power of this test is 0.916, which represent a moderate probability of rejecting the null hypothesis (as it was the case) if the alternative hypothesis is in fact true.

This author speculates that among the reasons why this validation effort yields statistically significant results over a rather small sample is the fact that the estimation was performed over only two variables. Such variables also happen to be very dense in information regarding crash occurrence, as they are computed from a model with significant coefficients. These coefficients, in turn, are based on a probability sample of Oregon roads.

6. General Conclusions and Recommendations

This chapter consists of two subsections: A set of conclusions and recommendations with their corresponding rationale from this author, and a summary on how the research questions stated in Chapter 1 were addressed by this work.

6.1. Conclusions, Recommendations and their Rationale

This work proposes and develops two new engineering tools to determine advisory speeds for horizontal curves. The proposed tools are expected to improve upon current practices, as the analysis of the data available from the state of Oregon suggested. The first tool is a fully computational posting method named the Oregon State University (OSU) method; the second tool is a BBI based posting methodology coined the Hybrid-OSU method. This research shows that both of these methods result in more consistent advisory speeds, thus sensibly improving upon the results from the ubiquitous traditional BBI methodology. Because of their improved results and easy applicability, this author deems the proposed tools sensible contributions to the transportation community, particularly to practitioners and local jurisdictions.

The engineering tools developed in this work are based on the concept of the optimal advisory speed as derived from the Advisory Speed Crash Factor (ASCF) formulation. The optimal speed is the speed anticipated to minimize the number of crashes. Developing these tools was possible because the functional form of the ASCF is convex at the feasible domain of advisory speeds and speed limits, as well as it exhibits a local extreme value in this domain. Both these characteristics are the conditions of local optimality of advisory speeds. This research showed that these conditions are satisfied for virtually every 2-lane, 2-way rural road scenario.

This author recommends, first and foremost, the Oregon adoption of the OSU posting method, as it has been shown to produce more consistent advisory speeds, and it also translates to the larger expected reduction in number of crashes at curve locations. However, this author recognizes that some jurisdictions may be reluctant to adopt a computational approach to determine advisory speeds at this time, especially because of the availability of equipment such as the Ball-Bank Indicator (BBI) and crews already proficient in their use. In those cases this author recommends that the BBI be used as outlined for the Hybrid OSU method, instead of the traditional methodology. This research demonstrated that there is a sensible consistency improvement when using the BBI with the Hybrid OSU method, though the results are not as consistent as those expected from the OSU method, its computational counterpart.

The Hybrid OSU method is also recommended as a transitional alternative prior to fully adopting the computational OSU method. This author expects that computational methods would be more appealing as road inventories become more reliable and easily accessible. In any case, based on the information at hand, this author recommends the implementation of the proposed methods at 2-lane, 2-way rural roads in Oregon only because of the geographic scope of the data used to develop and test these procedures.

Though these procedures may be already adequate for other jurisdictions, as suggested by the close performance of their resulting speeds to those stemming from the nationally accepted MUTCD guidelines, this author recommends a calibration to local conditions before implementing these methods outside of Oregon.

This author coded the two proposed posting methods into a self-explaining spreadsheet as a supplement to this dissertation. By making it publicly available, this author expects this spreadsheet to help in the process of adoption of the proposed procedures by any jurisdiction that so desires. However, the spreadsheet is provided as is, with no promise of future updates.

§

The basis of the engineering tools hereby proposed is a statistical analysis that focused on characterizing the relationship between crashes and curve site characteristics, including advisory speed signs, among other factors. The statistical model from the analysis included a sub-model for the effect of the advisory speed, which this author named the Advisory Speed Crash Factor, or ASCF. This sub-model convincingly links advisory speeds to a safety enhancement, thus justifying the practice of posting these signs.

Not only was the ASCF sub-model statistically significant, there also is a plausible Human Factors interpretation of its constituent elements: the Advisory Speed Differential (ASD) and the Side Friction Demand (SFD). According to this interpretation, advisory speeds enhance safety to the extent that they convey information about the severity of the horizontal curve immediately downstream and to the extent that this information is accurate and meaningful to the driving population. Even so, the safety enhancement could be relatively diluted for advisory speeds that are either too high or too low. In addition, the author concurs with the stance of previous researchers that inconsistency is an issue that very likely claims a toll on the safety associated with these signs. The methodologies proposed in this work are expected to be more consistent and also associated with a balanced Side Friction Demand.

In hindsight, from the standpoint of the statistical modelling effort, this author considers the inherent inconsistency exhibited by currently posted advisory speeds as an advantage rather than a liability for the research effort. The range used to estimate the ASCF response surface is considerably expanded as a direct result of this inconsistency. For instance, Figure 3-2 shows that the scatter of currently posted advisory speeds is the most appropriate to estimate the two ‘hills’ that take off around both the ASD and SFD axes. If, for example, the posted speeds available from the sample would have been those of the MUTCD method, the statistical estimation of the ‘hill’ that climbs over the ASD axis then would have been inadequate. This is because no points from the

MUTCD set of speeds fall in this area of the surface, as some of the currently posted speeds do.

§

The use of a model that incorporates multiple interaction terms, as well as the use of expectedly correlated covariates, may impose on this work the burden of an increased degree of criticism. This criticism was evidenced by a handful of reviewers of the first and second manuscripts who expressed concerns about interactions and multicollinearity. Even so, this author deems the use of such a model decisive to arrive at a meaningful ASCF function. The use of correlated covariates was necessary in order to simultaneously include variables that the literature has documented to exert an effect on curve safety. Not including any of these variables would have resulted in what is known as Omitted Variable Bias. That is the case of Radius and Curve length. Additionally, the use of interactions among some covariates ultimately provided the ASCF function with the flexibility to account for both speed differential and side friction demand as the joint determinants of advisory speed safety rather than an average effect captured by a single rate coefficient.

However, the use of interacting terms also increases the complexity of interpreting effects of variables in the traditional sense (i.e. their marginal effect on the number of crashes). For instance, the apparent contradicting sign of the curve length coefficient was pointed out by one of the reviewers of the second manuscript. Yet, Section 5.3.3 shows that regardless of the sign of this coefficient, the ultimate behaviour of this variable is as expected: more crashes at longer curves. That section also demonstrates that the discordant negative sign even changes into positive as the curve flattens into a tangent section.

In general, the model assumptions are satisfactorily met. In this respect, the author was initially concerned about treating both directions of travel from every site as independent points when fitting a univariate Generalized Linear Model, because of the paired-structure to the data that this practice overlooks. However, this author tested the degree of correlation in such data structure and found that it can be satisfactorily explained by the communalities in covariates exhibited by each pair, as it was shown in the first manuscript and expanded in section 5.2. Additionally, Appendix B shows an exploratory modelling effort this author performed by fitting a statistical model with a bivariate Poisson response, which is a more complex parameterization, but that explicitly accounts for the correlation between directions of travel in question. Although this modelling effort showed that there is an information quality improvement when using Bivariate Poisson models, thus making the residual correlation meaningful, the actual estimates of the paired-sites covariance provided statistically insignificant results. Even for the best fitting parameterization of the BV Poisson model exhibiting significant drop in the AIC statistic, a Bootstraps Estimation showed all coefficients in the covariance term were statistically insignificant. Because of the 'Ockhams Rasiermesser' principle, this author embraces the univariate Poisson specification as a better, more parsimonious alternative to carry this work upon. However, the use of BV Poisson models remains a viable and attractive option to further study of the subject of curve safety.

This author concludes that the model specification that yields the ASCF function is a robust basis to develop the proposed engineering methodologies. Repeated adequacy testing of different aspects of the model showed convincing results to this author. The model covariates behave as expected, even in the cases where abnormality was apparent. Finally, a validation analysis rejected the hypothesis of a null ASCF effect, which points out the thesis of a safety effect of advisory speed signs, as outlined in this work. However, a mild statistical power in the validation analysis provides but suggestive evidence in favor of the alternative hypothesis of the underlying effect being distinctly characterized by the best available ASCF coefficients estimates.

§

As just mentioned, the validation analysis verified the significance of both the model for total crashes and the ASCF sub-model for the effect of advisory speeds. However, the statistical power of this validation was convincing for the full model but only just satisfactory for the ASCF sub-model. Although the current analysis rejects the hypothesis of a null ASCF effect, if the estimated ASCF coefficients are indeed the true parameters, a statistical power of 71.7% for this test means that if the validation analysis were to be repeated multiple times on a Sampling Space of samples of 44-sites, the null hypothesis would be rejected only 28.3% of the time. Under the assumption of a true ASCF effect, this author concludes that a sample of 44 sites is still associated with some degree of uncertainty in order to validate the ASCF sub-model coefficients. An obvious way to reduce this uncertainty would be to increase the sample size for the validation; unfortunately, such a measure is beyond the scope and timeframe of this work.

This author recommends a new validation of the sub-model over a larger sample of sites. This author believes that the insights from Table 5-9 discussed in section 5.4.4 may provide the basis for a more efficient validation of the ASCF than the effort presented in Chapter 3. A validation analysis using a new sample of sites with abundant number of sites with statistically significant ASCF effect may prove a more powerful test without the need of significantly increasing the sample size. However, with the intent of assuring an increased statistical power, this author recommends the use of this targeted sample strategy still in combination with an increased sample size.

Though this author recommends a new validation of the sub-model over a larger sample of sites, he also embraces the hypothesis of a true ASCF effect regardless. This endorsement is justified as follows:

First, this dissertation demonstrates, through comparisons of posting procedures, that those procedures with more consistent advisory speeds are also those with the best safety performance as of the ASCF. The literature cites numerous efforts that maintain that inconsistent and conservative advisory speeds may explain the wide lack of adherence from drivers to these signs, to a large extent. This author strongly agrees with that premise. In that regard, both ASCF-based posting methods, proposed in this work, result in advisory speeds that are more consistent and associated with larger SFDs.

Second, this author considers that although the ASCF emerges from a modelling effort that started with many candidate parameterizations for the safety of advisory speeds, the selected functional form emerged from the simultaneous inclusion of two terms and their interaction in the larger model, all of which terms were incorporated in contest with other candidate parameterizations at the latest stage of the model selection. Nevertheless, the resulting bi-linear polynomial incidentally involves all of the key components that are used in the practice to determine advisory speeds. Not only are all the relevant variables involved, but their behavior, interrelationship and performance resonates with the guiding principles of almost 80 years of engineering practice. In this regard, the Human Factors implications of the ASCF and their relation to the dynamics of negotiating a horizontal curve, as articulated throughout this dissertation, are convincing and satisfactory to the author.

Third and finally, it is interesting that the expected performance of the speeds based on the proposed optimal advisory speed concept closely approximates the performance of the updated MUTCD guidelines. This was so even when optimal speeds were derived from the ASCF estimate obtained from a set of sites characterized by the conservative historic Oregon policy. This point is demonstrated in the second manuscript. This author argues that the fact that the optimal advisory speed correlates more with the advisory speed from the current MUTCD guidelines could be explained by the actuality of an underlying optimal advisory speed, a value that has been approached on the one hand empirically by the subsequent updates of MUTCD posting thresholds, and on the other, by the safety analysis presented in this work.

§

Despite his recommendation of further verifying the actuality of the ASCF function, this author argues that the specific engineering applications proposed in this work represent a sensible contribution to the state of the practice, even in the hypothetical case that further research does not find evidence in favor of the actuality of the ASCF effect. Both the OSU and Hybrid OSU methods result in more consistent advisory speeds (i.e. less variability in their SFDs), which is per se a significant safety benefit when compared to the state of the practice. This fact was verified beyond the modelling data set (i.e. state maintained sites) as both proposed methods were applied to a large independent data set of county maintained sites. This evaluation verified not only the expected improvement in consistency of the fully computational OSU method but also confirmed the expected, though more modest, consistency improvement associated with the Hybrid OSU method.

§

As mentioned before, this author looks forward to further work on this topic. Research coming from the areas of safety performance, Human Factors, and road operations should produce evidence in favor of the actuality of the safety effect of advisory speeds. This author recognizes that the statistical analysis in this dissertation is but an early attempt to characterize the relationship of advisory speed signs and crash occurrence. This characterization, along with the engineering tools also developed in this dissertation, are the most current developments on the safety implications of advisory speeds, to the extent of this author's knowledge. Independent verification efforts of the functional form, of independently developed alternative formulations, as well as the transferability of the function and the adequacy of the proposed engineering tools to other states and jurisdictions, are still to be explored.

6.2. Research Questions Addressed

This section finalizes the conclusions and recommendations by outlining how the research questions were successfully addressed:

Research Question 1:

1. After accounting for other relevant factors with known safety effects, is there a safety benefit associated with the use of advisory speed warning signs?

This work convincingly suggests that there is a safety benefit associated with posted advisory speed signs. Chapter 2 in this dissertation develops a statistical model based on an Oregon probability sample. From this model, many associations between safety and advisory speed signs become apparent: (1) the presence of these signs plays a significant role in shifting the safety effect of relevant geometric parameters –radius and deflection angle- via statistically significant interactions in the model; (2) not only does the presence of advisory speed signs influence the safety effects of other variables, but also the speed that they display has a safety association, in conjunction with the regulatory speed. This work accounted for this association on the variable introduced as the Advisory Speed Differential (ASD). The marginal effect of this variable at sites with explicitly posted advisory speeds clearly differs from that of the sites not displaying the signs (as Figure 2-2 shows); (3) the side friction demand (i.e. the SFD variable) associated with an advisory speed exhibits a statistically significant marginal effect on safety (shown in Figure 2-3); and (4) the statistical interaction between the ASD and the SFD, in conjunction with their constituent coefficients, jointly describe how both the advisory speed sign (or the lack thereof) and its associated SFD affect the horizontal curve safety. When these safety associations were observed for a large set of sites (i.e. Figure 2-6) it became obvious that the practice of posting advisory speed signs is associated with a safety benefit.

Research Question 2:

Is [the safety benefit] dependent of the advisory speed value displayed in these signs?

This work convincingly suggests that it is. As discussed in answering the previous research question, the safety benefit depends on the difference between the regulatory speed limit and the advisory speed, as well as on the side friction demand associated, which is itself a function of the actual advisory speed.

Research Question 3:

1. *Is this benefit also dependent on the criteria that were used to determine the advisory speed?*

This work convincingly suggests that the safety benefit of these signs depends on the posting criteria. Different posting criteria determine advisory speeds based on limiting the side friction factors associated with a range of values that would prevent vehicles from departing their travel lane. Since this research found that the safety benefit of these signs significantly associates with the corresponding side friction demand, it is expected that different criteria would have different safety performance in general. Particularly, this work showed that the performance may become marginal if posting criteria leans toward either excessively permissive or excessively prohibitive side friction values.

Research Question 4:

How robust is the evidence in favor of such a safety benefit?

This work puts forward convincing evidence that the newfound safety benefit exists, but the evidence in favor of the particular quantification of such a safety benefit is not as strong. This dissertation presents various pieces of evidence in favor of the existence of said safety benefit. Because this body of evidence proceeds from different directions and proved self-consistent, this work constitutes a robust case for the safety benefit of advisory speeds.

The main pieces of evidence in this dissertation are the two different validation analyses shown in chapter 3 and chapter 4. The validation effort in chapter 3 showed statistical significance of the ASCF function on a new and independent set of curve sites, which represents convincing evidence against the hypothesis of a ‘null’ ASCF effect (formally shown in the first half of Table 5-11). Furthermore, the validation effort for the Hybrid OSU method shown in chapter 4 verified the predicted safety trends of different posting methods in yet another set of independent sites (i.e. 90 curve sites at county-maintained roads). This constitutes additional evidence that the proposed ASCF formulation is not specific to the original data set in the modelling effort, but rather, it transcends the sample at hand. All this evidence jointly put forward the thesis that the ASCF estimates an underlying effect, inherent to a larger set of curve sites in Oregon’s two-lane, two-way rural highways.

However, the validation effort in chapter 3 also shows that the best estimates available for the ASCF parameters may still differ from said underlying effect (i.e. mild statistical power for the alternative hypothesis shown in the second half of Table 5-11).

This author confidently concludes that the evidence for a safety benefit is robust, but more evidence is necessary in order to increase the confidence in the actual magnitude of such safety benefit.

Research Question 5:

2. *Is it possible and feasible to determine an advisory speed value such that it will yield maximum safety benefit?*

Given the evidence provided in this work, such estimation is possible and feasible. Chapters 3 and 4 in this dissertation propose specific methodologies that are based precisely on the principle of maximizing the safety benefit that may be expected from the posted advisory speeds.

7. Bibliography

AASHTO. (2004). *A Policy on Geometric Design of Highways and Streets (5th Edition).* Washington, D.C.: AASHTO.

AASHTO. (2010). *Highway Safety Manual.* Washington, D.C.: AASHTO.

Avelar, R. E. (2010, August 16). *Effectiveness of Curve Advisory Speed Signs. A Characterization of Road Operations in Western Oregon.* Retrieved November 08, 2010, from Scholars Archive at OSU: http://hdl.handle.net/1957/17673

Avelar, R. E., & Dixon, K. K. (2011). Modelling the Safety Effect of Advisory Speed Signs: A Bivariate Multiplicative Factor on Number of Crashes based on the Speed Differential and the Side Friction Demand. *3rd International Conference on Road Safety and Simulation, September 14-16, 2011, Indianapolis, USA.* 3rd International Conference on Road Safety and Simulation. Indianapolis, IN: Transportation Research Board.

Avelar, R. E., & Dixon, K. K. (2012). How Far are Current Advisory Speeds from being Optimal? An Analysis Based on Safety Performance. Washington D.C.: Transportation Research Board.

Bonneson, J. A. (1999). Side Friction Demand and Speed as Controls for Horizontal Curve Design. *Journal of Transportation Engineering*, 473-480.

Bonneson, J. A., Pratt, M. P., & Miles, J. (2009). Evaluation of Alternative Procedures for Setting Curve Advisory Speed. *Transportation Research Record 2122*, 9-16.

Bonneson, J., Pratt, M., & Carlson, P. (2007). *Horizontal Curve Signing Handbook.* Austin, TX: Texas Department of Transportation. Report No. FHWA/TX-07/0-5439-P1.

Bonneson, J., Pratt, M., Miles, J., & Carlson, P. (2007). *Development of Guidelines for Establishing Effective Curve Advisory Speeds.* Springfield, VA: FHWA.

Brambor, T., Roberts Clark, W., & Golder, M. (2006). Understanding Interaction Models: Improving Empirical Analyses. *Political Analysis* , 63-82.

Carlson, P. J., Burris, M. W., Black, K., & Rose, E. R. (2005). Comparison of Radius-Estimating Techniques for Horizontal Curves. *Transportation Research Record*(1918), 76-83.

Charlton, S. G., & De Pont, J. J. (2007). *Curve Speed Management. Land Transportation New Zealand Research Report 323.* Waterloo Quay, Wellington, New Zealand: Land Transportation New Zealand.

Chowdhury, M. A., Warren, D. L., Bissell, H., & Taori, S. (1998). Are the Criteria for Setting Advisory Speeds on Curves Still Relevant? *ITE Journal. February,* 32-45.

Courage, K. G., Bastin, H. E., Byington, S. R., Cook, A. R., Ferro, W. N., Freeman, R. L., et al. (1978). Review of Usage and Effectiveness of Advisory Speeds. *ITE Journal. September*, 43-46.

Dixon, K. K., & Avelar, R. E. (2011). *SPR 685: Safety Evaluation of Curve Warning Speed Signs. Final Report.* Salem, OR: Oregon Department of Transportation.

Dixon, K. K., & Rohani, J. W. (2008, January). *SPR 641: Methodologies for Estimating Advisory Curve Speeds on Oregon Highways.* Salem, OR: Oregon Department of Transportation.

Eccles, K. A., & Hummer, J. E. (n.d.). Safety Effects of Fluorescent Yellow Warning Signs at Hazardous Sites in Daylight Curves. Washington, DC: Transportation Research Board.

Elvik, R., & Vaa, T. (2004). *"Handbook of Road Safety Measures."*. Oxfort, U.K.: Elsevier.

Farrar, D. E., & Glauber, R. R. (1967). Multicollinearity in Regression Analysis: The Problem Revisited. *The Review of Economics and Statistics, Vol. 49, No. 1,* 92-107.

FHWA. (2009). *Manual on Uniform Traffic Control Devices.* Washington, D.C.: U.S. Department of Transportation.

Fox, J., & Weisberg, S. (2011). An {R} Companion to Applied Regression, Second Edition. Thousand Oaks, CA: Sage. Retrieved from http://socserv.socsci.mcmaster.ca/jfox/Books/Companion

Gates, T. J., Carlson, P. J., & Hawkins Jr., H. G. (2004). Field Evaluations of Warning and Regulatory Signs with Enhanced Conspicuity Properties. *Transportation Research Record 1862*, 64-76.

Glennon, J., Newman, T., & Leisch, J. (1985). *Safety and Operational Considerations for Design of Rural Highway Curves.* Washington, D.C.: Federal Highway Administration.

Haitovsky, Y. (1969). Multicollinearity in Regression Analysis: Comment. *The Review of Economics and Statistics*, 486-489.

Institute of Transportation Engineers. (2009). *Traffic Engineering Handbook, 6th Edition.* Washington, DC: ITE.

Iwasaki, M., & Tsubaki, H. (2006). Bivariate Negative Binomial Generalized Linear Models for Environmental Count Data. *Journal of Applied Statistics*, 909-923.

Kanellaidis, G. (1995). Factors Affecting Drivers' Choice of Speed on Roadway Curves. *Journal of Safety Research, Vol. 26*(Spring 1995), 49-56.

Karlis, D., & Ntzoufras, I. (2005, September). Bivariate Poisson and Diagonal Inflated Bivariate Poisson Regression Models in R. *Journal of Statistical Software*.

Koorey, G., Page, S., Stewart, P., Gu, J., Ellis, A., Henderson, R., et al. (2002). *Curve Advisory Speeds in New Zealand.* Lambton Quay, Wellington, New Zealand: Transfund New Zealand.

Lord, D., & Miranda-Moreno, L. F. (2007). Effects of Low Sample Mean Values and Small Sample Size on the Estimation of the Fixed Dispersion Parameter of

Poisson-gamma Models for Modeling Motor Vehicle Crashes: a Bayesian Perspective. Paper #07-1247. Washington, DC: TRB.

Lyles, R. W. (1982). Advisory and Regulatory Speed Signs for Curves: Effective or Overused? *ITE Journal*. *August* , 20-22.

Lyles, R. W., & William, C. T. (2006). *Communicating Changes in Horizontal Alignment.* Washington, D.C.: Transportation Research Board.

May, A. D. (1990). *Traffic Flow Fundamentals.* Upper Saddle River, NJ 07458: Prentice Hall.

McGee, H. W., & Hanscom, F. R. (2006). *Low-Cost Treatments for Horizontal Curve Safety*. Washington, DC: FHWA-SA-07-002.

ODOT. (2006). *Traffic Manual and the ODOT Sign Policy and Guidelines.* Salem, OR: Oregon Department of Transportation.

Pline, J. L. (2001). *Traffic Control Devices Handbook.* Washington, DC: Institute of Transportation Engineers.

Pratt, M. P., Bonneson, J. A., & Miles, J. D. (2011). Measuring the Non-Circular Portions of Horizontal Curves: An Automated Data Collection Method using GPS. *TRB 90th Annual Meeting.* Washington, DC: Transportation Research Board.

R Development Core Team. (2009). *R: A Language and Environment for Statistical Computing*. Vienna, Austria: R Foundation for Statistical Computing. Retrieved from http://www.R-project.org

R Development Core Team. (2011). *R: A language and environment for statistical computing*. Vienna, Austria: R Foundation for Statistical Computing. Retrieved from http://www.R-project.org/

Ramsey, F. L., & Schafer, D. W. (2002). *The Statistical Sleuth. A Course in Methods of Data Analysis. Second Editon.* Pacific Grove, CA: Duxbury.

Ritchie, M. L. (1972). Choice of Speed in Driving Through Curves as a Funcion of Advisory Speed and Curve Sign. *Human Factors*, 533-538.

Samaniego, F. J. (1976). A Characterization of Convoluted Poisson Distributions with Applications to Estimation. *Journal of the American Statistical Association*, 475-479.

Silvey, S. D. (1968). Multicollinearity and Imprecise Estimation. *Journal of the Royal Statistical Society. Series B (Methodological)*, 539-552.

Thompson, S. K. (1992). *Sampling.* New York: John Wiley & Sons, Inc.

Torbic, D. J., Harwood, D. W., Gilmore, D. K., Pfefer, R., Neuman, T. R., Slack, K. L., et al. (2004). *A Guide for Reducing Collisions on Horizontal Curves.* Washington, DC: Transportation Research Board.

Venables, W. N., & Ripley, B. D. (2002). *Modern Applied Statistics with S. Fourth Edition.* New York: Springer.

Wackerly, D. D., Mendenhall III, W., & Scheaffer, R. L. (2008). *Mathematical Statistics with Applications. 7th Edition.* Toronto, Canada: Thomson.

Winkelmann, R., & Zimmermann, K. (1991). A New Approach for Modeling Economic Count Data. *Economics Letters 37*, 139-143.

Zegeer, C. V., Stewart, J. R., Council, F. M., Reinfurt, D. W., & Hamilton, E. (1992). *Safety Effects of Geometric Improvements on Horizontal Curves. (pp. 11-19)*. Transportation Research Board.

Zwahlen, H. T. (1987). Advisory Speed Signs and Curve Signs and Their Effect on Driver Eye Scanning and Driving Performance. *Transportation Research Record* (1111), 110-120.

Zwahlen, H. T., Russ, A., & Schnell, T. (2003). *Driver Eye Scanning Behavior While Viewing Ground-Mounted Diagrammatic Guide Signs before Entrance Ramps at Night*. Washington, D.C.: Transportation Research Board.

Appendices

Appendix A. Computing the Marginal Effect of an Interacting Variable in a Regression Model

This Appendix demonstrates the details of how to obtain the marginal effect of a variable with a constituent term and also involved in an interaction term in a regression model. In this section, this author uses an early version of the final model presented in this work. In that early version, the variable for the horizontal radius was involved only in one interaction with another variable. That is not the case for the final model, where the horizontal radius interacts with several other variables. The purpose of this exercise is to exemplify the interpretation of a marginal effect from the model as discussed in chapter 2, where this procedure is implied in order to obtain the marginal effects of the ASD and SFD components of the ASCF. Equation A-1 shows the horizontal radius terms in the early model. The complete parameterization in the early model is shown in Table A-1.

Equation A-1: Early Model Terms that Included Horizontal Radius

$$\{0.0004(Radius) - 0.0045(AdvSpdPresent \times Radius)\}$$

The total effect of the horizontal radius is contained in the two terms shown in Equation A-1. In order to find the marginal effect of the horizontal radius, one needs to know if there is an advisory speed present in the curve. If it is not so, then the marginal effect of horizontal radius is simply the main constituent coefficient (+0.0004, because the interaction coefficient is multiplied by *AdvSpdPresent*, zero in this case). The statistical significance in this case is given simply by a measure of the coefficient estimate (p-value of 0.1603, as of Table A-1).

The model suggests then that the effect of the horizontal radius at locations without advisory speeds is an increase of crashes (a positive coefficient *AdvSpdPresent*=0), and that such increase is proportional to the magnitude of the horizontal radius. This is counter intuitive with what one would expect. However, such an increase of crashes is statistically insignificant. So, for practical purposes, there is no sufficient statistical evidence in the model of such an adverse effect.

Table A-1: Early Version of Poisson Regression Model for Crash Data

Term	***Estimate***	***Standard Error***	***z-value***	***p-value***	***Signi-ficance***
(Intercept)	-3.678	0.692	-5.314	1.07×10^{-7}	***
AADT	5.097×10^{-4}	6.399×10^{-5}	7.966	1.64×10^{-15}	***
AADT:HigherAADT	-4.578×10^{-4}	9.134×10^{-5}	-5.011	5.41×10^{-15}	***
HigherAADT	2.007	0.678	2.960	0.003	**
Radius	4.430×10^{-4}	3.172×10^{-4}	1.396	0.163	
Radius:AdvSpdPresent	-4.459×10^{-3}	1.052×10^{-3}	-4.237	2.26×10^{-5}	***
AdvSpdPresent	4.644	0.745	6.237	4.47×10^{-10}	***
CurveLength:AdvSpdPresent	-2.557×10^{-3}	6.965×10^{-4}	-3.671	2.42×10^{-4}	***
CurveLength	8.485×10^{-4}	3.170×10^{-4}	2.677	7.431×10^{-3}	**
SFD	7.711	2.381	3.239	1.198×10^{-3}	**
ASD:SFD	-0.863	0.201	-4.152	3.300×10^{-5}	***
ASD	4.926×10^{-2}	2.594×10^{-2}	1.899	5.760×10^{-2}	
LowAdv	-1.301	0.504	-2.584	9.759×10^{-3}	***

In the case advisory speed signs are present, however, the marginal effect of horizontal radius would result from a composite coefficient (+0.0004 - 0.0045, the last factor resulting from substituting *AdvSpdPresent=1* for this case). So, in the case of locations with posted advisory speeds, the effect of horizontal radius is a decrease in the number of crashes (a negative coefficient when *AdvSpdPresent=1*) and such decrease is proportional to the horizontal radius. The general trend of this effect is in the way expected (more crashes at sharper curves), but such an effect would appear relevant if its statistical significance becomes convincingly high from the model, converse to the irrelevant effect of radius when there is no advisory speed present. The computation of a p-value of this marginal effect is slightly more complicated, however. For the Poisson regression generalized linear model, the canonical link function is the natural logarithm. Defining *z=ln(y)*, where y is the number of crashes, the regression model may be expressed as of Equation A-2.

Equation A-2: General Multiplicative Interactive Regression Model

$$z = \beta_0 + (\beta_1.X_1 + \beta_2.X_1.X_2 + \beta_3.X_2) + \cdots + \beta_j.X_i + \cdots + \beta_m.X_n,$$

Where:

z	=	natural logarithm of y;
y	=	Number of Crashes;
X_i	=	i-th explanatory variable; and
β_j	=	j-th regression coefficient.

The marginal effect of x_1 may be obtained easily by taking the first partial derivative with respect to x_1: $\frac{\partial z}{\partial x1} = \beta_1 + \beta_2.X_2$. This is a linear combination of two random variables, β_1 and β_2, the first with coefficient 1 and the other with coefficient X_2. The variance for this linear combination is then given by Equation A-3:

Equation A-3: Variance for the Marginal Effect of a Single Variable in a Multiplicative Interactive Model

$$V\left(\frac{\partial z}{\partial x1}\right) = V(\beta_1) + (X_2)^2.V(\beta_2) + 2.(X_2).Cov(\beta_1, \beta_2)$$

Where:

V(.)	=	denotes the variance of the variable in the parenthesis; and
Cov(. , .)	=	denotes the covariance of the two quantities in parenthesis.

The computation of such a variance requires that the covariance structure among the regression coefficients be known. The required covariance matrix may be easily obtained from most available statistical analysis packages. Table A-2 shows the intermediate results for the calculation based on Equation A-3.

This table shows an inversely proportional effect, as expected, of the horizontal curve radius on the crash frequency (determined by the negative value). But more importantly, such effect is statistically significant (p-value of 0.00011).

Table A-2: Radius Effect at Sites with Posted Advisory Speeds

Radius effect when *AdvSpPresent*=1 ($\beta_1 + \beta_2 .(1)$)	-0.00402
Variance of *Radius* Coefficient ($V(\beta_1)$)	$1.006\text{x}10^{-07}$
Variance of *Radius*:*AdvSpPresent* Interaction ($V(\beta_2)$)	$1.108\text{x}10^{-6}$
Covariance of *Radius* and *Radius:AdvSpPresent* Interaction ($Cov(\beta_1, \beta_2)$)	$-1.350\text{x}10^{-8}$
Standard Error for *Radius* Marginal Effect	0.0011
z-value	-3.695
p-value	0.00011

A complete interpretation of the marginal effect of the horizontal radius may now be crafted. Using the radius partial effects at both possible levels of the variable *AdvSpdPresent*, the model predicts, with statistical significance, fewer crashes at curves with larger radii, but only at curves displaying advisory speed plaques (p-value of

0.00011). The model shows an opposite effect at curves without advisory speed plaques, at least in its mathematical form; but the model provides only narrow statistical evidence of such a counterintuitive effect (p-value of 0.1603).

It is important to notice that the just computed marginal effect of horizontal radius is not yet an independent effect. The total number of crashes is affected when *AdvSpdPresent* changes from 0 to 1. This change occurs because there is a single constituent coefficient for the variable *AdvSpdPresent*, as of Table A-1. Furthermore, in addition to shifting the baseline number of crashes, the presence of advisory speed plaques interacts with the curve length variable as well in this model. Such interaction should be interpreted as a conditioning of the effect of the curve length to both levels of the variable *AdvSpdPresent*.

Additionally, it is important to notice that the complete mathematical form of the sub-model that captures the joint effect of radius, curve length and the presence of advisory speed plaques, as of this early model, is that of a trilinear polynomial in the statistical model. Although mathematically feasible, this author did not establish the detailed intricacies of this tri-linear interpolant polynomial because it diverges from the main focus of this work.

Appendix B. Explicit Treatment of Structural Correlation in the Data by use of a Bivariate Poisson Model

In this appendix, this author explored a bivariate Poisson parameterization as a way to assess to which extent deeming the structural correlation in the data may have affected the statistical modelling effort this dissertation bases upon.

B.1. The Bivariate Poisson Specification

Karlis and Ntzoufras (2005) developed a maximum likelihood estimation procedure for bivariate Poisson models. The authors developed a computational package for the statistical analysis software R, which implements an Expected-Maximization (EM) iterative algorithm to perform the estimation.

In this model specification, the response variable is a vector: $\begin{bmatrix} Y_R \\ Y_L \end{bmatrix}$, where the sub-indexes correspond to the direction of curvature. This author stipulated so in order to provide some sense of order to the vector, and to explore the effect of the direction of travel. The direction of travel, however, did not prove a significant piece of information.

Instead of single parameter estimation such that $Y \sim Poisson(\lambda)$, the bivariate Poisson model can be specified as a vector response whose distribution depends on three parameters: $\begin{bmatrix} Y_R \\ Y_L \end{bmatrix} \sim BV.Poisson(\,\lambda_1, \lambda_2, \lambda_3)$

This specification is such that:

$$Y_R \sim Poisson(\lambda_1 + \lambda_3) \ \ \wedge \ \ Y_L \sim Poisson(\lambda_2 + \lambda_3)$$

Where:

$$\lambda_3 = Cov(Y_R, Y_L).$$

The parameter λ_3 is then a direct measure of the codependence between the crash counts from two directions of travel in a single site.

Marginally, the parameterization of each of the three parameters is similar to that of a GLM Poisson model:

$$\lambda_1 = \exp\left(\vec{\beta_i}^T . \overrightarrow{X_1}\right)$$

$$\lambda_2 = \exp\left(\vec{\beta_{ii}}^T . \overrightarrow{X_2}\right)$$

$$\lambda_3 = \exp\left(\vec{\beta_{iii}}^T . \overrightarrow{X_3}\right)$$

B.2. Performance of Alternative Bivariate Specifications

By use of the R library developed by Karlis and Ntzoufras (2005), this author fitted various alternative BV Poisson models, after reordering the data into 105 curve sites with all the covariates conforming a single vector per site. It is important to point out that the data was originally broken down into 210 directions of travel in order to parameterize univariate Poisson and NB2 regression models as described in chapter 2. Since this exploration of alternative specifications is a supplement to the main body of this dissertation, this author only explored five basic specifications of bivariate response models:

1. A Double Poisson model with the same structure for λ_1 and λ_2 and shared coefficients. This specification assumes a null covariance between the components of the response vector, namely $\lambda_3 = 0$. This specification yielded, as expected, the same coefficients and same AIC as obtained from the simpler GLM version discussed in Appendix A (i.e. AIC of 440.59). The 13 coefficients are exactly the same shown in Table A-1.
2. A Double Poisson model with independent coefficient sets for λ_1 and λ_2, still specifying $\lambda_3 = 0$. The AIC increased very significantly (450.79), which

indicates that nearly doubling the parameters (from 13 to 21) steeply decreases the quality of information in the model.

3. A simple bivariate Poisson model with the same structure and shared coefficients for λ_1 and λ_2. In this case, λ_3 was subject to estimating a flat value only. Although there is a significant improvement in the AIC (drops from the reference point 440.59 to 438.41), which means that λ_3 is a significant addition in terms of quality of information, an actual covariance between directions of travel of $\lambda_3 = 0.0958$ seems to this author a scientifically insignificant value. Even when there is an improvement in information quality, the actual value of the covariance corresponds to an average correlation of 0.2824 (as computed from all the realizations of the three BV Poisson parameters available in the sample). The corresponding standard deviation is, however, 0.2431, which makes it statistically insignificant.
4. A more complex bivariate Poisson model with same structure and shared coefficients for λ_1 and λ_2, but parameterizing λ_3 as:

$$\lambda_3 = \exp(\beta_{iii.1} + \beta_{iii.2}.Radius + \beta_{iii.3}.CurveLength)$$

This parameterization was selected because these variables are common to both directions of travel. The AIC dropped to (435.06), but in an attempt to reduce duplicity of information in the model specification, this author attempted various permutations of removing these two variables from λ_1 and λ_2, resulting the best model the one without Radius but still including *CurveLength* in λ_1 and λ_2. In this specification, both said variables were kept in λ_3. The corresponding AIC was (434.00).
5. A complex bivariate Poisson model resulting from some empirical model selection. This author considered such a parameterization of interest, so to assess the extent to which parameterizing λ_3 could be associated with a gain

in information quality of the model. Both λ_1 and λ_2, were kept as in the previous bivariate model. The best parameterization for λ_3 was then:

$$\lambda_3 = \exp(\beta_{iii.1} + \beta_{iii.2}.Radius + \beta_{iii.3}.CurveLength + \beta_{iii.4.}AdvSpPresent + \beta_{iii.5}.AdvSpPresent \times Radius + \beta_{iii.3}.AdvSpPresent \times CurveLength)$$

This parameterization yielded an AIC value of 420.92, a very good return at the cost of estimating 20 parameters instead of 13 of the nested univariate model.

Finally, a bootstrap estimation was performed over the best BV Poisson model, in order to shed some light on the aspect of statistical significance. Unfortunately, obtaining p-values for the estimates is not as simple as in the case of GLM specifications.

The bootstrap procedure consists on re-sampling from the available data set and estimating all the regression coefficients every time. Statistics can be computed from the results. In such a way, this author performed 200 re-sampling replications from the 105 pairs of curve directions in the data set. P-values were obtained from the standard normal distribution, as the sample size confidently allows the required assumption of normality. The significance of the coefficients parameterizing λ_1 and λ_2 were comparable to the significance of the corresponding coefficients from the univariate model. However, all coefficients parameterizing λ_3 resulted statistically insignificant (where the smallest p-value was 0.8689 for the CurveLenght variable). This resonates with the observation in chapter 2 that after accounting for communalities, the unexplained residual correlation can be considered insignificant.

Table B-1 shows a comparison of the ASCF coefficients for different model specifications. The ASCF estimation appears relatively resilient to the more complex bivariate Poisson specification.

Table B-1: ASCF Coefficients and AICs for Different Model Specifications

	ASD	**SFD**	**SFD:ASD**	**AIC**
Early Poisson Model	0.0493	7.7115	-0.8625	440.59
Simple BV Poisson Model	0.0476	9.5066	-0.9923	438.41
Best BV Poisson Model	0.0406	9.3679	-1.0981	420.92
Final Poisson Model (Including more covariates)	0.0240	5.7993	-0.5532	424.85

The only set of coefficients that appears significantly different is that from the final Poisson model. Such coefficients suggests that the inclusion of additional covariates made the ASCF effect less pronounced (i.e. smaller ASD and SFD constituent coefficients) and it made its marginal effect more independent (i.e. smaller SFD:ASD interaction coefficient).

From this exploratory analysis, this author concludes that not much can be gained in terms of better ASCF estimates or statistically significant effects of other variables when using the BV Poisson specification, especially if one compares the similar AICs of the best BV Poisson model and the Final Poisson Model, though such a comparison is not necessarily appropriate. The mean structure in the final Poisson Model was not tested by using the BV Poisson specification, which this is a critical difference, given that the latest structure includes the deflection angle and the lane width as new covariates. This latest mean structure also changes the mathematical form of the curve length, now associated with two coefficients. Because of these reasons, this author recommends that future work related to this topic explores alternative parameterizations for the mean.

Regardless, the use of the BV Poisson specification unnecessarily complicates, in this author's opinion, the process of obtaining the statistical significance of the coefficients by techniques such as jackknife, CV, and bootstrap estimation. These techniques are significantly more costly in terms of computational power, coding efforts, preparation of the data, and processing times. However, the significant drop in AIC (from 440.59 to 420.92) associated with the best available BV Poisson specification makes it a very promising alternative for future works modelling horizontal curve safety. This author speculates that the BV Poisson specification may provide an even larger entropy reduction if the most recent specification for the univariate Poisson model (i.e. the one presented in chapter 2) were to be used instead of the early version shown in this section.